

Offshore Wind Farm

Eneco Luchterduinen

Ecological Monitoring of Seabirds

T3 (Final) Report



December 2018

ISO 9001
Management System Certification

BUREAU VERITAS
Certification Denmark A/S



Offshore Wind Farm

Eneco Luchterduinen

Ecological Monitoring of Seabirds

T3 (Final) Report

Prepared for ENECO
 Represented by Ms. Sytske van den Akker



Photo by Thomas W Johansen

Project manager	Henrik Skov
Author	Stefan Heinänen Henrik Skov
Quality supervisor	Henrik Skov

Project number	11813060
Approval date	10 December 2018
Revision	Final
Classification	Confidential

CONTENTS

1	Abbreviations	7
2	Executive summary	8
3	Introduction	10
4	Materials and methods	11
4.1	Monitoring approach	11
4.2	Survey design and available data	12
4.3	Seabird counting techniques	14
4.4	Quality control and post-processing of survey data	16
4.5	Distance analysis	16
4.6	Distribution models	17
4.7	Analysis of displacement and number of included surveys	20
4.8	Presentation of data	20
5	Results	20
5.1	Effort and sample sizes	20
5.2	Distance analysis	23
5.3	Species accounts	23
5.3.1	<i>Divers: Red-throated Gavia stellata and Black-throated Divers Gavia arctica</i>	23
5.3.2	<i>Great Crested Grebe Podiceps cristatus</i>	27
5.3.3	<i>Northern Gannet Morus bassanus</i>	31
5.3.4	<i>Great Cormorant Phalacrocorax carbo</i>	36
5.3.5	<i>Little Gull Hydrocoloeus minutus</i>	40
5.3.6	<i>Black-headed Gull Chroicocephalus ridibundus</i>	44
5.3.7	<i>Common Gull Larus canus</i>	48
5.3.8	<i>Lesser Black-backed Gull Larus fuscus</i>	52
5.3.9	<i>Herring Gull Larus argentatus</i>	56
5.3.10	<i>Great Black-backed Gull Larus marinus</i>	60
5.3.11	<i>Black-legged Kittiwake Rissa tridactyla</i>	64
5.3.12	<i>Common Guillemot Uria aalge</i>	68
5.3.13	<i>Razorbill Alca torda</i>	73
5.3.14	<i>Marine mammal observations</i>	78
6	Discussion and conclusion	81
6.1	Characterisation of LUD site	81
6.2	Monitoring design	82
6.3	Modelling approach and performance.....	83
6.4	Displacement and attraction effects	84
7	References	86
8	APPENDIX A – Detailed results of species distribution models for the T-2 surveys	88

FIGURES

Figure 4.1. Primary (blue) and secondary (red) transects with indications of Luchterduinen, Prinses Amalia and Egmond aan Zee wind farms indicated.	13
Figure 4.2. The ‘Ivero’ above and ‘Coastal Chariot’ below used as the survey ships.	15
Figure 4.3. Schematic overview of the seabird survey method (see above for definitions of bands A-E).	15
Figure 4.4. Environmental variables (mean values) for the four LUD-T3 surveys.	19
Figure 5.1. The spatial coverage of survey effort (km ²) obtained during the three ship-based surveys in the LUD-T3 season (2017-2018).	21
Figure 5.2. Observed density (birds/km ²) of Diver sp. during LUD-T3 surveys 2017-2018. Densities have been corrected for distance bias.	24
Figure 5.3. Mean observed density (birds/km ²) of Diver sp. in the entire surveyed area during OWEZ, PAWP and LUD pre- and post-construction surveys. Densities have been corrected for distance bias.	25
Figure 5.4 Mean density of Diver species during surveys included in the modelling. The mean density within the OWEZ footprint is shown as well as the mean in the whole surveyed area (including wind farms).	26
Figure 5.5. Predicted mean density (birds/km ²) and distribution of wintering Diver sp. during four LUD pre- and four LUD post-construction surveys, and the relative change in predicted density between the two periods. Note that all included surveys are OWEZ and PAWP post-construction surveys.	27
Figure 5.6. Observed density (birds/km ²) of Great Crested Grebe during LUD-T3 surveys 2017-2018. Densities have been corrected for distance bias.	28
Figure 5.7. Mean observed density (birds/km ²) of Great Crested Grebe in the entire surveyed area during OWEZ, PAWP and LUD pre- and post-construction surveys. Densities have been corrected for distance bias.	29
Figure 5.8. Mean density of Great Crested Grebe species during surveys included in the modelling. The mean density within the OWEZ footprint is shown as well as the mean in the whole surveyed area (including wind farms). Surveys above the dashed line are LUD post-construction surveys.	30
Figure 5.9. Predicted mean density (birds/km ²) and distribution of wintering Great Crested Grebe during three LUD pre- and three LUD post-construction surveys, and the relative change in predicted density between the two periods. Note that all included surveys are OWEZ and PAWP post-construction surveys.	31
Figure 5.10 Observed density (birds/km ²) of Northern Gannet during LUD-T3 surveys 2017-2018. Densities have been corrected for distance bias.	32
Figure 5.11. Mean observed density (birds/km ²) of Northern Gannet in the entire surveyed area during OWEZ, PAWP and LUD pre-construction and post-construction surveys. Densities have been corrected for distance bias.	33
Figure 5.12. Mean density of Northern Gannet during surveys included in the modelling. The mean density within each of the three wind farm footprints (OWEZ, PAWP and LUD) is shown as well as the mean in the whole surveyed area (including wind farms). Surveys above the dashed line are LUD post-construction surveys.	34
Figure 5.13. Predicted mean density (birds/km ²) and distribution of wintering Northern Gannet during eight LUD pre-construction and 12 LUD post-construction surveys, and the relative change in predicted density between the two periods. Note that all included surveys are OWEZ and PAWP post-construction surveys.	35
Figure 5.14. Model predictions (on model data) for Northern Gannet during the eight LUD post-construction surveys, with (fitted values) and without the response of the wind farm, when taking into account the dynamic environmental conditions. The difference indicate a mean displacement with model errors, i.e. what is the difference in probability of presence (to the left) or the density (to the right) if the wind farm(s) would not be present compared to a WF present. The mean displacement in % is indicated above the estimates for the footprints (GAMM model errors, SE, are indicated as error bars).	36
Figure 5.15. Observed density (birds/km ²) of Great Cormorant in the entire surveyed area during LUD-T3 surveys 2017-2018. Densities have been corrected for distance bias.	37
Figure 5.16. Mean observed density (birds/km ²) of Great Cormorant during OWEZ, PAWP and LUD pre- and post-construction surveys. Densities have been corrected for distance bias.	38

Figure 5.17. Mean density of Great Cormorant during surveys included in the modelling. The mean density within each of the three wind farm footprints (OWEZ, PAWP and LUD) is shown as well as the mean in the whole surveyed area (including wind farms). Surveys above the dashed line are LUD post-construction surveys. 39

Figure 5.18. Predicted mean density (birds/km²) and distribution of wintering Great Cormorant during eight LUD pre- and 12 LUD post-construction surveys, and the relative change in predicted density between the two periods. Note that all included surveys are OWEZ and PAWP post-construction surveys. 40

Figure 5.19. Observed density (birds/km²) of Little Gull during LUD-T3 surveys 2017-2018. Densities have been corrected for distance bias. 41

Figure 5.20. Mean observed density (birds/km²) of Little Gull in the entire surveyed area during OWEZ, PAWP and LUD pre- and post-construction surveys. Densities have been corrected for distance bias. 42

Figure 5.21. Mean density of Little Gull during surveys included in the modelling. The mean density within OWEZ wind farm footprint is shown as well as the mean in the whole surveyed area (including wind farms). Surveys above the dashed line are LUD post-construction surveys. 43

Figure 5.22. Predicted mean density (birds/km²) and distribution of wintering Little Gull during eight LUD pre- and 12 LUD post-construction surveys, and the relative change in predicted density between the two periods. Note that all included surveys are OWEZ and PAWP post-construction surveys. 44

Figure 5.23. Observed density (birds/km²) of Black-headed Gull during LUD-T3 surveys 2017-2018. Densities have been corrected for distance bias. 45

Figure 5.24. Mean observed density (birds/km²) of Black-headed Gull in the entire surveyed area during OWEZ, PAWP and LUD pre- and post-construction surveys. Densities have been corrected for distance bias. 46

Figure 5.25. Mean density of Black-headed Gull during surveys included in the modelling. The mean density within each of the three wind farm footprints (OWEZ, PAWP and LUD) is shown as well as the mean in the whole surveyed area (including wind farms). Surveys above the dashed line are LUD post-construction surveys. 47

Figure 5.26. Predicted mean density (birds/km²) and distribution of wintering Black-headed Gull during eight LUD pre- and 12 LUD post-construction surveys, and the relative change in predicted density between the two periods. Note that all included surveys are OWEZ and PAWP post-construction surveys. 48

Figure 5.27. Observed density (birds/km²) of Common Gull during LUD-T3 surveys 2017-2018. Densities have been corrected for distance bias. 49

Figure 5.28. Mean observed density (birds/km²) of Common Gull in the entire surveyed area during OWEZ, PAWP and LUD pre- and post-construction surveys. Densities have been corrected for distance bias. 50

Figure 5.29. Mean density of Common Gull during surveys included in the modelling. The mean density within each of the three wind farm footprints (OWEZ, PAWP and LUD) is shown as well as the mean in the whole surveyed area (including wind farms). Surveys above the dashed line are LUD post-construction surveys. 51

Figure 5.30. Predicted mean density (birds/km²) and distribution of wintering Common Gull during eight LUD pre- and 12 LUD post-construction surveys, and the relative change in predicted density between the two periods. Note that all included surveys are OWEZ and PAWP post-construction surveys. 52

Figure 5.31. Observed density (birds/km²) of Lesser Black-backed Gull during LUD-T3 surveys 2017-2018. Densities have been corrected for distance bias. 53

Figure 5.32. Mean observed density (birds/km²) of Lesser Black-backed Gull in the entire surveyed area during OWEZ, PAWP and LUD pre- and post-construction surveys. Densities have been corrected for distance bias. 54

Figure 5.33. Mean density of Lesser Black-backed Gull during surveys included in the modelling. The mean density within each of the three wind farm footprints (OWEZ, PAWP and LUD) is shown as well as the mean in the whole surveyed area (including wind farms). Surveys above the dashed line are LUD post-construction surveys. 55

Figure 5.34. Predicted mean density (birds/km²) and distribution of wintering Lesser Black-backed Gull during eight LUD pre- and 12 LUD post-construction surveys, and the relative change in predicted density between the two periods. Note that all included surveys are OWEZ and PAWP post-construction surveys. 56

Figure 5.35. Observed density (birds/km ²) of Herring Gull during LUD-T3 surveys 2017-2018. Densities have been corrected for distance bias.....	57
Figure 5.36. Mean observed density (birds/km ²) of Herring Gull in the entire surveyed area during OWEZ, PAWP and LUD pre- and post-construction surveys. Densities have been corrected for distance bias.....	58
Figure 5.37. Mean density of Herring Gull during surveys included in the modelling. The mean density within each of the three wind farm footprints (OWEZ, PAWP and LUD) is shown as well as the mean in the whole surveyed area (including wind farms). Surveys above the dashed line are LUD post-construction surveys.....	59
Figure 5.38. Predicted mean density (birds/km ²) and distribution of wintering Herring Gull during eight LUD pre- and 12 LUD post-construction surveys, and the relative change in predicted density between the two periods. Note that all included surveys are OWEZ and PAWP post-construction surveys.	60
Figure 5.39. Observed density (birds/km ²) of Great Black-backed Gull during LUD-T3 surveys 2017-2018. Densities have been corrected for distance bias.	61
Figure 5.40. Mean observed density (birds/km ²) of Great Black-backed Gull in the entire surveyed area during OWEZ, PAWP and LUD pre- and post-construction surveys. Densities have been corrected for distance bias.....	62
Figure 5.41. Mean density of Great Black-backed Gull during surveys included in the modelling. The mean density within each of the three wind farm footprints (OWEZ, PAWP and LUD) is shown as well as the mean in the whole surveyed area (including wind farms). Surveys above the dashed line are LUD post-construction surveys.	63
Figure 5.42. Predicted mean density (birds/km ²) and distribution of wintering Great Black-backed Gull during eight LUD pre- and 12 LUD post-construction surveys, and the relative change in predicted density between the two periods. Note that all included surveys are OWEZ and PAWP post-construction	64
Figure 5.43. Observed density (birds/km ²) of Black-legged Kittiwake during LUD-T3 surveys 2017-2018. Densities have been corrected for distance bias.	65
Figure 5.44. Mean observed density (birds/km ²) of Black-legged Kittiwake in the entire surveyed area during OWEZ, PAWP and LUD pre- and post-construction surveys. Densities have been corrected for distance bias.....	66
Figure 5.45. Mean density of Black-legged Kittiwake during surveys included in the modelling. The mean density within each of the three wind farm footprints (OWEZ, PAWP and LUD) is shown as well as the mean in the whole surveyed area (including wind farms). Surveys above the dashed line are LUD post-construction surveys.	67
Figure 5.46. Predicted mean density (birds/km ²) and distribution of wintering Black-legged Kittiwake during eight LUD pre- and 12 LUD post-construction surveys, and the relative change in predicted density between the two periods. Note that all included surveys are OWEZ and PAWP post-construction surveys.	68
Figure 5.47. Observed density (birds/km ²) of Common Guillemot during LUD-T3 surveys 2017-2018. Densities have been corrected for distance bias.....	69
Figure 5.48. Mean observed density (birds/km ²) of Common Guillemot in the entire surveyed area during OWEZ, PAWP and LUD pre-construction surveys (indicated by a blue rectangle) and post-construction surveys (green rectangle). Densities have been corrected for distance bias.	70
Figure 5.49. Mean density of Common Guillemot during surveys included in the modelling. The mean density within the three wind farm footprints (OWEZ, PAWP and LUD) are shown as well as the mean in the whole surveyed area. Surveys above the dashed line are LUD post-construction surveys.....	71
Figure 5.50. Predicted mean density (birds/km ²) and distribution of wintering Common Guillemot during eight LUD pre- and 12 LUD post-construction surveys, and the relative change in predicted density between the two periods. Note that all included surveys are OWEZ and PAWP post-construction surveys.	72
Figure 5.51. Model predictions (on model data) for Common Guillemot during the eight LUD post-construction surveys, with (fitted values) and without the response of the wind farm, when taking into account the dynamic environmental conditions. The difference indicate a mean displacement with model errors, i.e. what is the difference in probability of presence (to the left) or the density (to the right) if the wind farm(s) would not be present compared to a WF present. The mean displacement in % is indicated above the estimates for the footprints (GAMM model errors, SE, are indicated as error bars).	73

Figure 5.52. Observed density (birds/km²) of Razorbill during LUD-T3 surveys 2017-2018. Densities have been corrected for distance bias. 74

Figure 5.53. Mean observed density (birds/km²) of Razorbill in the entire surveyed area during OWEZ, PAWP and LUD pre- and post-construction surveys. Densities have been corrected for distance bias. 75

Figure 5.54. Mean density of Razorbill during surveys included in the modelling. The mean density within the three wind farm footprints (OWEZ, PAWP and LUD) are shown as well as the mean in the whole surveyed area. Surveys above the dashed line are LUD post-construction surveys. 76

Figure 5.55. Predicted mean density (birds/km²) and distribution of wintering Razorbill during eight LUD pre- and 12 LUD post-construction surveys, and the relative change in predicted density between the two periods. Note that all included surveys are OWEZ and PAWP post-construction surveys. 77

Figure 5.56. Model predictions (on model data) for Razorbill during the eight LUD post-construction surveys, with (fitted values) and without the response of the wind farm, when taking into account the dynamic environmental conditions. The difference indicate a mean displacement with model errors, i.e. what is the difference in probability of presence (to the left) or the density (to the right) if the wind farm(s) would not be present compared to a WF present. The mean displacement in % is indicated above the estimates for the footprints (GAMM model errors, SE, are indicated as error bars). 78

Figure 5.57. Observations of marine mammals during the LUD-T3 surveys 2017-2018. No corrections for possible double registrations have been made. 79

Figure 6.1. The distribution of the coastal and North Sea water masses and currents in relation to the location of the LUD site as reflected by the frequency (%) of modelled salinity (above 34 psu or below 32 psu), current speed (above 0.5 m/s) and current gradient (above 0.00003) at 10 m depth. The hydrodynamic model data from the period January-March 2018 have been processed. Areas close to the coast which are shallower than 10 m are shown with grey colour indicating no data values. 82

TABLES

Table 1. Design parameters for LUD, OWEZ and PAWP wind farms. 11

Table 2. List of 27 available surveys included in the analyses of seabird displacement from LUD. Survey No indicate the factor levels used in the statistical analyses (Appendix A). 13

Table 3. List of observers engaged in the LUD-T3 seabird surveys. 16

Table 4. Grouping of species for distance analysis. 17

Table 5. Survey effort (km² covered by observation transect) obtained during the three ship-based surveys in the LUD-T3 winter season (2017-2018). 20

Table 6. Numbers of seabirds observed during the four LUD-T3 surveys in winter 2017/2018. 22

Table 7. Distance statistics for sitting birds in each species group. 23

Table 8. Overview of observations of marine mammals during the LUD Seabird monitoring program 2014-2018. 80

1 Abbreviations

AIC	Akaike Information Criterion
AUC	Area Under Curve. Probability of correctly predicting presence of species
EEZ	Dutch Exclusive Economic Zone
EIA	Environmental Impact Assessment
ESW	Effective Strip Width
GAM	Generalized Additive Model
LUD	Offshore Wind Farm Eneco Luchterduinen
LAT	Lowest Astronomical Tide
MEP	Monitoring and Evaluation Program
OWEZ	Offshore Wind Farm Egmond aan Zee
OWF	Offshore Wind farm
PAWP	Prinses Amalia wind farm
TOR	Terms of Reference
UTM	Universal Transverse Mercator
WTG	Wind Turbine Generator

2 Executive summary

The T3 report provides the results from the third and last year post-construction of the LUD seabird monitoring program regarding displacement of seabirds from LUD as well as updated results from PAWP and OWEZ. The dynamic modelling framework, which was tested during LUD-T1 was applied on all available data from the three wind farms including the data collected during the three LUD-T3 surveys. The LUD-T1 and LUD-T2 reports indicated that high power would be achievable after LUD-T3 for Common Guillemot (detection of a displacement of 50%), and possibly for Northern Gannet depending on the number of birds recorded. Due to the high number of Gannets recorded during the second T3 survey displacement effects were detected for both Northern Gannet and Common Guillemot, and additionally also for Razorbill, Lesser Black-backed Gull (LUD only) and Black-legged Kittiwake (PAWP only). Although reductions in the number of several species were recorded and modelled during the LUD post-construction period, these changes were not related to the three wind farms. Red-throated/Black-throated Diver, Great Crested Grebe and Little Gull all declined in the coastal zone, and there was a general decline in the occurrence of Black-headed Gull. The reduction in the presence of Red-throated/Black-throated Diver in OWEZ and in the buffer zones of all three wind farms, of Little Gull in OWEZ and of Black-headed Gull in LUD (footprint and buffer) may therefore be unrelated to displacement, and rather reflects large-scale changes in environmental conditions beyond what was accounted for by the models.

When incorporating all data collected in relation to the monitoring programs of the three offshore wind farms the displacement impact on Northern Gannet from the three footprints was significant and at a level of 74% for LUD, 89% for PAWP and 90% for OWEZ. The impact was manifested as a decline in the presence of the birds in spite of an increase in the occurrence of gannets in the offshore zone during the LUD post-construction period. No significant displacement impact on gannets could be detected beyond the footprints, within the 2 km buffer zone analysed. Displacement impact on the presence of Lesser Black-backed Gull was detected in the LUD footprint and of Black-legged Kittiwake in PAWP in spite of a general increase of both species in the offshore zone during LUD post-construction.

The significant displacement impact on Common Guillemot was manifested as a decline in presence in all three offshore wind farm footprints and also in the PAWP buffer (2 km), as well as a decline in the density when present in the footprints of LUD and PAWP. The level of the displacement of guillemots (density) was 52% in LUD, 70% in PAWP and 28% in OWEZ. The significant displacement impact on Razorbill presence was apparent in the footprints of all three wind farms, but only significant for LUD and PAWP due to higher level of variability in the occurrence of this species in OWEZ. The level of displacement (density) was 52% in LUD, 72% in PAWP and 52% in OWEZ. The displacements of Common Guillemot and Razorbill were detected in spite of the general recent increase in the occurrence of both species on the Dutch shelf. Overall the impact on both species was highest in PAWP, followed by LUD and lowest in OWEZ, thus reflecting both the variation in the density of turbines between the three wind farms and the difference in terms of location relative to areas of highest densities of auks.

No signs of habituation of Northern Gannet, Razorbill and Common Guillemot to the three wind farms were observed.

Great Cormorants were clearly attracted to the footprints and buffers of all three wind farms. Although higher numbers of Common Gull, Herring Gull and Great Black-backed Gull were also recorded in LUD and PAWP during post-construction, only the Great Black-backed Gull may reflect attraction as this species was recorded in slightly lower numbers everywhere else during this period. Common Gull and Herring Gull displayed a general increase in occurrence off the Dutch coast during this period.

The LUD-T3 results are generally in line with the results from LUD-T1 and other studies like Krijgsveld (2014) and Welcker & Nehls (2016), see Table 0. The updated results now indicate that displacement of Northern Gannet, Common Guillemot and Razorbill mainly takes place from the footprint and only the Guillemots seem to be displaced from the 2 km buffer around PAWP. Based on these results and the higher level of displacement seen in Guillemots and Razorbills in PAWP as compared to LUD and OWEZ it seems plausible that the distance between turbines plays an important role in determining the strength of displacement of seabirds.

The modelling framework included data on intensity of shipping. However, the updated results indicate that the density of ships mainly affected the distribution of Little gull, divers and grebes. Hence, none of the species affected by displacement from the wind farms seemed also to be significantly affected by shipping.

Due to the detailed oceanographic data included in the modelling framework the LUD seabird monitoring program has highlighted several hydrodynamic features in the surveyed area which are of importance to the distribution of seabirds. In particular, it should be noted that the zone of high frontal activity off the Dutch coast had a significant effect on the distribution of Common Gull, Black-headed Gull, Lesser Black-backed Gull, Herring Gull, Great Black-backed Gull and Common Guillemot.

The T3 surveys also resulted in a total of 116 sightings of marine mammals, of which the majority (91) were harbour porpoise *Phocoena phocoena*, which were recorded in the whole area, including inside PAWP and LUD (Figure 5.57).

Table 0. Summary of species-specific responses to the LUD, PAWP and OWEZ wind farm footprints, significant displacement/attraction or no significant impact. Brackets mark responses which may not only be related to the wind farm but also to large-scale changes in environmental conditions. Significance of both model parts are given as *p* values for each wind farm (presence-absence/positive model part), ns = not significant. Significant responses to the wind farms are marked in bold letters. In the last column the results of a review of displacement patterns from several wind farms presented in Welcker & Nehls 2016 are given for comparison with other studies.

Species	LUD	PAWP	OWEZ	General review (Welcker & Nehls 2016)
Divers	Out of range (not included)	Out of range (not included)	(Displacement), <0.001/-	10/10 displacement
Great Crested Grebe	Out of range (not included)	Out of range (not included)	(<0.05 /ns)	-
Northern Gannet	Displacement 0.001 /ns	Displacement <0.001 /ns	Displacement <0.001 /ns	8/10 displacement
Great Cormorant	Attraction <0.001 /ns	Attraction <0.001 /ns	Attraction <0.001/<0.001	-
Little Gull	(not included)	(not included)	(Displacement) <0.01 /ns	5/8 displacement
Black-headed Gull	(Displacement) <0.001 /ns	No sig. impact ns/ns	No sig. impact ns/ns	-
Common Gull	(Attraction) ns/ <0.05	No sig. impact ns/ns	No sig. impact ns/ns	5/6 no displacement
Lesser Black-backed Gull	Displacement <0.01 /ns	No sig. impact ns/ns	No sig. impact ns/ns	5/8 no displacement
Herring Gull	(Attraction) <0.05 /ns	(Attraction) <0.05 /ns	No sig. impact ns/ns	6/8 no displacement
Greater Black-backed Gull	Attraction <0.05 /ns	Attraction <0.01 /ns	No sig. impact ns/ns	5/7 no displacement, 2 attractions
Black-legged Kittiwake	No sig. impact ns/ns	Displacement 0.01/<0.05	No sig. impact ns/ns	5/7 no displacement
Common Guillemot	Displacement <0.001/<0.05	Displacement <0.001/<0.001	Displacement <0.001 /ns	9/11 displacement (Alcids pooled)
Razorbill	Displacement <0.05 /ns	Displacement <0.01 /ns	No sig. impact ns/ns	9/11 displacement (Alcids pooled)

3 Introduction

Construction of the Offshore Wind Farm Eneco Luchterduinen (LUD) started in 2014, and the 129 MW (43 turbines) were fully operational by summer 2015. The wind farm covers an area of 16 km². The location for the LUD is 17 km south of the existing Prinses Amaliawindpark (PAWP), roughly 23km off the coast of IJmuiden in block Q10 of the Netherlands Continental Shelf (NCS) in the Dutch Exclusive Economic Zone (EEZ). The water depth at this location ranges between 19 m and 24 m relative to LAT. The water depth and composition of the sediment underground allow for steel mono-piles to be used in conjunction with the preferred wind turbine generator (WTG) type which, under these circumstances, is the most cost effective solution. At a water depth of 25 m the WTGs require mono-piles of 51.5 m in length, with a diameter between 4.2 and 4.6 m and a transition piece of 19.1 m in length with a diameter of 4.5 m. Pile penetration in the seabed is approximately 23 m. An offshore high voltage station (OHVS) collects the generated energy at all WTGs and transforms the voltage from MV level to HV level, suited for export to shore. The wind farm is connected to the 150 kV onshore substation in Sassenheim.

OWEZ was constructed between April and August 2006, while PAWP was constructed between October 2006 and June 2008. The two wind farms have very different designs; PAWP has a much higher turbine density than OWEZ (60/17km² [3.5 WTG·km⁻²] and 36/24 km² [1.5 WTG·km⁻²] resp.) and has been built in slightly deeper waters (19-24 m versus 18-20 m) and further offshore (ca 23 km versus ca 15 km) than OWEZ.

As part of the Wbr-permit application an ‘Environmental Impact Assessment’ (EIA) and an ‘Appropriate Assessment’ were carried out. The outcome of these studies resulted in the requirement by the Competent Authority for a ‘Monitoring and Evaluation Program’ (MEP). The MEP is undertaken in conjunction with and for approval by the Competent Authority. Currently the MEP consists of eleven monitoring topics, of which seabirds is one topic. LUD is obliged to carry out a 3-5 year monitoring program on seabirds. According to the license permit the objective of the Luchterduinen seabird monitoring program is to conduct the seabird monitoring program in a way that location specific and cumulative avoidance behaviour can be measured in LUD and the two existing offshore wind farms (OWEZ and PAWP). For this purpose, a ship-based line transect monitoring program of seabirds focusing on the winter season has been proposed by Clusius CV and approved by the Competent Authority. The program covers pre-construction (baseline), construction and post-construction phases. This report covers the results of the third year of post-construction monitoring with ship-based surveys (T-3) undertaken December 2017 and February 2018. The main aim of the report is to present the results of the T3 surveys and assess the displacement (including cumulative displacements) of seabirds from LUD, PAWP and OWEZ based all data collected in the post-construction studies of OWEZ and PAWP and both pre-and post-construction data from LUD.

Pelagic seabirds such as gannets, divers and alcids flying in the vicinity of offshore wind farms consistently show strong avoidance behaviour, with only a few exceptions (Krijgsveld 2014). Evaluations of the habitat displacement of seabirds from OWEZ and PAWP indicated strong avoidance of Northern Gannet and Common Guillemot (although they not fully avoided the wind farms). Other species showing significant avoidance behaviour were divers, Great Crested Grebe, Little Gull, Lesser Black-backed Gull, Black-legged Kittiwake and Razorbill (Leopold et al. 2013). The lay-out of the wind farms seemed to be an important factor, as the widely distributed birds avoided PAWP to a larger degree than the more widely spaced OWEZ (Leopold et al. 2013), which also partly could be due to distance from coast and differences in environmental factors related to this.

4 Materials and methods

4.1 Monitoring approach

The TORs for the seabird monitoring were to study the distribution and abundance of seabirds in the region of the three wind farms before, during and after construction of the LUD wind farm. After the post-construction surveys, the results were evaluated to determine to what extent the behavioural responses of species of seabirds had been determined, and whether the ship-based surveys could be curtailed. The collected data should be used to assess the avoidance behaviour of seabirds both in relation to the LUD wind farm and as a secondary priority cumulatively to the LUD, OWEZ and PAWP wind farms. The study should be undertaken using three sets of four NE-SW oriented transects traversing the three wind farms. Each of the proposed transects measures approximately 20 km. Results of the monitoring of habitat displacement of seabirds and waterbirds at other offshore wind farms have strongly indicated displacements to a distance of 1-2 kilometers (Petersen et al. 2006, Skov et al. 2012, Welcker & Nehls (2016)). Hence, the use of relatively short transect lines in the three wind farms was suitable for detecting gradients in abundance (densities) within a relatively well-defined area around each of the wind farms. Thus, the design allowed to detect changes in densities between pre- and post-construction periods which can be attributed to ecological habitats (by integration of hydrodynamic data), shipping activity (by integration of AIS data) and the presence of the wind farms (Skov et al. 2015). This meant that the degree of habitat displacement from all three wind farms could be tested statistically by gradient analysis.

In addition to the three series of four 20 km long primary transects through each of the LUD, OWEZ and PAWP wind farms, the monitoring approach included a number of 30-40 km long secondary transects running east-west through the entire survey region. As habitat displacement of seabirds from offshore wind farms is typically small-scaled, this survey design provided a good basis for determining to what degree the different species of seabirds are impacted by habitat displacement, which could be determined by testing for changes in densities at increasing distances from the wind farms. The design parameters of the three wind farms are provided in Table 1.

Table 1. Design parameters for LUD, OWEZ and PAWP wind farms.

Design parameter	LUD	OWEZ	PAWP
Capacity	129 MW	108 MW	120 MW
Total turbine height	137 m	115 m	99 m
Rotor diameter	112 m	90 m	80 m
Height of lowest tip of rotor	25 m	25 m	19 m
Height of nacelle	81 m	70 m	59 m
Number of turbines	43	36	60
Number of turbines per km ²	2.69	1.50	3.53
Minimum distance to shore	24 km	10 km	22 km
Minimum water depth	20.7 m	17.1 m	20.8 m

4.2 Survey design and available data

The survey design is shown in Figure 4.1, showing the three series of four dense primary transects through LUD, OWEZ and PAWP designed to detect habitat displacement and the coarse set of secondary transects covering a larger region surrounding the three wind farms designed to describe distributions over a wider region. Between LUD and PAWP-OWEZ the shipping lane to/from IJmuiden is located. Two anchoring sites are associated with the shipping lane. The study area extends from about 52°30'N (Noordwijk) to about 52°45'N (Hondsbosse Zeewering) and from the shore to circa 18 nm out to sea. The size of the study area is circa 725 km². The primary transects are oriented NE-SW to capture the expected density gradient in seabirds, whereas the secondary transects are largely perpendicular to the main physical and ecological parameters, such as distance from the coast, water depth, temperature and salinity.

Four surveys in winter 2017-2018 were undertaken following the construction of the LUD wind farm. The survey strategy has been to cover primary transects during all surveys, and as many of the secondary transects as possible. The primary transects were surveyed first, and surveying of the secondary transects was only initiated once the primary transects had been surveyed. The primary transects measure 209 km (+ 11 km transit) which can be covered in 12-14 hours of survey time. The secondary transects measure 660 km (+ 48 km transits). It was the strategy to achieve as much coverage as possible in the coastal and offshore environment surrounding the Luchterduinen survey area. The coverage of the secondary transects was therefore designed to achieve as much survey effort as possible on the secondary transects in the southern part of the survey region.

When crossing the three wind farms a safety distance of 250 m was kept to the turbines. During crossing of the shipping lane a minimum distance of 1000 m was maintained to all vessels in the shipping lane.

Surveys were initiated only on the basis of a forecasted weather window (less than Beaufort 5, good visibility (≥ 2 km), no heavy precipitation) of at least 2 days. Surveys should only be undertaken during sea states less than or equal to 4 and visibility of 2 km or more. Cancellation of a survey would only take place in situations with adverse weather conditions in relation to surveying (sea state above 4, visibility < 2 km) extending beyond the 5 day period of a survey.

By including the T1 data from OWEZ and PAWP (Leopold et al. 2013) data from 13 additional surveys could be included in the analyses of bird distributions, which adds up to a total of 27 surveys (Table 2). In the analyses the OWEZ and PAWP T1 survey data were treated as part of the LUD baseline. The surveys during construction were not included in the analyses.

Table 2. List of 27 available surveys included in the analyses of seabird displacement from LUD. Survey No indicate the factor levels used in the statistical analyses (Appendix A).

Year	Survey dates	Survey No.	Reference
2007	5-6/11 and 20-24/11	4	PAWP/OWEZ T1
2008	14-18/1 and 3-7/11	5, 6	PAWP/OWEZ T1
2009	19-22/1, 5-9/10 and 2-6/11	7, 8, 9	PAWP/OWEZ T1
2010	18-22/1 and 22-26/2	10, 11	PAWP/OWEZ T1
2011	3-7/10 and 31/10-4/11	12, 13	PAWP/OWEZ T1
2012	9-13/1 and 20-23/2	14, 15	PAWP/OWEZ T1
2013	18-22/10	16	LUD T0
2014	10-14/1 and 19-23/1	17, 18	LUD T0
2015	19-23/10 and 13-17/12	21, 22	LUD T1
2016	11-16/2 and 4-8/3 30/10 – 3/11 and 3-7/12	23 ,24, 25, 26	LUD T1 LUD T2
2017	16-20/1 and 6-10/3 20-23/12	27, 28 29	LUD T2 LUD T3
2018	16-23/2 25-28/2	29, 30, 31	LUD T3 LUD T3

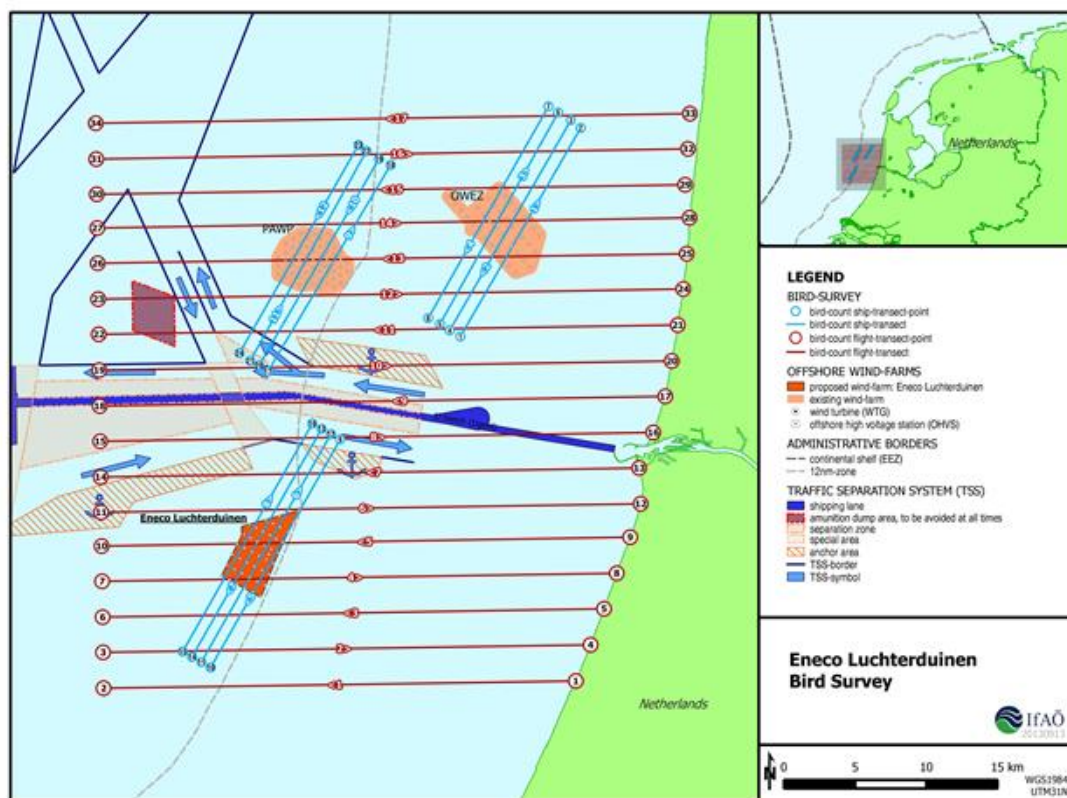


Figure 4.1. Primary (blue) and secondary (red) transects with indications of Luchterduinen, Prinses Amalia and Egmond aan Zee wind farms indicated.

4.3 Seabird counting techniques

Seabirds were recorded according to the method for surveying seabirds from ship by means of the strip-transect method as suggested by Tasker et al. 1984, Camphuysen et al. 2004 and Leopold et al. 2004, and implemented as a standard by the European Seabirds at Sea Database (ESASD). As the search mode used during previous surveys for OWEZ and PAWP was ‘naked-eye’ (Leopold et al. 2013) this mode was also used during the monitoring of seabirds for LUD. The observation height was between 6.5 and 10 m above sea level. The method is a modified strip transect with a width of 300 meter, and five perpendicular distance sub-bands:

- A. 0-50 m;
- B. 50-100 m;
- C. 100-200 m;
- D. 200 – 300 m;
- E. \geq 300 m.

Transect lines were broken up into 1 minute (time) stretches and birds seen “in transect” in each individual 1 minute count were pooled (from $t=0$ to $t=1$ mins and for portside and starboard). At $t=1$ mins, the next count commenced, from $t=1$ mins to $t=2$ mins, etc. Densities were calculated as numbers seen in transect, divided by area surveyed. Area surveyed is the segment length covered in that particular 1 minute period, depending on sailing speed (average 9 knots) and strip width (300 m), which were both continuously monitored, corrected for the proportion of birds that were missed by the observers (see next section: distance sampling). The location of each count was taken as the mid-position between the positions at $t=0$ and $t=1$ mins, for each count, on the ship’s transect line.

Birds were counted from the roof of the survey ship by four bird observers (Table 3), two on each side of the ship (Figure 4.2). Swimming seabirds were counted on both sides of the ship, and snap-shot counts of flying birds were made whereby every minute all birds were counted within an area of 300 by 300 m transverse and directly in front of the ship (Figure 4.3). Two vessels were used during the T3 surveys. The Ivero was used during the first survey in December 2017. As the Ivero was not available in 2018 the Coastal Chariot (Acta Marine) was used during the surveys in February 2018.



Figure 4.2. The 'Ivero' above and 'Coastal Chariot' below used as the survey ships.

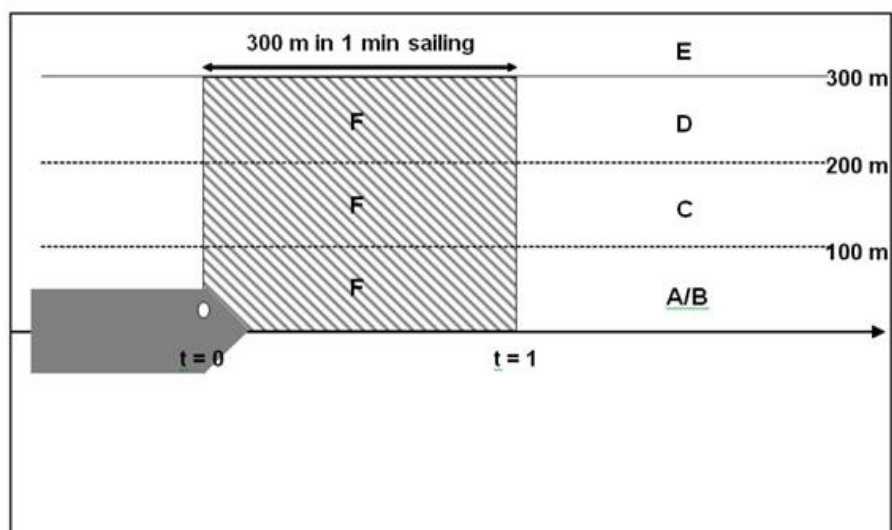


Figure 4.3. Schematic overview of the seabird survey method (see above for definitions of bands A-E).

Table 3. List of observers engaged in the LUD-T3 seabird surveys.

Survey	Observers
LUD-3-01	Jörn Hartje*, Thomas Schubert, Troels Ortvad, Thomas W. Johansen
LUD-3-02	Jörn Hartje*, Thomas Schubert, Troels Ortvad, Thomas W. Johansen
LUD-3-03	Jörn Hartje*, Thomas Schubert, Troels Ortvad, Thomas W. Johansen

*Cruise leader

4.4 Quality control and post-processing of survey data

General quality assurance and management were conducted and documented in accordance with internationally accepted principles for quality and environmental management as described in the DS/EN ISO 9001 standard. Post-processing of the survey data followed Leopold et al. (2013).

Before and after every survey an equipment check was carried out following an approved checklist. On the ship all routines followed strictly briefing rules with the party chief as outlined in the Work Method Statement. All observations of seabirds, marine mammals and ships were recorded on sheets and the ship's position and speed in a GPS. After each survey the GPS-track was downloaded to a computer and checked for completeness. As soon as possible after the survey the sheets were transcribed by one of the observers directly into a special developed database. Unusual data were marked and commented and the observers were asked for clarification or confirmation if needed. This procedure is very important to get rid of erroneous data as soon as possible. Later on, the data sets were run through different automated routines to detect mistyping and other errors.

All observations and GPS positions were stored in a special SQL geo-database (FULMAR) held by IfAÖ for aerial and ship-based surveys, which is linked to ArcGIS, and which exports the results to a Microsoft Access® database. The post-processing chain starts by transcribing the general survey metadata (e.g. date, observer, observation height etc.) from the observation sheets into the database. The next step is to import the GPS-track into the database by using a special extension for ArcGIS, which is started by the database. In ArcGIS the whole track is shown. The start and end points of each transect line are marked and then the track points with their position and time are imported into the database. The user of the database can now view track points, time and the columns for the sightings. Every observation will be sorted by time to the nearest 1 minute count period. Also the weather conditions which are monitored continuously during the survey are stored into the database during this step.

After finishing the data input, different tools are used to visualize the observed seabirds along the transect lines. The next step was the validation of the data by a senior biologist, who also checked the weather conditions along all the transect lines on each side of the ship according to sea state, glare and visibility. If the observations of parts of the lines are affected by strong glare, sea state over Bft 4 or poor visibility, he marks that period as "invalid". After the evaluation, and if necessary by additional confirmation of the observer, the data will be exported to a report-file, which is a Microsoft Access® database file. Here, all common types of results are generated by queries. Two tools are generating the export files for ArcGIS and population estimation in Distance.

4.5 Distance analysis

The term 'Distance analysis' used in this report refers to analyses following standard distance sampling techniques (Buckland et al. 2001) conducted using the Distance package in R (<https://cran.r-project.org/web/packages/Distance>). These analyses were conducted to calculate distance detection functions for swimming seabirds. Sitting seabirds like auks or divers may be difficult to detect in the outer distance bands (farther away from the ship) and may also respond to the approaching survey vessel, and hence the collected densities of sitting seabirds are biased. As flying seabirds are comparatively easy to

detect the collected densities of flying seabirds have been treated as unbiased, and no distance correction was applied. Flying birds were included (uncorrected) for Divers, Northern Gannet, Common Guillemot and Razorbill. In the distance analysis all birds are assumed to be detected in the distance band closest to the ship, further away detectability decreases with increasing distance from the ship. A set of different detection function models were fitted. Half normal, hazard rate and uniform detection functions were fitted and Cosine adjustment terms were added to the models as well as Hermite polynomials (for Half-normal detection function) and simple polynomial (for the hazard rate detection function). Bird abundance and sea state were available as covariates in the models. Finally the best fitting function was chosen on the basis of the smallest Akaike Information Criterion (AIC) values (Burnham and Anderson 2002).

Detection functions were calculated for the entire dataset (dedicated project surveys) for each species with sufficient number of observations, assuming that detectability of bird species was similar among surveys. Estimated detection functions were used to estimate species-specific effective strip widths (ESW), which represent the width within which the expected number of detected seabirds would be the same as the numbers actually detected within the full width of 300 m (Buckland et al. 2001). Correction factors were then calculated by $1/(ESW/300)$. In line with Leopold et al. (2013), seabird species were pooled into species groups before Distance analysis (Table 5). The abundance of each species in each segment was thereafter corrected using the correction factor. The corrected abundance was merged with the effort data and species-specific densities (birds/km²) were calculated. The data was finally re-segmented (mean density) into approximately 1 km segments, to resemble the historic data resolution. Distance correction of the historic data was done using the corrections factors (and method) reported by Leopold et al. (2013). The historic and dedicated survey data was finally merged and used in species distribution modelling.

Table 4. Grouping of species for distance analysis.

Group	Species
Divers	Red-throated Diver (<i>Gavia stellata</i>)
Divers	Black-throated Diver (<i>Gavia arctica</i>)
Gannets	Northern Gannet (<i>Morus bassanus</i>)
Cormorants	Great Cormorant (<i>Phalacrocorax carbo</i>)
Small gulls	Little Gull (<i>Hydrocoloeus minutus</i>)
Small gulls	Black-headed Gull (<i>Chroicocephalus ridibundus</i>)
Small gulls	Common Gull (<i>Larus canus</i>)
Small gulls	Black-legged Kittiwake (<i>Rissa tridactyla</i>)
Large gulls	Herring Gull (<i>Larus argentatus</i>)
Large gulls	Lesser Black-backed Gull (<i>Larus fuscus</i>)
Large gulls	Great Black-backed Gull (<i>Larus marinus</i>)
Auks	Common Guillemot (<i>Uria aalge</i>)
Auks	Razorbill (<i>Alca torda</i>)

4.6 Distribution models

For the assessment of potential displacement from LUD and cumulative displacement with PAWP and OWEZ, fine-scale distribution models capable of describing the distribution during the LUD post-construction period were developed in line with the baseline models (Skov et al. 2015). To enhance the power of detecting a displacement in a highly variable environment it is important to include the factors causing the large variability and account for any unexplained spatial autocorrelation (Perez-Lapena 2010).

In one survey seabirds might be in a specific location due to suitable oceanographic conditions which enhance the availability of prey fish. In another survey the condition might be unsuitable and the seabirds therefore absent. If this location happens to be the wind farm it can be difficult to assess a displacement effect if the important factors driving the distribution are not included. In order to assess the impact of LUD (in terms of statistically significant displacement) and map the survey-specific distribution of seabirds during the LUD-T3 winter of 2017-2018, prediction models were therefore applied taking both static (depth treated as static) and dynamic habitat conditions (salinity, current speed, eddy potential, current gradient and water depth) as well as pressures (location of the wind farms and shipping intensity AIS) into account. AIS counts of ships were analysed by MARIN www.marin.nl by aggregating the number of ships entering a grid cell of 1000 by 1000 meter over the course of each of the 26 survey periods (see Table 1). A factor variable with each survey as a level was also included as a fixed factor, enabling survey specific predictions and simulations.

The hydrodynamic variables (fixed factors) salinity, current speed, eddy potential (vorticity) and current gradient were added to the survey data as mean values during each survey period (whole days), together with water depth and wind farm footprints and 2 km buffer around the wind farms as factor levels (for each wind farm compared to the area outside, i.e. 7 levels in total). In the baseline and T1 report a distance to wind farms truncated at 4 km was used however as there is a potential problem with collinearity with separate distance variables for each wind farm we changed the response variable to a factor variable in the analyses. The environmental variables are mapped in Figure 4.4 for the four surveys during LUD-T3. Data from 2007 until 2018 were included and the two surveys conducted during construction (October 2014 and December 2014) were excluded from the species-specific models, so in total 27 surveys were included. Surveys with no-records (or only 1-2 records) of the model species were also dropped, if any. Generalized additive mixed models (GAMMs) were used as these are capable of fitting different family distributions and nonlinear responses (Hastie & Tibshirani 1990), which are expected between seabirds and habitat variables. The mixed models can also account for potential temporal and spatial autocorrelation in model residuals. To account for zero inflation a two-step model (hurdle model) was fitted consisting of a presence-absence model and a positive model part (densities) where all zeroes were excluded.

The autocorrelation was accounted for by adding a correlation structure (corAR1 or corARMA), grouped by survey hour (in accordance with Leopold et al. 2013), to account for the temporal and spatial autocorrelation. The “`gamm`” function in “`mgcv`” (Wood 2006) R package (R Development Core Team 2004) was used for fitting the models. The species-specific models were fitted in a stepwise manner, an initial full model was first fitted including all environmental variables and further simplified by dropping uninfluential variables in a stepwise manner. Variables displaying ecologically unrealistic shapes (for example if divers would show a preference for high shipping intensity, or grebes would prefer very deep water response that we know from experience is wrong) were also dropped. The wind farm factor variable were always retained in the model, being significant or not. The model residuals were checked for autocorrelation using a correlogram. The models were evaluated for predictive accuracy by fitting the model on 70% or 80% of the data (randomly selected) and predicted on the 30%/20% withheld data. However, many of the models do not converge on smaller sample sizes and for these models no evaluation results are shown. The presence-absence model part was tested using AUC and the combined density predictions using Spearman’s correlation coefficient.

The species-specific models were finally used for predicting the distribution of mean densities in the whole study area during a range of different surveys. The mean density of the 12 post construction (LUD) surveys were calculated and mapped together with eight pre-construction surveys. The change in density between these two periods was also mapped to illustrate potential predicted displacement or attraction.

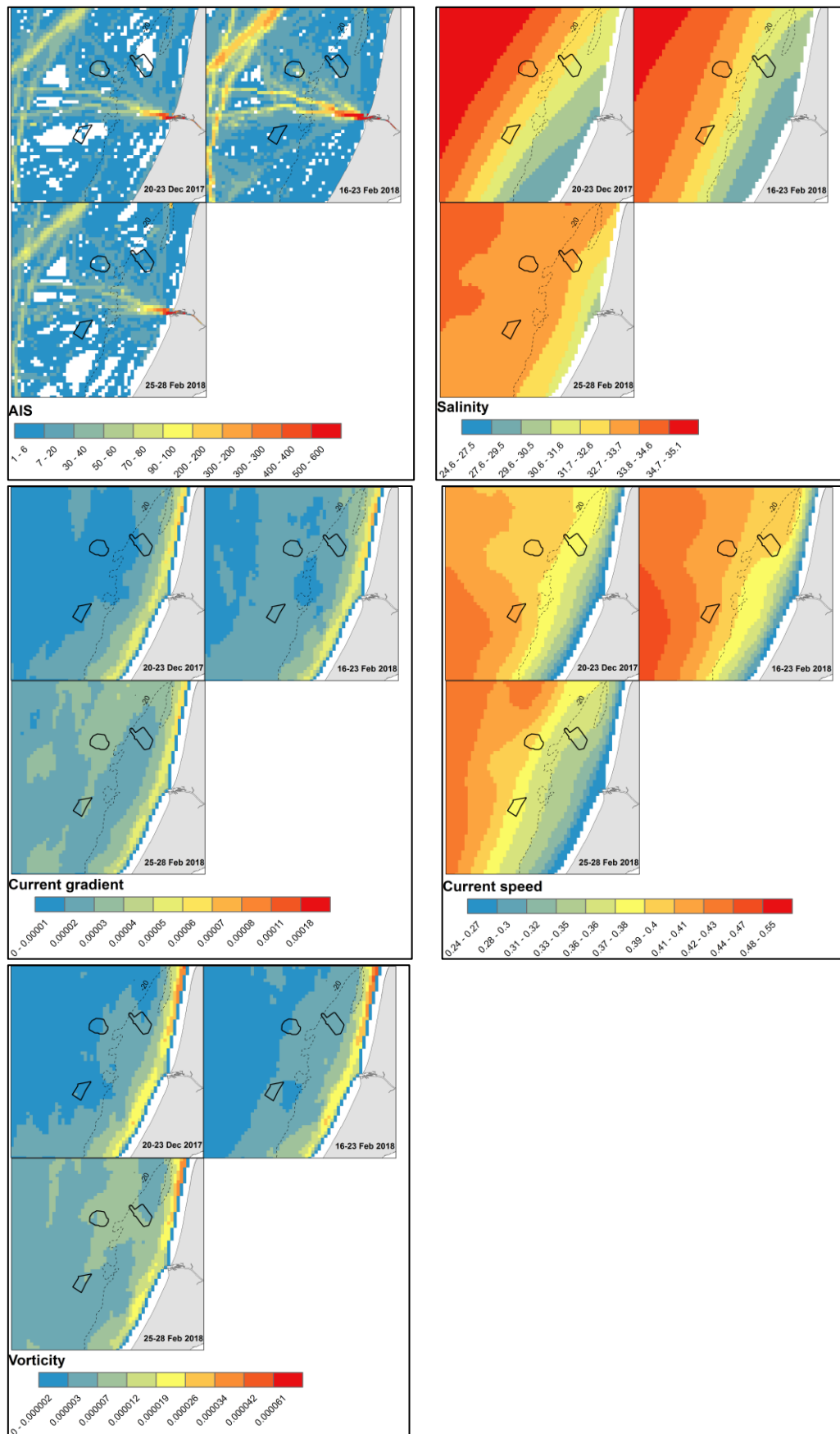


Figure 4.4. Environmental variables (mean values) for the four LUD-T3 surveys.

4.7 Analysis of displacement and number of included surveys

This report includes the results from the third and final year post-construction of LUD Seabird Monitoring Program of the analyses of displacement of seabirds at LUD and updated results for PAWP and OWEZ. The results from the analyses are reported in two main ways, an assessment of significance of the factor levels describing wind farm footprints and 2 km buffers (indicating a statistically significant displacement) and the difference in predicted densities pre- and post-construction for LUD. For key species the degree of displacement is also estimated.

4.8 Presentation of data

Maps showing observed densities and predicted mean distributions during the LUD-T3 surveys in the winter 2017-2018 have been produced in UTM 32N WGS84 projection. The observed densities are shown for segments (mid points) of approximately 1 km and the mean predicted density is presented for cells with a resolution of 1 km. The mean of model predictions from four LUD pre-construction surveys are also presented together with a map displaying the change between pre and post construction. Note, that the predictions are based on the statistical models and should be interpreted as model results together with model statistical outputs, see Appendix A. The three disturbance areas (LUD, PAWP, OWEZ) and the 20 m depth contour are indicated.

5 Results

5.1 Effort and sample sizes

Three surveys were undertaken during the 2017-2018 winter using the Ivero in December 2017 and Coastal Chariot in February 2018. The first survey was conducted from 20th to 23rd of December 2017. Due to weather conditions the survey was not finalised before on the 17th of February 2018 when conditions improved following a long period dominated by strong cyclonic weather. The second survey was undertaken from 17th to 22nd of February 2018 and the third from 25th to 28th of February 2018. During the LUD-T3 surveys, the primary transects within PAWP, OWEZ and LUD were completed. Due to the prevailing conditions the majority of the secondary transects around LUD could only be completed during the second survey. An overview of the survey effort is given in Table 5 and Figure 5.1. Number of recorded seabirds during the T-3 surveys are listed in Table 6, and reflects to some extent the difference in survey effort between the three surveys. Relatively large numbers of Northern Gannets and Razorbills were observed during the T3-02 survey. During the T3-02 survey two European Shags were recorded – a rare species in the Netherlands and a first time for the LUD monitoring programme.

Table 5. Survey effort (km² covered by observation transect) obtained during the three ship-based surveys in the LUD-T3 winter season (2017-2018).

Period	Survey	Area covered (km ²)
LUD-T3-01	20-23/12 2017 and 17/2 2018	138.73
LUD-T3-02	16-23/2 2018	379.28
LUD-T3-03	25-28/2 2018	155.68

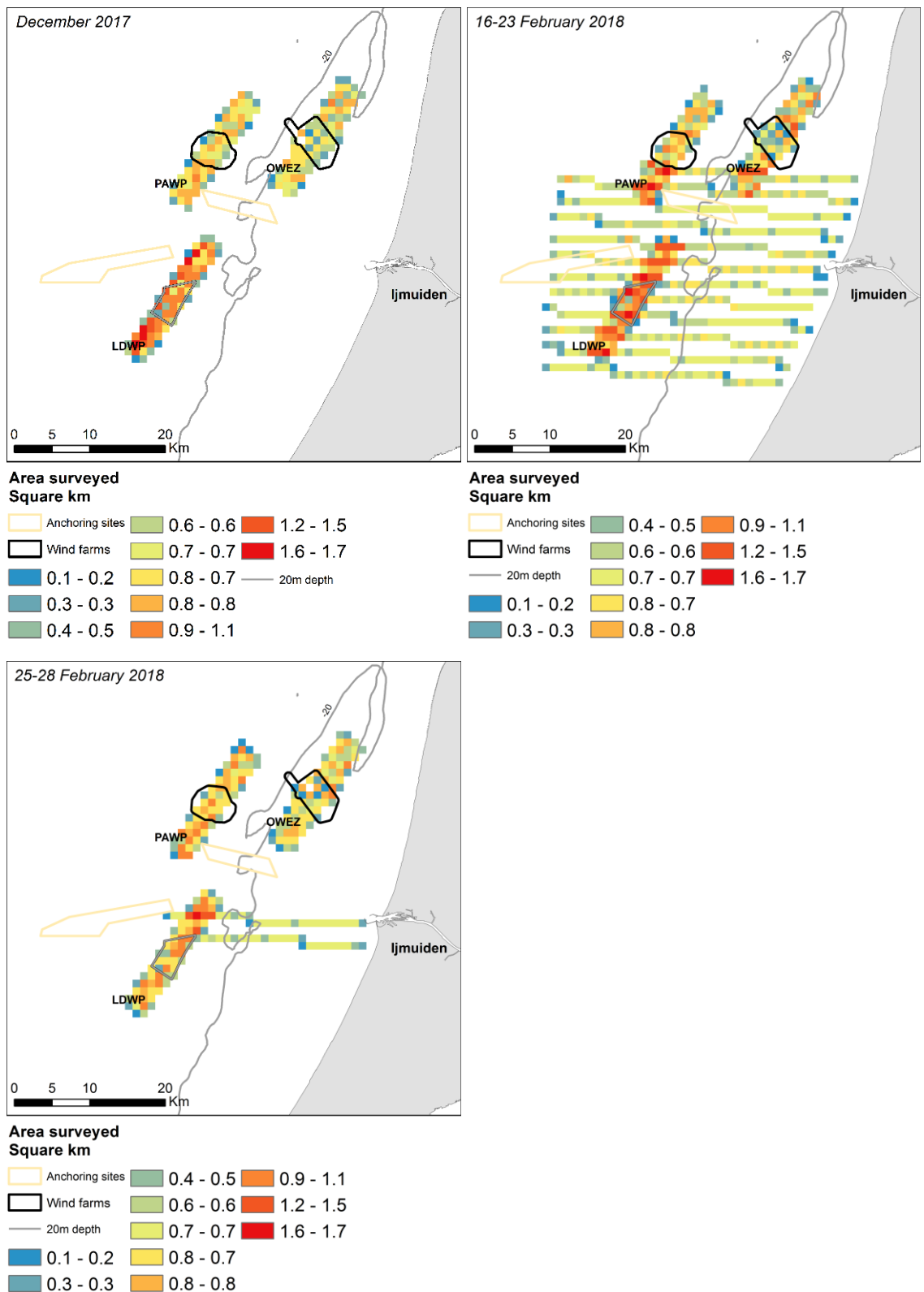


Figure 5.1. The spatial coverage of survey effort (km²) obtained during the three ship-based surveys in the LUD-T3 season (2017-2018).

Table 6. Numbers of seabirds observed during the four LUD-T3 surveys in winter 2017/2018.

Species	Total Dec 2017	Total Feb 2018-I	Total Feb 2018-II
Red-throated Diver	3	96	0
Red-Black-throated Diver	1	2	5
Great Crested Grebe	1	81	65
Northern Gannet	52	408	33
European Shag	0	2	0
Great Cormorant	159	290	206
Greylag Goose	3	2	0
Shelduck	0	1	0
Teal	0	7	0
Wigeon	0	29	0
Common Eider	0	1	0
Common Scoter	0	28	6
Red-breasted Merganser	0	3	0
Goosander	0	0	1
Dunlin	0	2	0
Lapwing	0	0	35
Curlew	0	1	0
Unid. wader sp.	0	20	0
Arctic Skua	1	0	0
Little Gull	1	69	4
Black-headed Gull	7	21	1
Common Gull	158	202	65
Lesser Black-backed Gull	72	141	5
Herring Gull	175	128	14
Great Black-backed Gull	75	189	3
Black-legged Kittiwake	401	152	16
Unid. Gull sp.	32	1347	0
Common Guillemot	982	909	242
Razorbill	122	576	12
Unidentified <i>Alcids</i>	3	198	48
Total	2248	4905	761

5.2 Distance analysis

Table 7 gives an overview of the selected models used for estimating detection of sitting birds with distance for the different species groups.

Table 7. Distance statistics for sitting birds in each species group.

Species group	Sample size	Key function*	Adjustment term	Effective strip width (ESW in m)	% CV ESW
Divers	81	HR	-	127	37.2
Grebes	213	HN	Cosine (2)	146	10.8
Gannets	236	HN	Cosine (2)	201	11.0
Cormorants	342	HN	-	300	5.5
Small gulls	994	HN	Cosine (2)	162	4.5
Large gulls	1068	Uniform	Cosine (1,2,3)	160	6.1
Auks	7898	HR	Cosine (2)	136	1.8

* HN=Half normal, HR= Hazard rate

5.3 Species accounts

In this chapter an account of the results of the analyses and modelling of the LUD-T3 data (together with T0, T1, T2 and the “historic” PAWP and OWEZ data) is given. For each species the description of the LUD-T3 status starts with a general introduction in which the results of the LUD-T3 surveys during the 2017-2018 winter are summarised. The results of the species-specific distribution models are given in a separate subsection called ‘model results’, based on all surveys.

5.3.1 Divers: Red-throated *Gavia stellata* and Black-throated Divers *Gavia arctica*

The LUD-T3 surveys showed similar distribution patterns to LUD baseline, T1 and T2 surveys with most of the overall few sightings done in the coastal zone shallower than 20 m, including the area to the east of LUD (Figure 5.2). Almost all birds were identified as Red-throated Diver. There is a large variability in mean density between surveys in the whole area as well as within the three wind farms as indicated by Figure 5.3 and 5.4.

Model results

Surveys with no or very few (sitting on water) diver sightings were not included in the analyses (Figure 5.3, Figure 5.4). The model did not “behave” properly when LUD and PAWP footprints were included in the model as factor levels and the reason is because these two areas are outside the general distribution range of the divers in the area. Therefore, only OWEZ was included as a factor level in the model, while the 2 km buffers for all three wind farms were included. The wind farms had no effect in the positive model part and were therefore dropped altogether. Probability of presence was significantly lower inside OWEZ and also within the 2 km buffer of all three wind farms. The results indicate that very few divers occur in areas of the wind farms, and those that do occur are displaced. An increasing probability of presence of divers was also explained by water depths lower than 20 m, where the water is less saline and the mean current speed lower and shipping intensity is low. Increasing density (when present) was further explained by decreasing current speed and low shipping intensity (Appendix A). All responses indicate a preference for coastal waters, which is also apparent from the predictions (Figure 5.5). The model had a good predictive ability with an AUC value of 0.87, indicating the model is good at distinguishing between presence and

absence. The Spearman's correlation between observed and predicted was also fair with a value of 0.41 (Appendix A). The predicted distributions indicate a general reduction in the density of divers in the coastal zone when the mean of post-construction surveys were compared against the mean of (LUD) pre-construction surveys (Figure 5.5). The general reduction, however, is most likely unrelated to the wind farms.

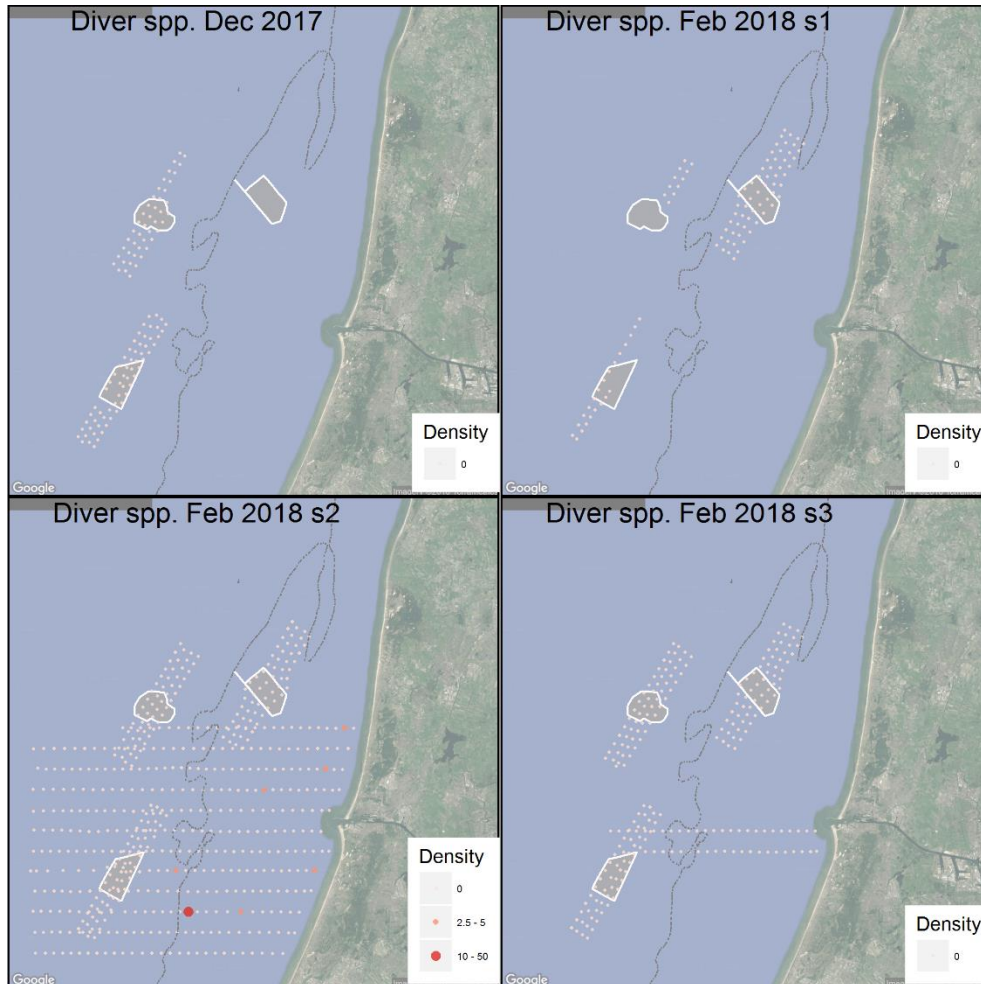


Figure 5.2. Observed density (birds/km²) of Diver sp. during LUD-T3 surveys 2017-2018. Densities have been corrected for distance bias.

Diver sp, 2002-2018

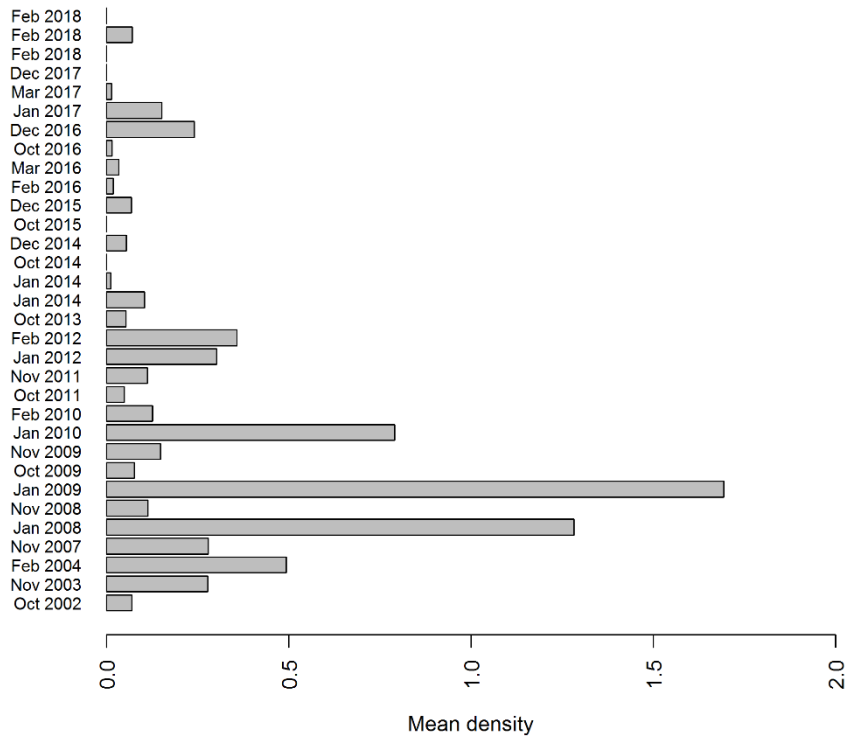


Figure 5.3. Mean observed density (birds/km²) of Diver sp. in the entire surveyed area during OWEZ, PAWP and LUD pre- and post-construction surveys. Densities have been corrected for distance bias.

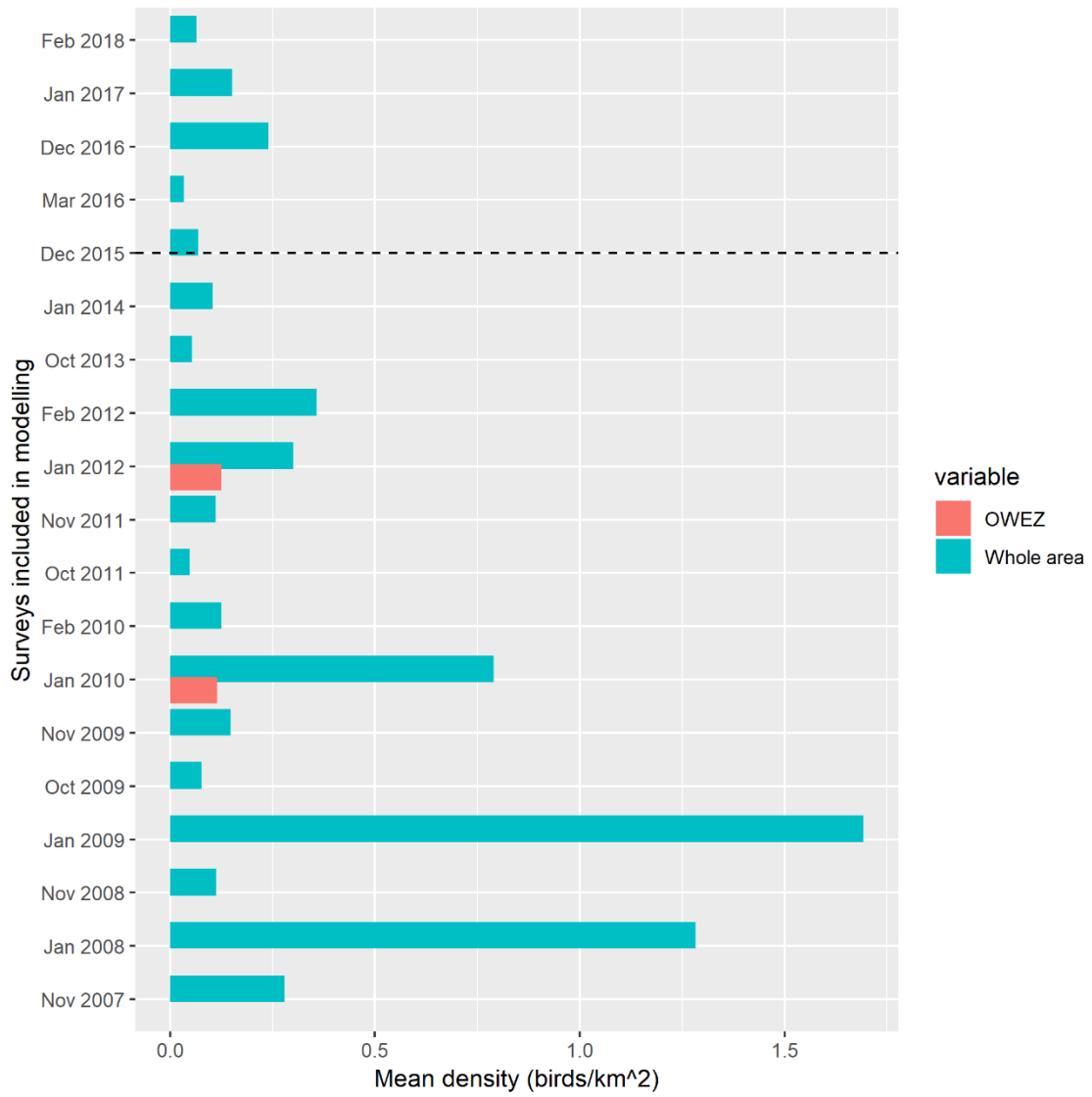


Figure 5.4. Mean density of Diver species during surveys included in the modelling. The mean density within the OWEZ footprint is shown as well as the mean in the whole surveyed area (including wind farms).

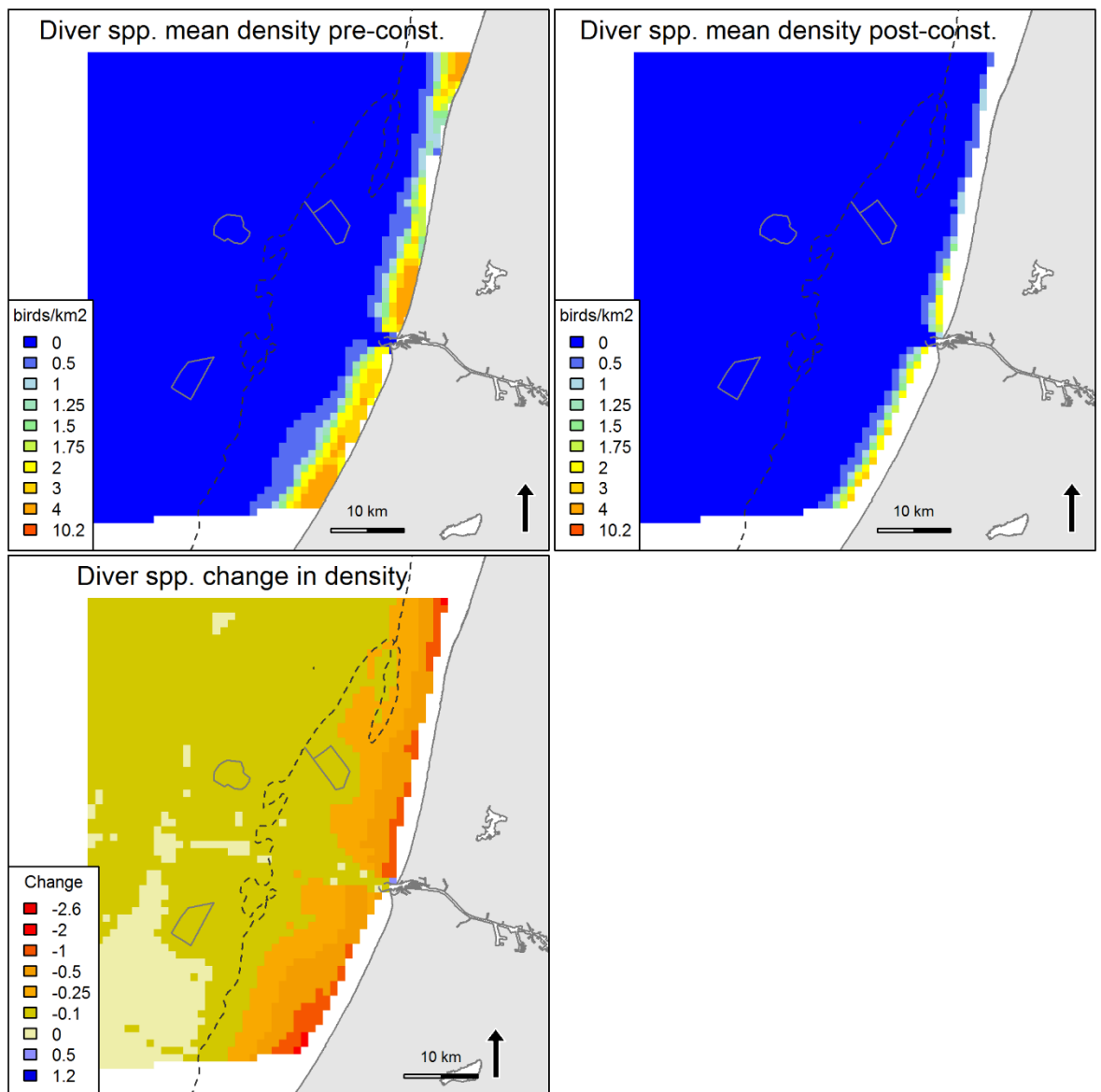


Figure 5.5. Predicted mean density (birds/km²) and distribution of wintering Diver sp. during four LUD pre- and four LUD post-construction surveys, and the relative change in predicted density between the two periods. Note that all included surveys are OWEZ and PAWP post-construction surveys.

5.3.2 Great Crested Grebe *Podiceps cristatus*

In the LUD seabird monitoring programme Great Crested Grebes have only been recorded in the near-coastal zone during mid-winter. During the T-3 surveys one bird was recorded just outside OWEZ during the T3-01 survey (second leg in February 2018, (Figure 5.7). There is a large variability in mean density between surveys in the whole area as well as within OWEZas indicated by Figure 5.37 and 5.8.

Model results

Surveys with no or very few (sitting on water) grebe sightings were not included in the analyses. As for divers only OWEZ footprint was included in the model together. PAWP and LUD was not included because they were outside the distribution range of the species in the region. The probability of presence was significantly lower in the OWEZ footprint ($p < 0.05$) indicating a displacement although also the OWEZ wind farm is outside the range of the general grebe distribution in the area (Figure 5.9). Further, depths between 10 and 15 m, low salinity, low mean current speed and low shipping intensity were included in the

presence-absence model part and had a significant influence on the distribution of grebes. Decreasing water depth and salinity were important in the positive part (Appendix A). The responses describes the preference of Great Crested Grebe for coastal waters (9). The split-sample evaluation model did not converge, however the explanation degree of the presence absence model was fair while very low for the positive part (Appendix A). The predicted distributions indicate a general reduction in Great Crested Grebe density in the coastal zone when the mean of post-(LUD)-construction surveys were compared against the mean pre-(LUD)-construction surveys (Figure 5-9), - a reduction which however, is clearly unrelated to the wind farms.

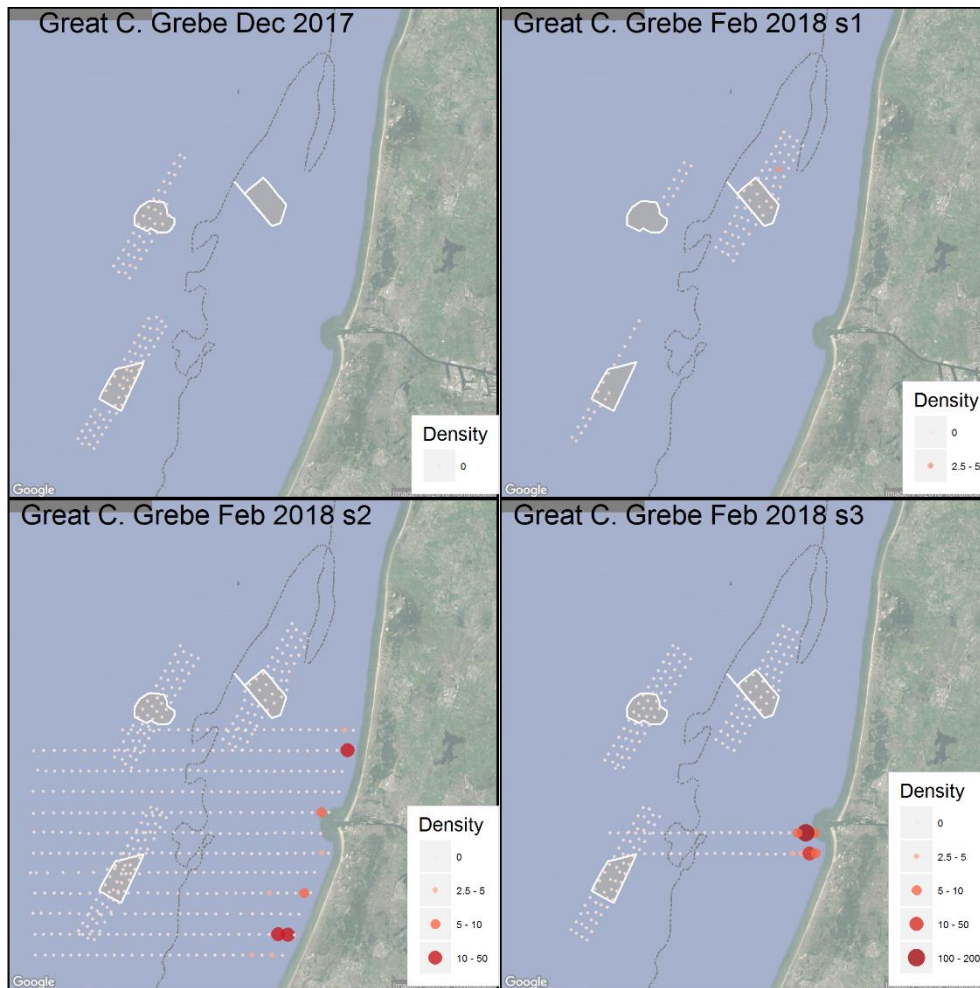


Figure 5.6. Observed density (birds/km²) of Great Crested Grebe during LUD-T3 surveys 2017-2018. Densities have been corrected for distance bias.

Great Crested Grebe, 2002-2018

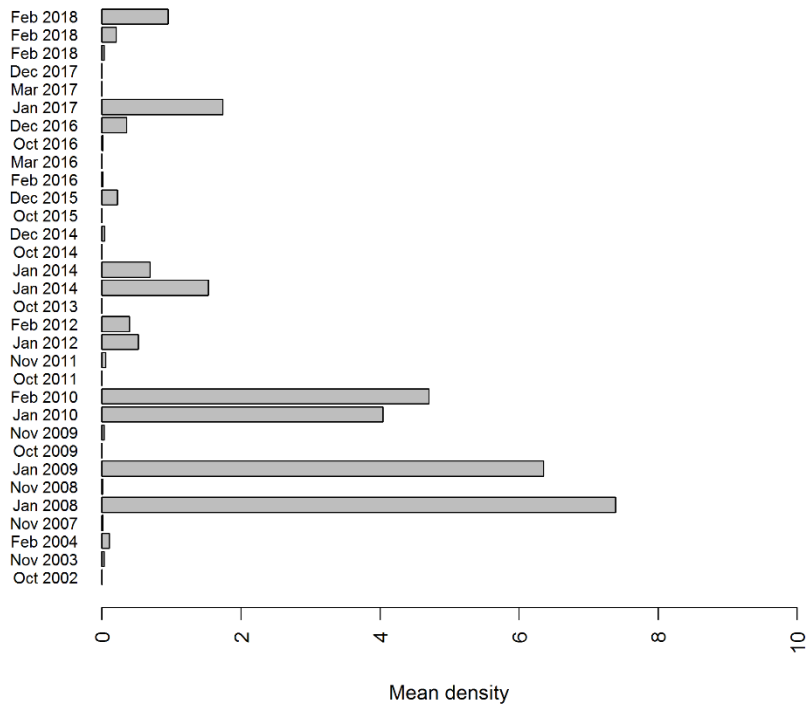


Figure 5.7. Mean observed density (birds/km²) of Great Crested Grebe in the entire surveyed area during OWEZ, PAWP and LUD pre- and post-construction surveys. Densities have been corrected for distance bias.

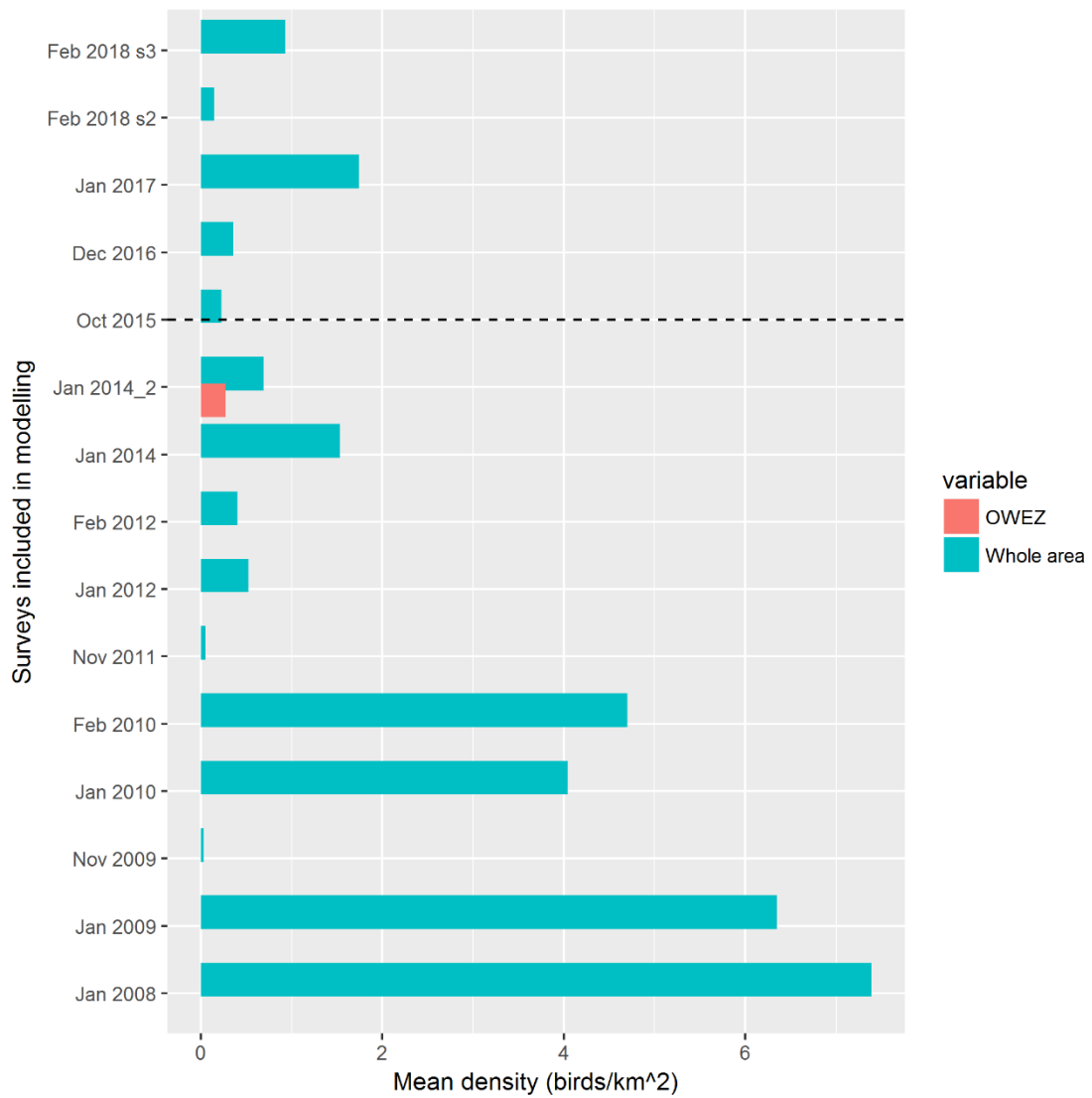


Figure 5.8. Mean density of Great Crested Grebe species during surveys included in the modelling. The mean density within the OWEZ footprint is shown as well as the mean in the whole surveyed area (including wind farms). Surveys above the dashed line are LUD post-construction surveys.

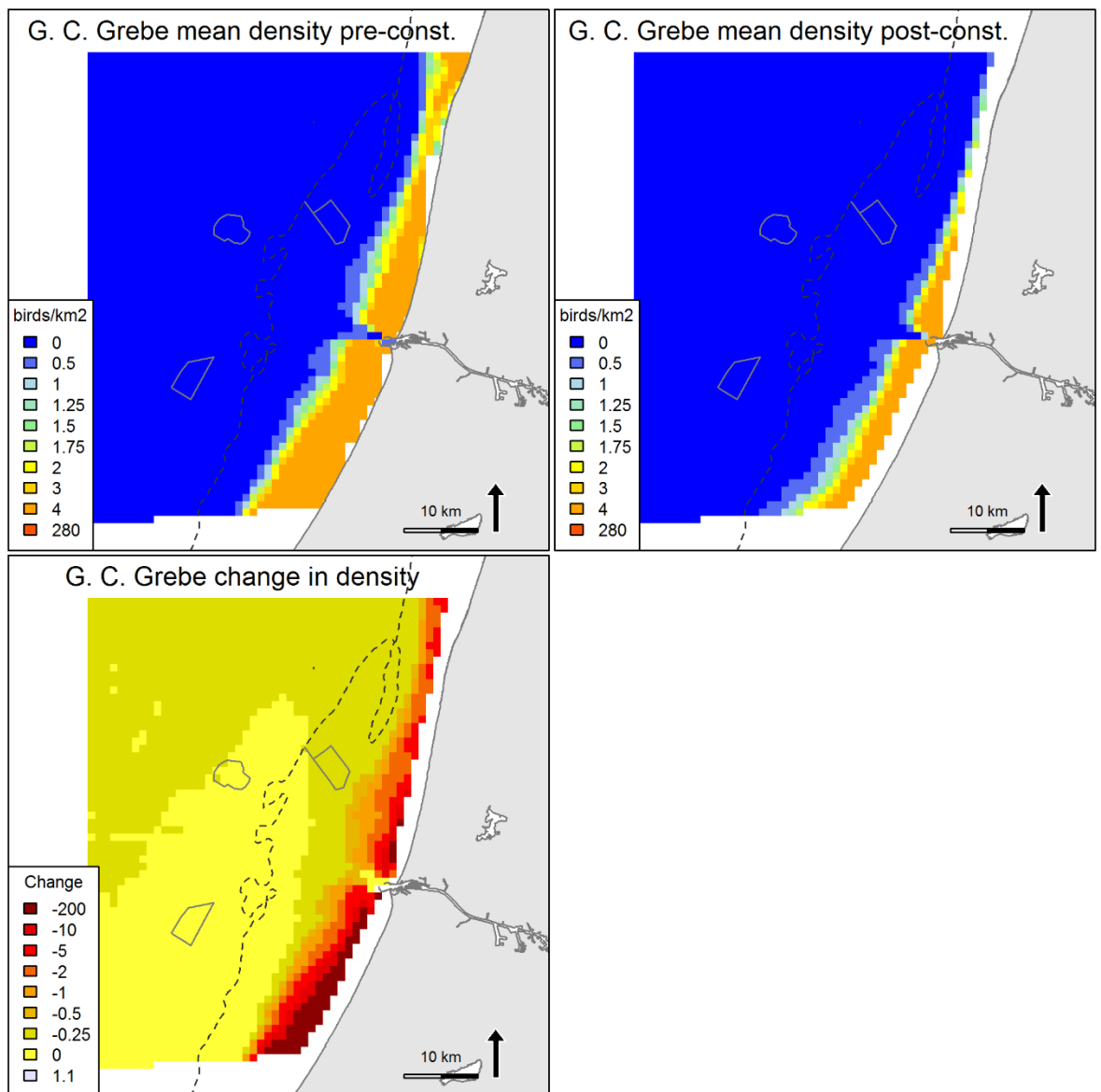


Figure 5.9. Predicted mean density (birds/km²) and distribution of wintering Great Crested Grebe during three LUD pre- and three LUD post-construction surveys, and the relative change in predicted density between the two periods. Note that all included surveys are OWEZ and PAWP post-construction surveys.

5.3.3 Northern Gannet *Morus bassanus*

During the LUD-T3 surveys the highest numbers of Gannets were recorded during the T3-02 survey in the offshore area between LUD and PAWP. Most Gannets were observed outside the wind farms, and only a few records inside LUD and PAWP during T3-02 indicating a potential displacement (Figure 5.10). A marked variation is apparent in the recorded densities of Gannet between the 32 surveys conducted (Figure 5.11) of which 27 were included in the distribution modelling (Figure 5.12). There is also a large variation in observed mean densities inside the wind farm footprints, however in most surveys the mean density is clearly lower than the average in the whole area or no Gannets were recorded at all inside the footprints (Figure 5.12). According to the results in the T1 report (Skov et al 2016) the Gannet did not seem to prefer the LUD footprint even before construction when comparing mean density within the wind farms with three buffers outside the wind farm.

Model results

The modelling results indicated that the Northern Gannets preferred saline and deeper North Sea water masses with lower mean current speeds. The Northern Gannet avoided all three wind farm footprints ($p < 0.01$) and the probability of presence was also significantly lower in a 2 km buffer around OWEZ wind farm (Appendix A). The explanation degree of the distribution model for the Northern Gannet was poor for the positive part, whereas the explanation degree was fair for the presence-part of the model (Appendix A). The AUC indicated that the presence-absence model part had a quite good predictive ability (i.e. the model is good at discriminating between presence and absence) while the Spearman's correlation coefficient indicated that the model is rather poor at explaining and predicting accurate density patterns (Appendix A).

The predicted patterns described a general increasing density in the North Sea water mass while there seem to be lower densities in the coastal water mass from 8 pre-construction to 12 post construction surveys. The significant displacement from LUD is clear from the predicted densities when comparing LUD pre-construction vs. post-construction (Figure 5.13). When evaluating predictions, by predicting on model input data with and without the response of the wind farm the results indicate that there is in average a 54% decrease in probability of detecting a Gannet inside the LUD wind farm, in comparison to a case without a wind farm. When both model parts are combined there is a 74% decrease in density within the wind farm when comparing model predictions including the wind farm response (factor variable) with model predictions excluding the wind farm response (Figure 5.14). This can be regarded as an indication of level of displacement, however it is important to consider the model errors as well as potential unknown uncertainties around the estimates (Figure 5.14). For comparison, the levels of displacement for PAWP and OWEZ were at a slightly higher level; 86%/89% for the predicted probabilities and 87%/90% for the predicted densities.

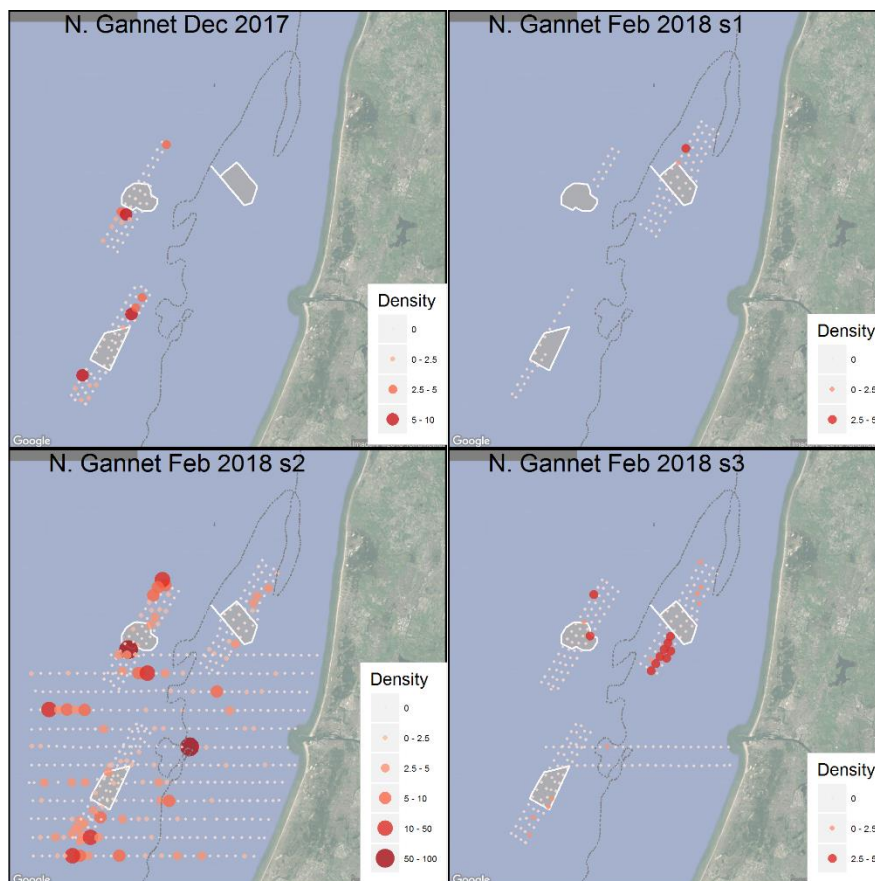


Figure 5.10 Observed density (birds/km²) of Northern Gannet during LUD-T3 surveys 2017-2018. Densities have been corrected for distance bias.

Northern Gannet, 2002-2018

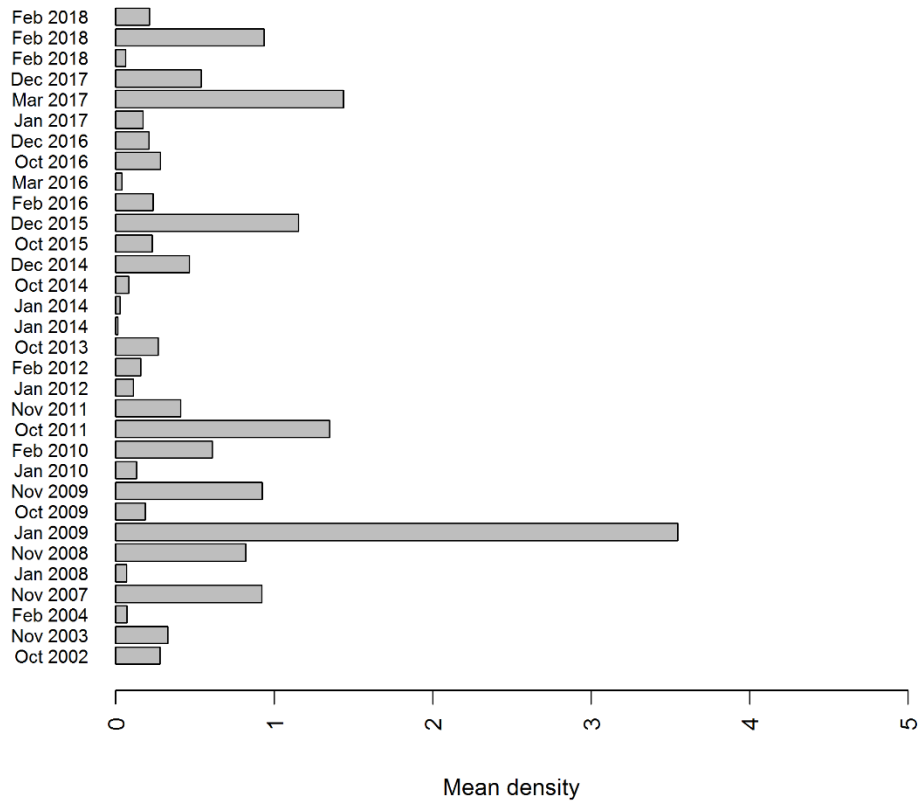


Figure 5.11. Mean observed density (birds/km²) of Northern Gannet in the entire surveyed area during OWEZ, PAWP and LUD pre-construction and post-construction surveys. Densities have been corrected for distance bias.

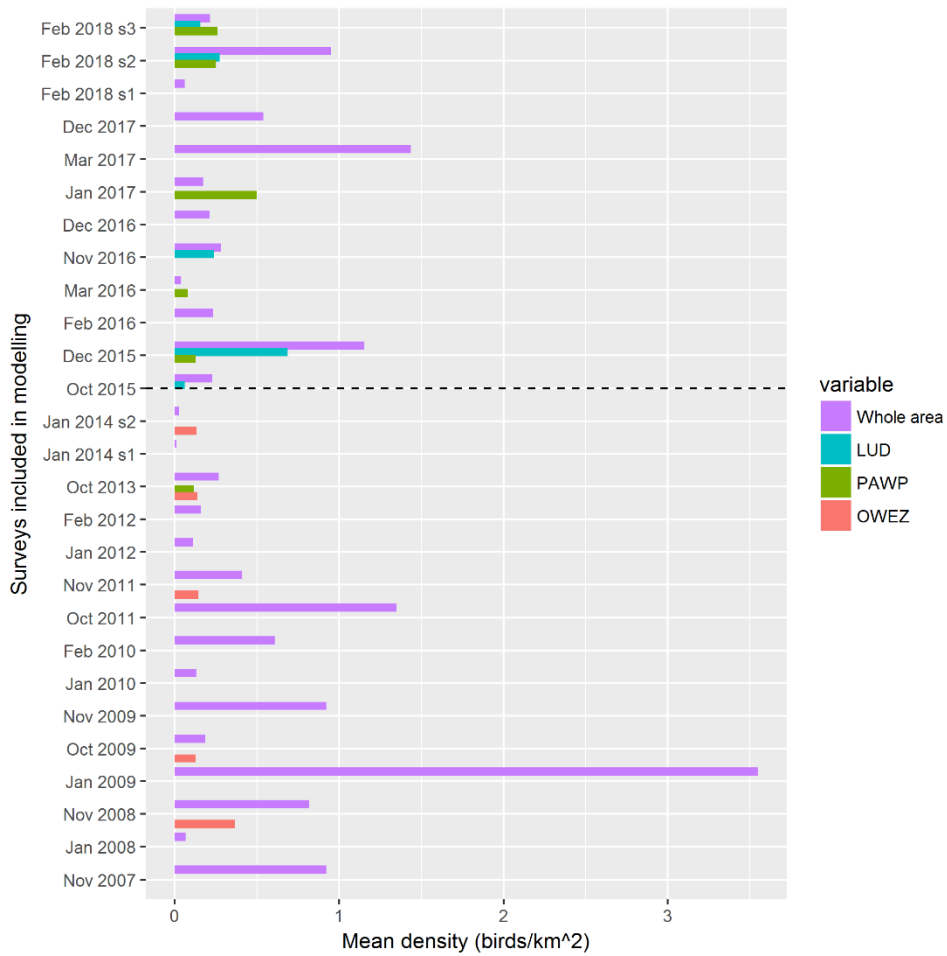


Figure 5.12. Mean density of Northern Gannet during surveys included in the modelling. The mean density within each of the three wind farm footprints (OWEZ, PAWP and LUD) is shown as well as the mean in the whole surveyed area (including wind farms). Surveys above the dashed line are LUD post-construction surveys.

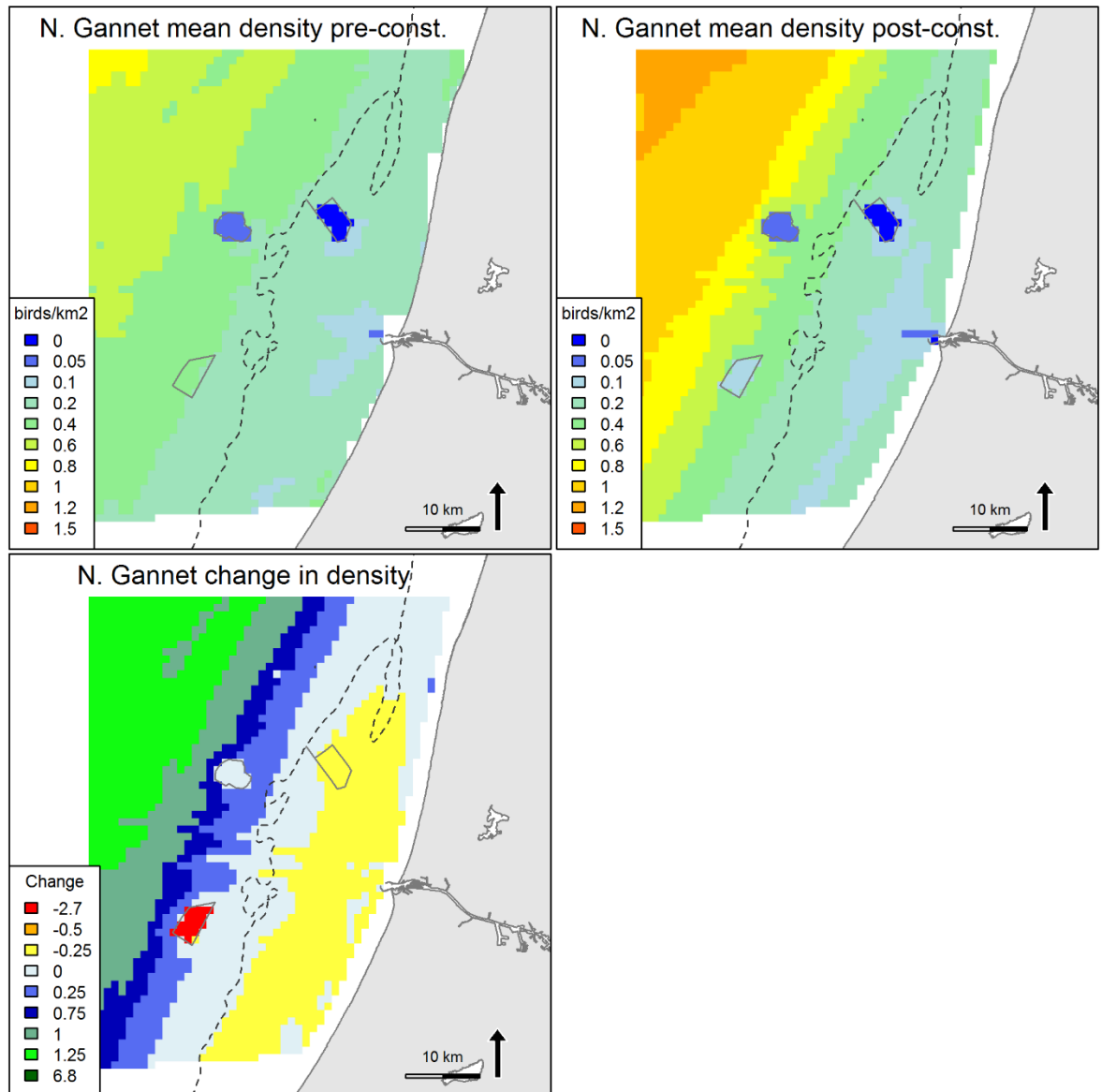


Figure 5.13. Predicted mean density (birds/km²) and distribution of wintering Northern Gannet during eight LUD pre-construction and 12 LUD post-construction surveys, and the relative change in predicted density between the two periods. Note that all included surveys are OWEZ and PAWP post-construction surveys

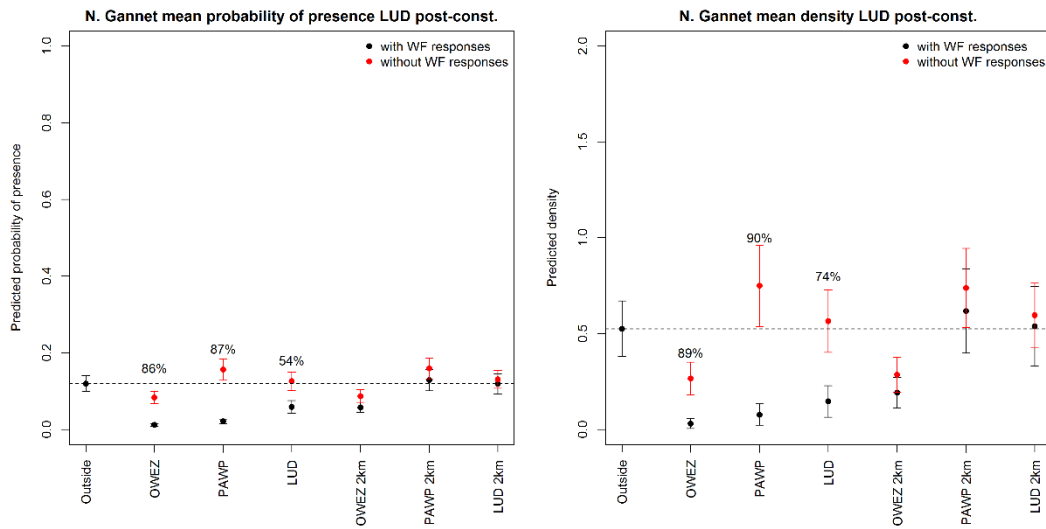


Figure 5.14. Model predictions (on model data) for Northern Gannet during the eight LUD post-construction surveys, with (fitted values) and without the response of the wind farm, when taking into account the dynamic environmental conditions. The difference indicate a mean displacement with model errors, i.e. what is the difference in probability of presence (to the left) or the density (to the right) if the wind farm(s) would not be present compared to a WF present. The mean displacement in % is indicated above the estimates for the footprints (GAMM model errors, SE, are indicated as error bars).

5.3.4 Great Cormorant *Phalacrocorax carbo*

The LUD-T3 surveys corroborated the findings of the LUD baseline, T1 and T2 surveys that the distribution of Cormorants offshore is exclusively associated with PAWP and OWEZ, and now also with LUD (Figure 5.15).

Model results

The modelling results stressed the importance of PAWP, OWEZ and LUD for the presence of Cormorants, as all wind farm footprints were significant ($p < 0.01$) as well as the 2 km buffer around each wind farm (Appendix A). However, with respect to the abundance (density) only the footprint of OWEZ, including the 2 km buffer had a significant effect on numbers of Cormorants. The large degree of variation seen in the overall abundance of recorded Cormorants during the 32 surveys is displayed in Figure 5.16 and Figure 5.17. The predicted patterns of change in density between pre-(LUD) and post-(LUD)-construction periods further underlined the attraction effect of the wind farms on the Cormorants (Figure 5.18). The explanatory degree of the distribution model for the Great Cormorant was poor for both the presence-absence and the density model parts (Appendix A). The model is nevertheless useful for describing the significant attraction effect of the three wind farms.

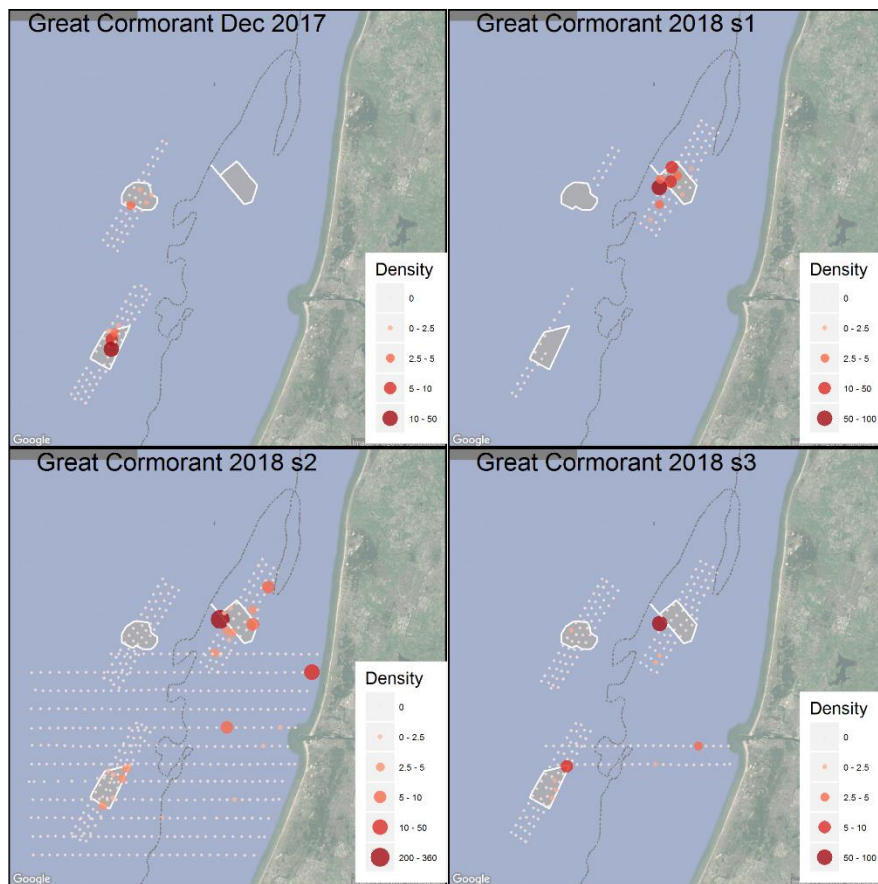


Figure 5.15. Observed density (birds/km²) of Great Cormorant in the entire surveyed area during LUD-T3 surveys 2017-2018. Densities have been corrected for distance bias.

Great Cormorant, 2002-2018

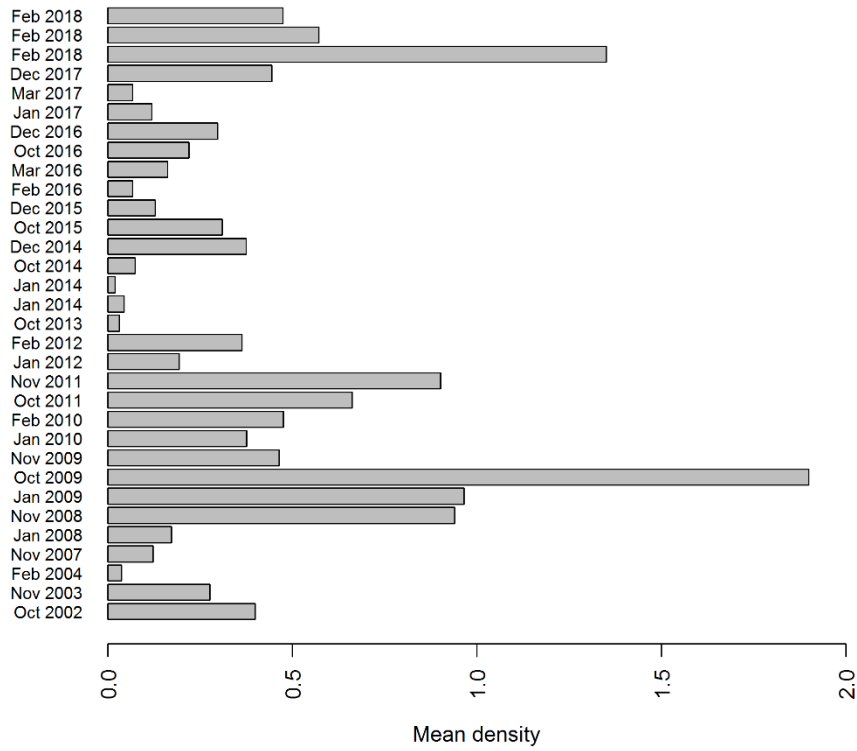


Figure 5.16. Mean observed density (birds/km²) of Great Cormorant during OWEZ, PAWP and LUD pre- and post-construction surveys. Densities have been corrected for distance bias.

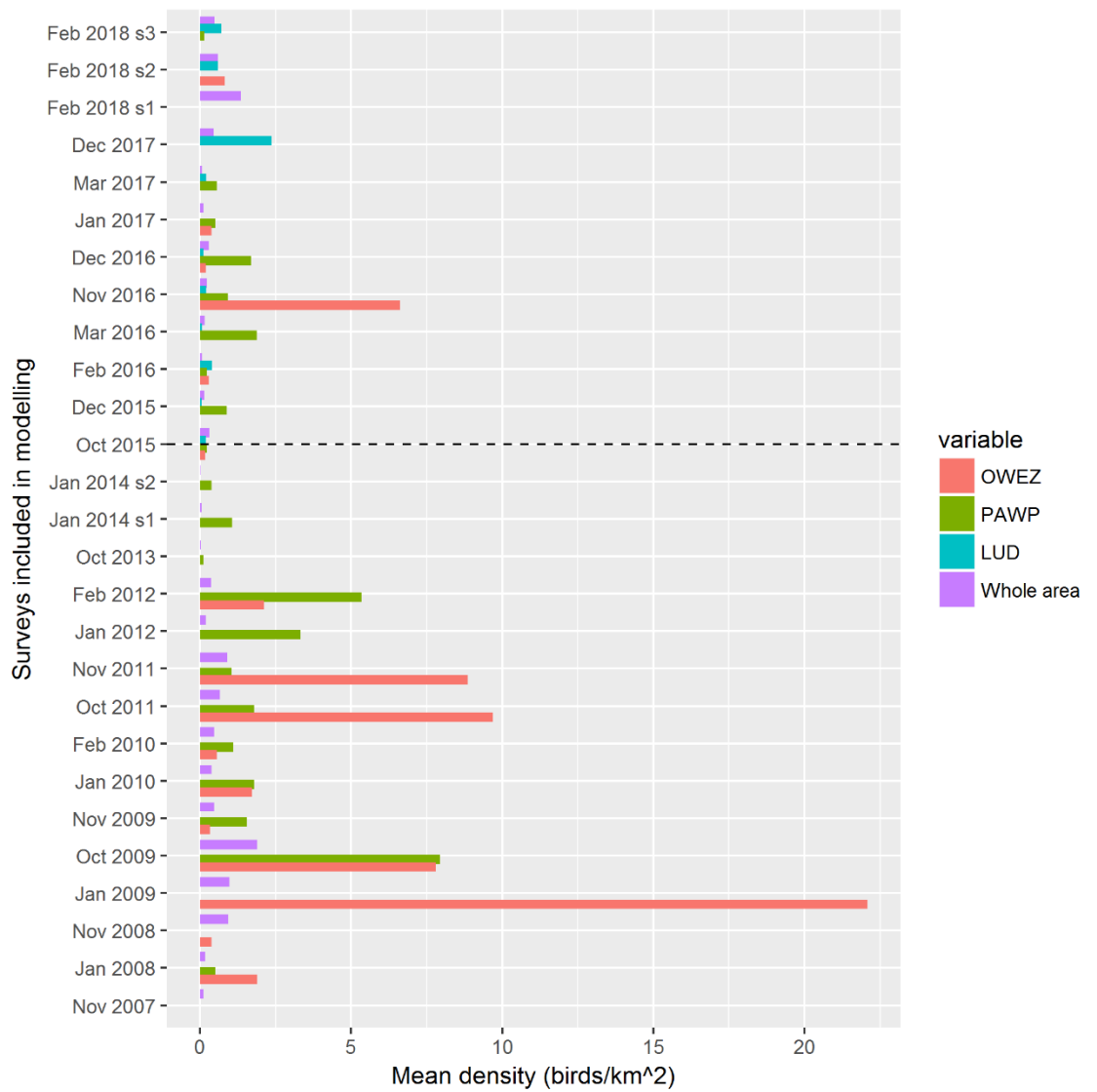


Figure 5.17. Mean density of Great Cormorant during surveys included in the modelling. The mean density within each of the three wind farm footprints (OWEZ, PAWP and LUD) is shown as well as the mean in the whole surveyed area (including wind farms). Surveys above the dashed line are LUD post-construction surveys.

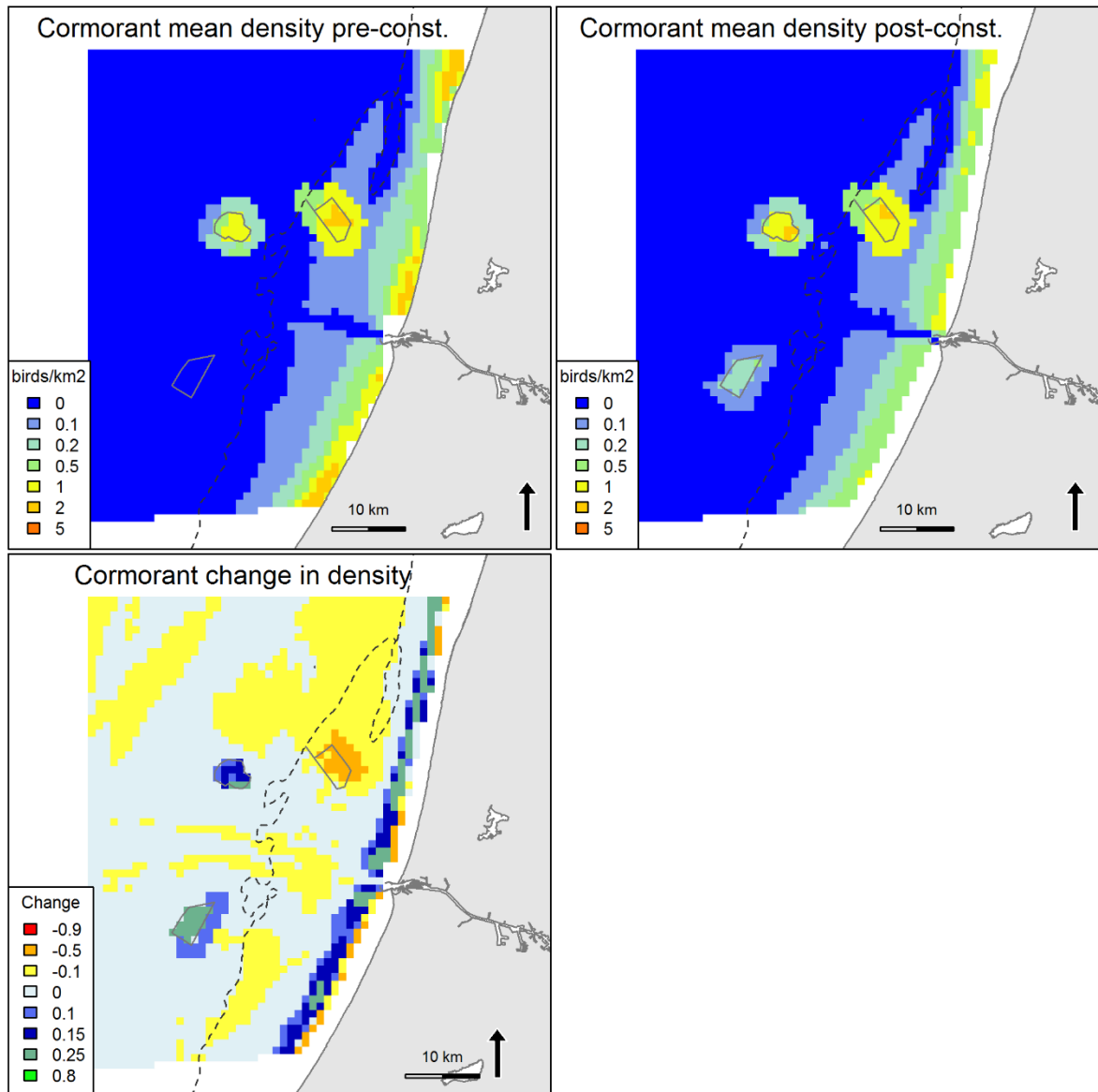


Figure 5.18. Predicted mean density (birds/km²) and distribution of wintering Great Cormorant during eight LUD pre- and 12 LUD post-construction surveys, and the relative change in predicted density between the two periods. Note that all included surveys are OWEZ and PAWP post-construction surveys.

5.3.5 *Little Gull Hydrocoloeus minutus*

During the LUD-T3-01 survey only one observation of Little Gull was made outside OWEZ. During the LUD-T3-02 survey spring migration was noted in the southern part of the area. Although most birds were recorded in the coastal zone a few birds including one bird inside LUD were seen offshore (Figure 5.19). During the LUD-T3-03 survey one Little Gull was observed outside OWEZ.

Model results

Surveys with no or very few Little Gull sightings were not included in the analyses (Figure 5.20, Figure 5.21). The footprints of LUD and PAWP were dropped from the model due to low overall presence of the species. The presence-absence model indicated a significantly lower probability in the OWEZ footprint ($p < 0.01$). The probability of presence also increased with decreasing water depth and shipping intensity and increasing salinity (Appendix A). The only smooth term included in the positive model part was current speed (Appendix A). The model was poor and strong conclusions should not be drawn based on the model

results. There seemed to be a discrete concentration of Little Gulls just outside LUD based on model predictions (Figure 5.22).

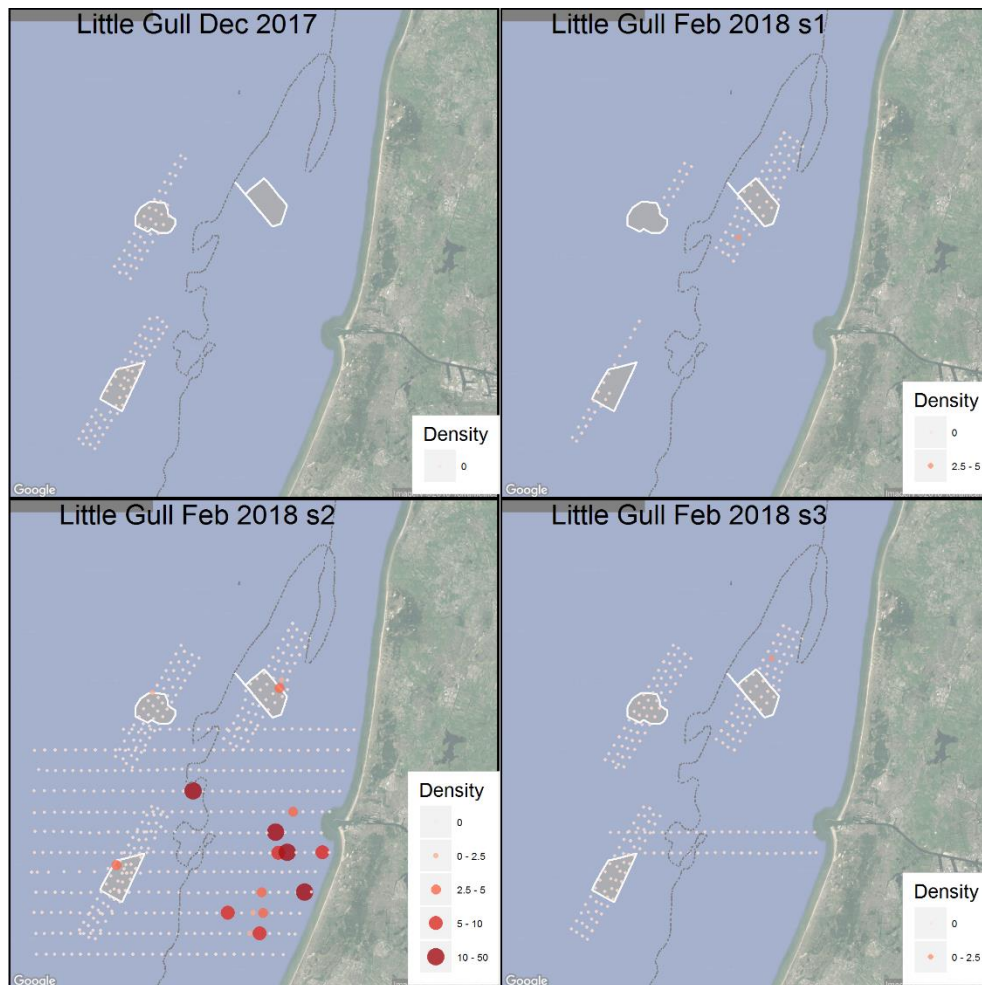


Figure 5.19. Observed density (birds/km²) of Little Gull during LUD-T3 surveys 2017-2018. Densities have been corrected for distance bias.

Little Gull, 2002-2018

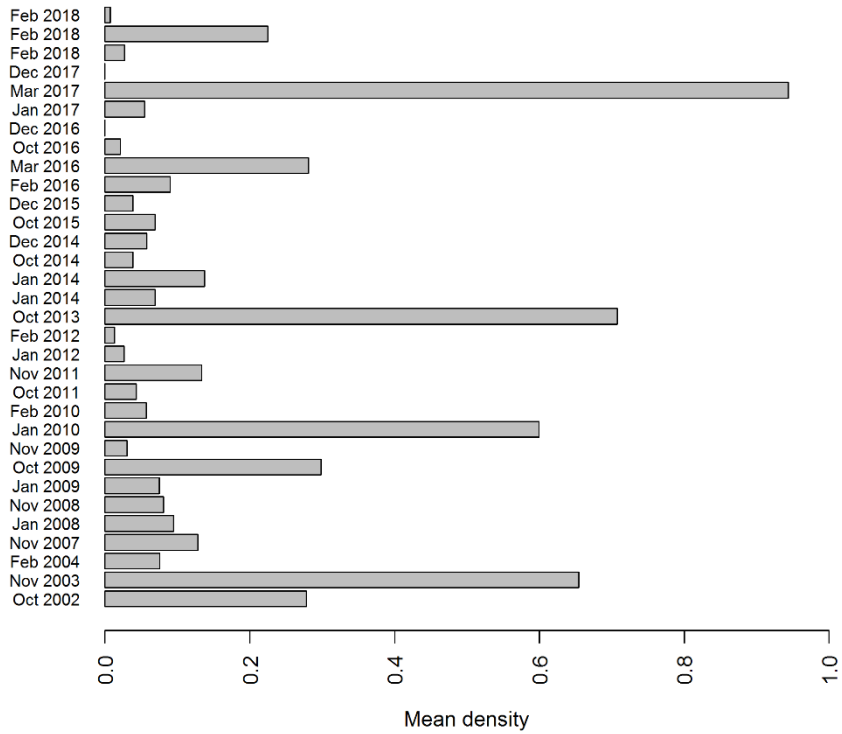


Figure 5.20. Mean observed density (birds/km²) of Little Gull in the entire surveyed area during OWEZ, PAWP and LUD pre- and post-construction surveys. Densities have been corrected for distance bias.

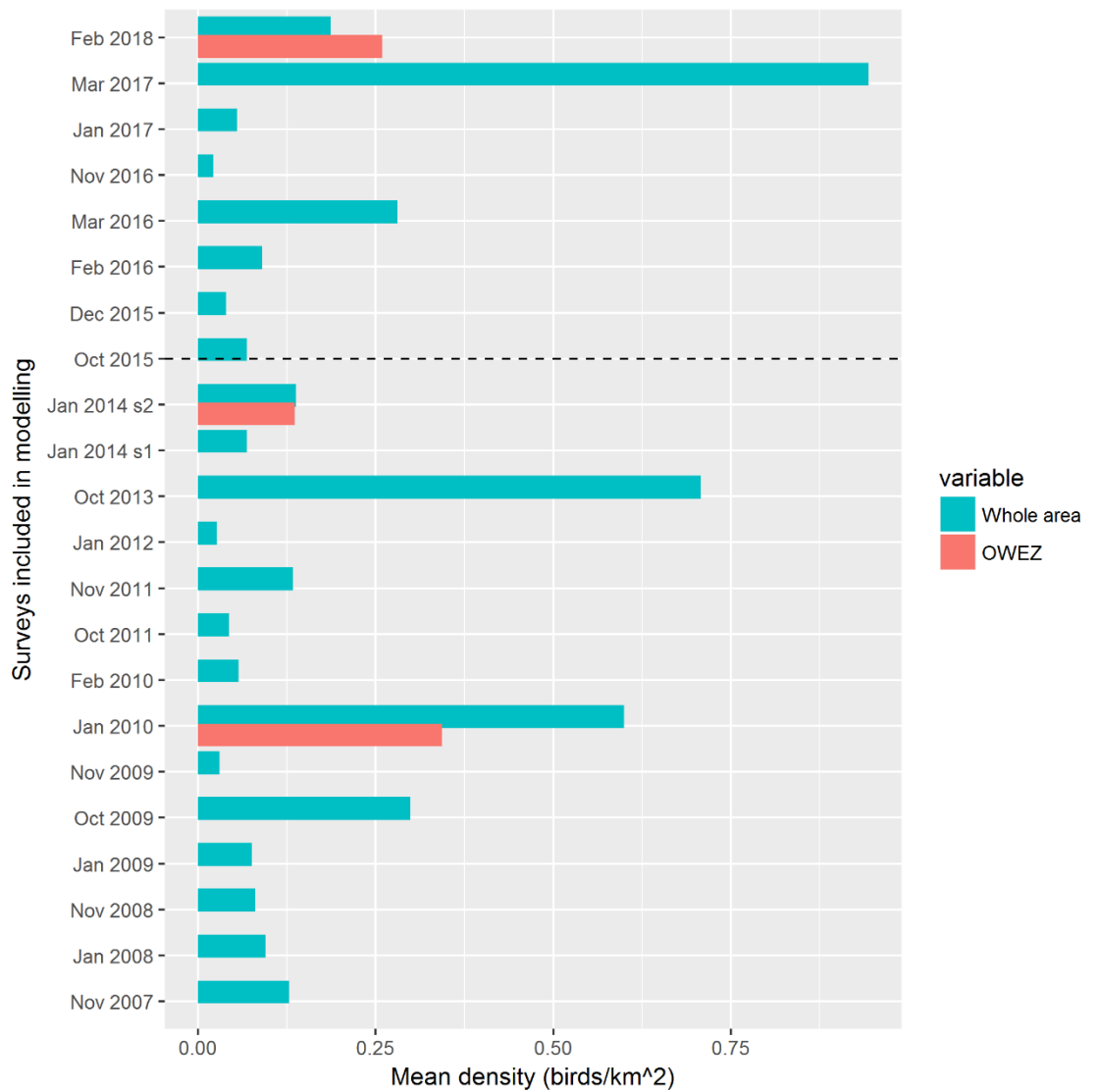


Figure 5.21. Mean density of Little Gull during surveys included in the modelling. The mean density within OWEZ wind farm footprint is shown as well as the mean in the whole surveyed area (including wind farms). Surveys above the dashed line are LUD post-construction surveys.

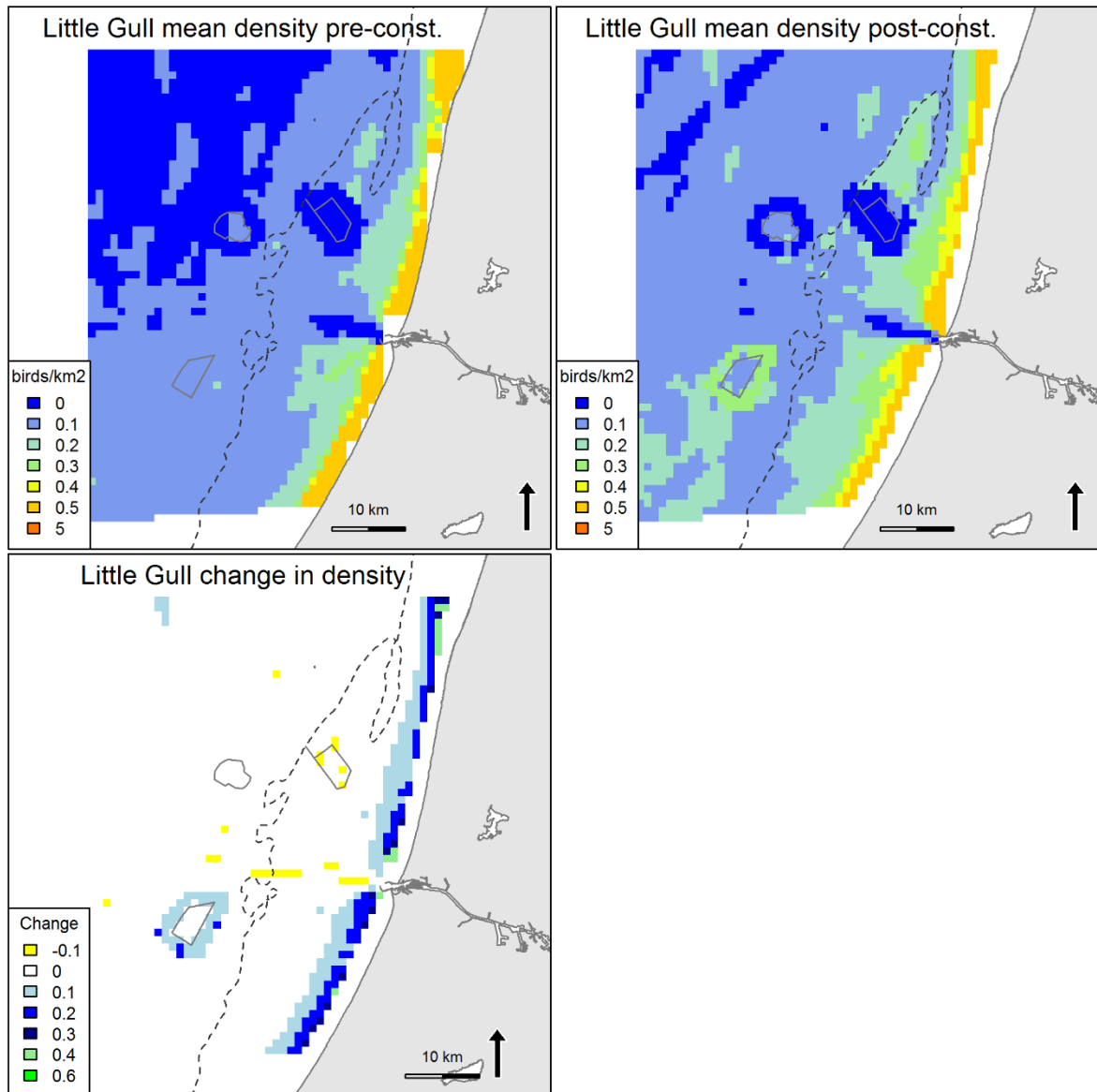


Figure 5.22. Predicted mean density (birds/km²) and distribution of wintering Little Gull during eight LUD pre- and 12 LUD post-construction surveys, and the relative change in predicted density between the two periods. Note that all included surveys are OWEZ and PAWP post-construction surveys.

5.3.6 Black-headed Gull *Chroicocephalus ridibundus*

During the LUD-T3 surveys low densities of Black-headed Gulls were recorded in the study area (Figure 5.23, Figure 5.24). Single Black-headed gulls were recorded in LUD and OWEZ. The observed density of Black-headed Gulls has dropped markedly in the whole area as well as inside all three wind farms between the LUD pre- and post-construction survey periods (Figure 5.23, Figure 5.245).

Model results

According to the model the probability of presence was significantly lower in LUD and in the 2 km buffer around LUD during post-construction. Other significant variables in the presence-absence model part were decreasing depth and salinity as well as increasing frontal activity (current gradient). In the positive model part depth and current speed were influential. As the model accounts for oceanographic changes between pre- and post-construction periods, the marked decline in the abundance of Black-headed Gulls is most likely linked to other factors. The significant drop in the densities in LUD may therefore be considered as

coincidental and not a displacement effect. Generally, the model was rather poor although, the explanation degree of the presence-absence part was fair 24% (Appendix A). The predictions indicate a preference to the coastal water mass (Figure 5.26).

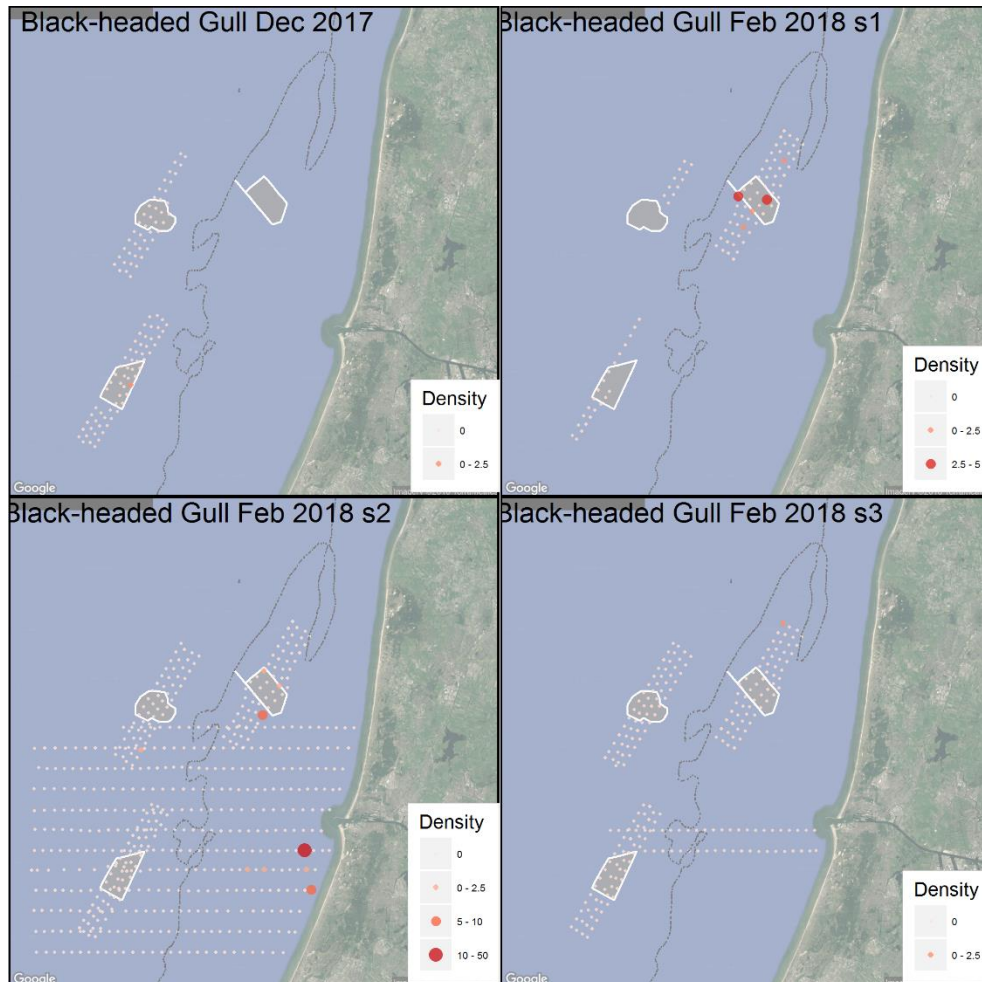


Figure 5.23. Observed density (birds/km²) of Black-headed Gull during LUD-T3 surveys 2017-2018. Densities have been corrected for distance bias.

Black-headed Gull, 2002-2018

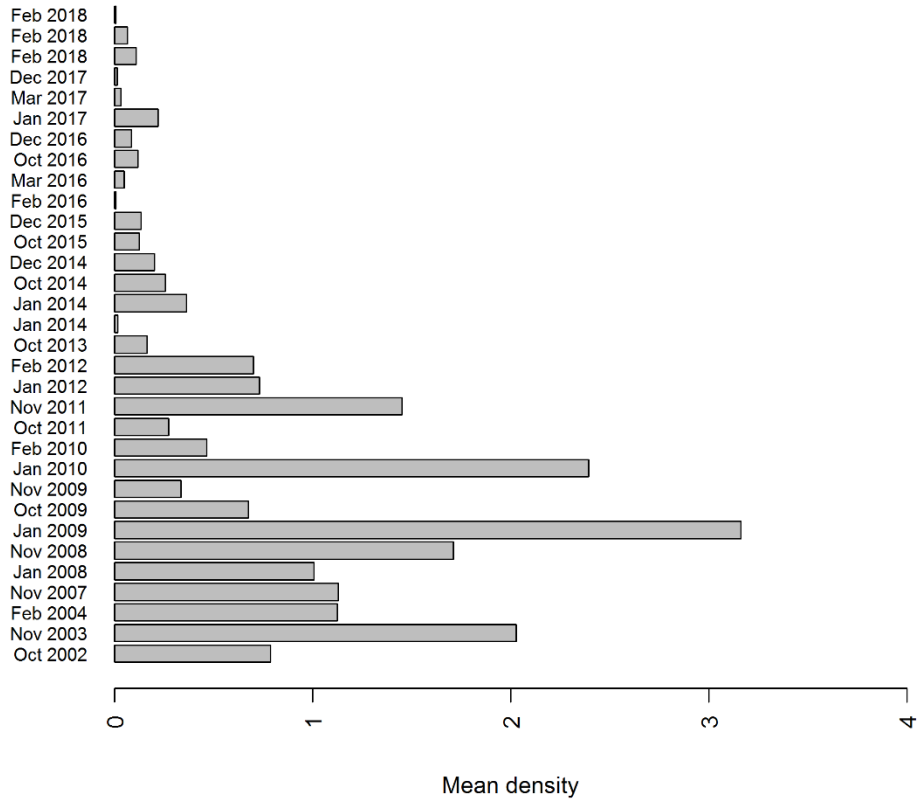


Figure 5.24. Mean observed density (birds/km²) of Black-headed Gull in the entire surveyed area during OWEZ, PAWP and LUD pre- and post-construction surveys. Densities have been corrected for distance bias.

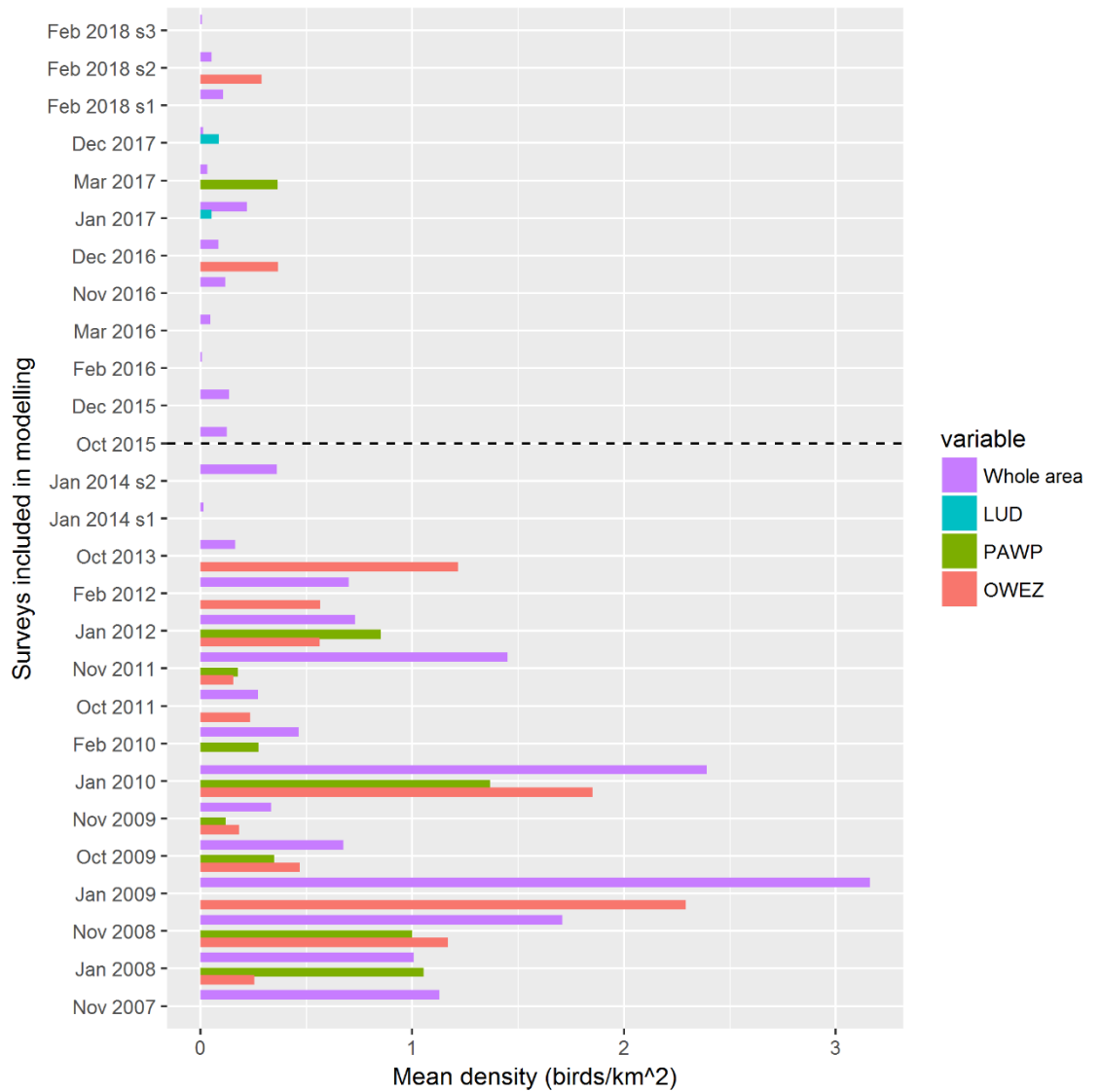


Figure 5.25. Mean density of Black-headed Gull during surveys included in the modelling. The mean density within each of the three wind farm footprints (OWEZ, PAWP and LUD) is shown as well as the mean in the whole surveyed area (including wind farms). Surveys above the dashed line are LUD post-construction surveys.

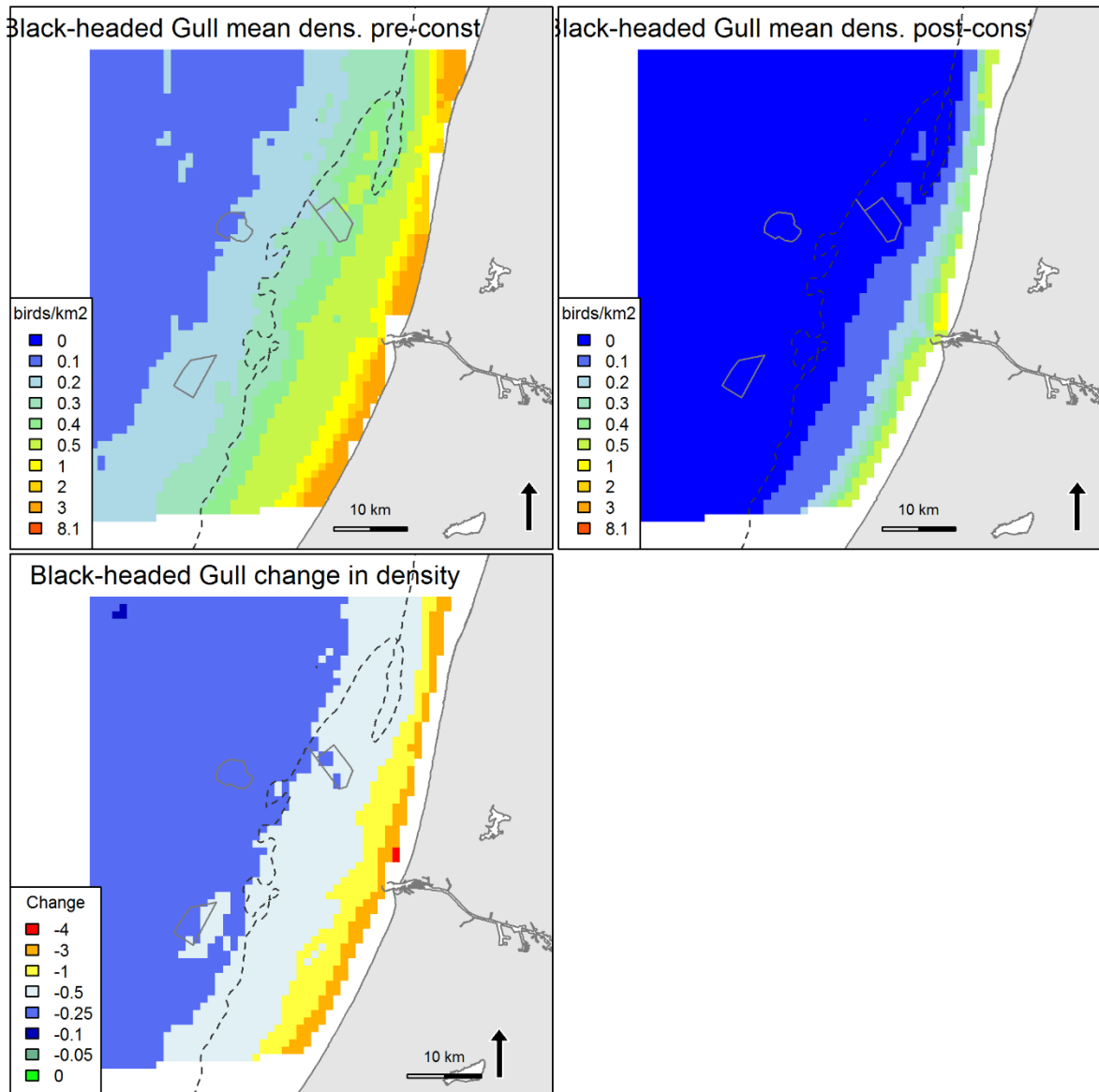


Figure 5.26. Predicted mean density (birds/km²) and distribution of wintering Black-headed Gull during eight LUD pre- and 12 LUD post-construction surveys, and the relative change in predicted density between the two periods. Note that all included surveys are OWEZ and PAWP post-construction surveys.

5.3.7 Common Gull *Larus canus*

During the LUD-T3 surveys highest densities were observed during the LUD-T3-02 survey with observations scattered around the study area (Figure 5.27). Birds were recorded frequently inside all three wind farm footprints (Figure 5.27). After the construction of LUD, a marked increase in the abundance of Common Gull has been recorded over the whole area, including the three wind farm footprints (Figure 5.28, Figure 5.29).

Model results

The model indicated that the probability of presence is highest in water depths around 15 m where mean current speed is low. Increasing density, when present, is further explained by increasing frontal activity (current gradient, Appendix A). The wind farm footprints were not significant in the model, however the model predictions indicate a potential small increase in the vicinity of the LUD wind farm (Figure 5.30). As the model accounts for oceanographic changes between pre- and post-construction periods, the marked

increase in the abundance of Common Gulls is most likely linked to other factors. The significant increase in the densities in the LUD buffer zone may therefore be considered as coincidental and not an effect of displacement or attraction to the wind farm.

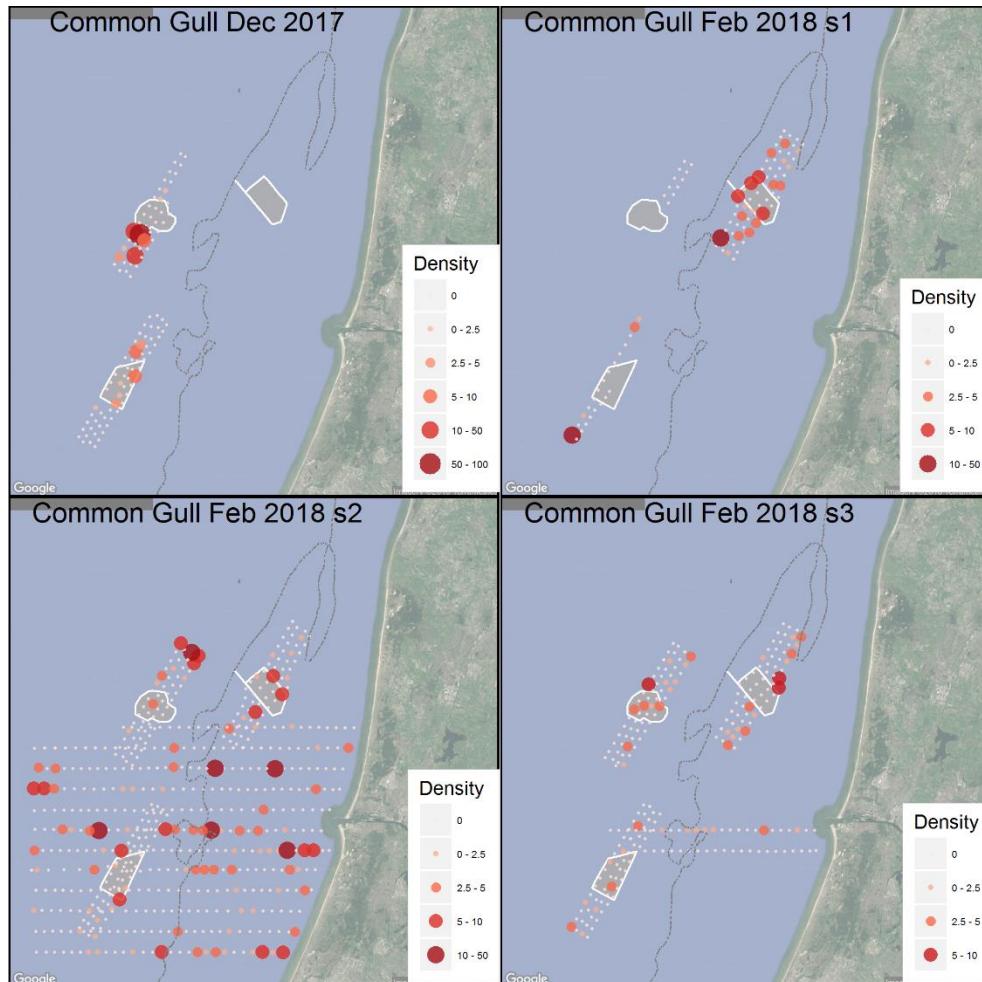


Figure 5.27. Observed density (birds/km²) of Common Gull during LUD-T3 surveys 2017-2018. Densities have been corrected for distance bias.

Common Gull, 2002-2018

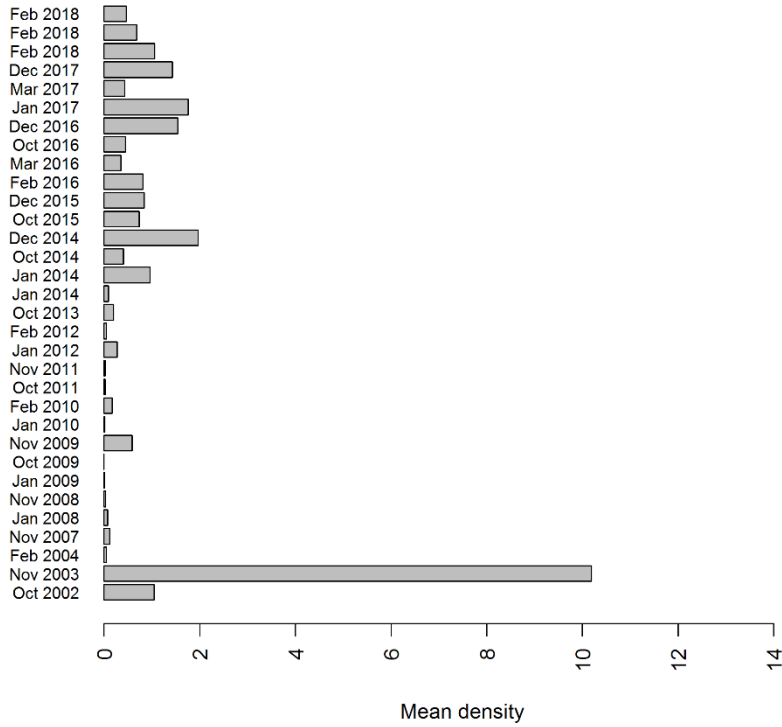


Figure 5.28. Mean observed density (birds/km²) of Common Gull in the entire surveyed area during OWEZ, PAWP and LUD pre- and post-construction surveys. Densities have been corrected for distance bias.

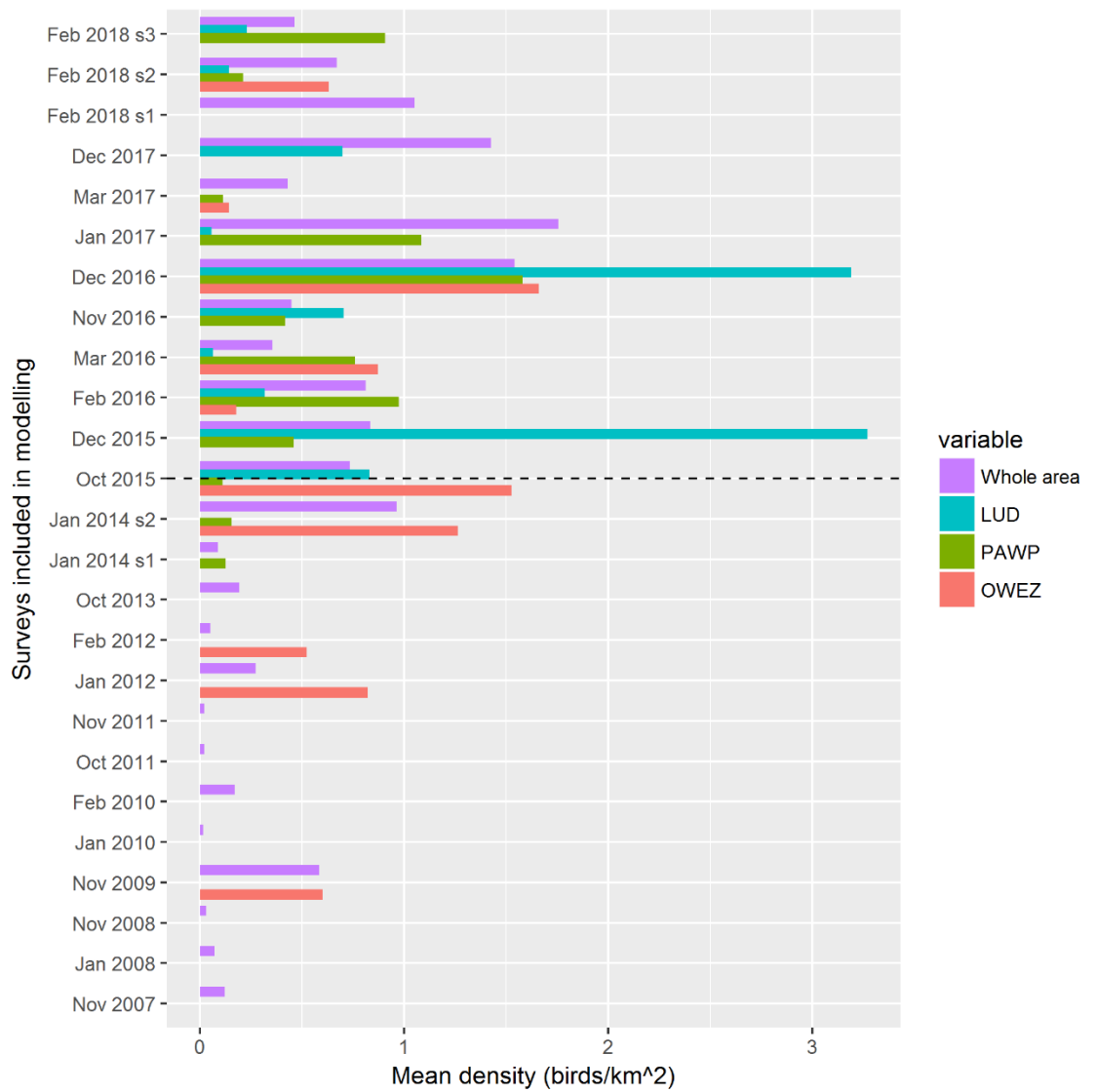


Figure 5.29. Mean density of Common Gull during surveys included in the modelling. The mean density within each of the three wind farm footprints (OWEZ, PAWP and LUD) is shown as well as the mean in the whole surveyed area (including wind farms). Surveys above the dashed line are LUD post-construction surveys.

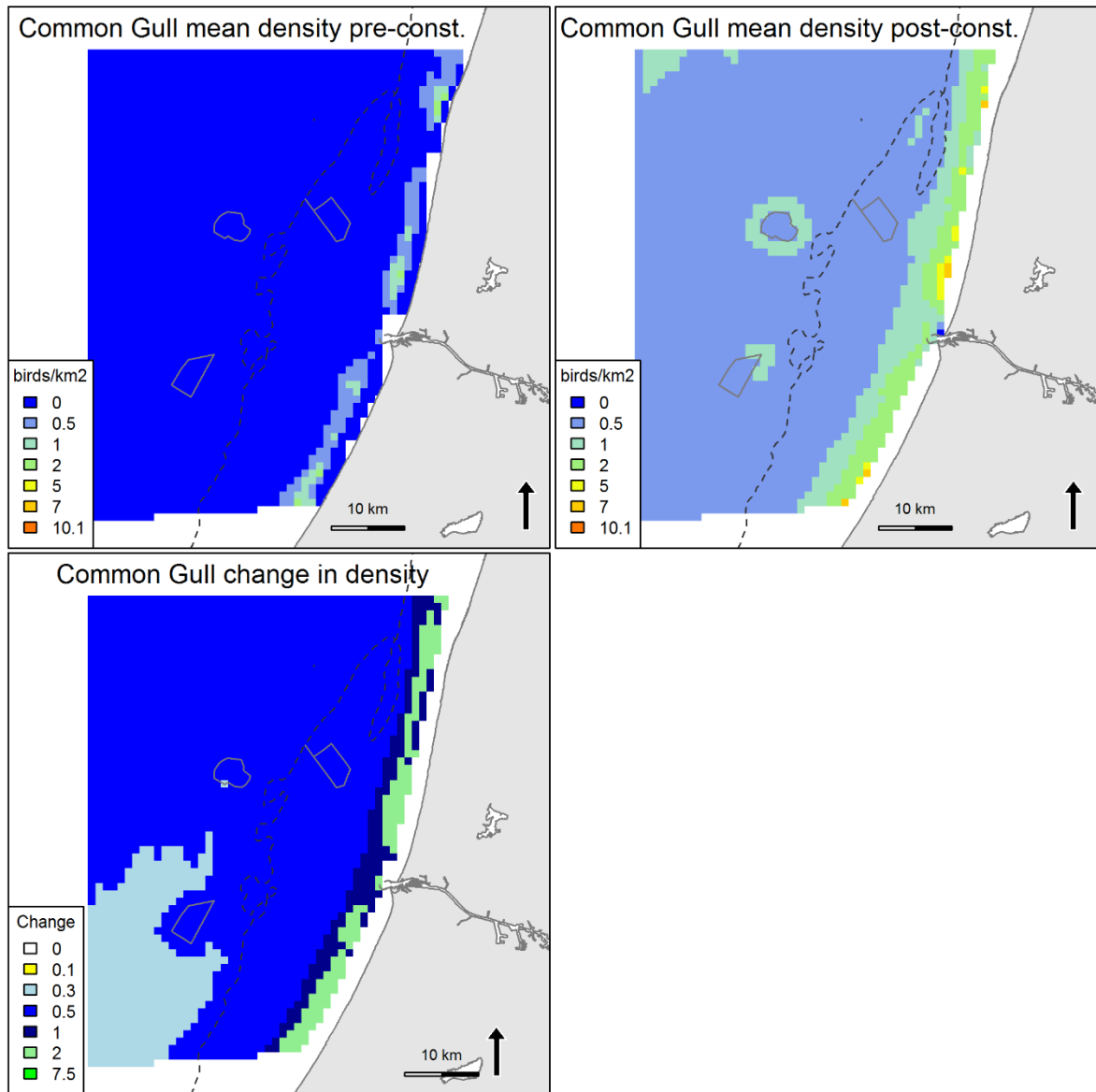


Figure 5.30. Predicted mean density (birds/km²) and distribution of wintering Common Gull during eight LUD pre- and 12 LUD post-construction surveys, and the relative change in predicted density between the two periods. Note that all included surveys are OWEZ and PAWP post-construction surveys.

5.3.8 Lesser Black-backed Gull *Larus fuscus*

During the LUD-T3 surveys the majority of Lesser Black-backed gulls was observed during the LUD-T3-02 survey, when birds were seen throughout the offshore zone (Figure 5.31). This pattern most likely reflected an influx of migrating birds (Figure 5.31, Figure 5.32). No apparent general trends were present in the observed numbers of Lesser Black-backed Gulls between LUD pre- and post-construction periods (Figure 5.32, Figure 5.33).

Model results

According to the model the probability of presence was significantly lower within the LUD footprint during post-construction ($p < 0.01$). Otherwise the same variables were influential in both model parts, decreasing water depth and increasing salinity and frontal activity (current gradient, Appendix A). The explanation degree of the model was low, indicating a rather poor model. The predictions indicate that the densities are highest within a narrow belt close to the coast and over a wider area farther offshore in areas deeper than

20 m (Figure 5.34). Further, the model predictions indicate a general increase in the latter zone during the LUD post-construction zone which may be linked to changes in oceanographic conditions between pre- and post-construction periods. Although LUD is located within the offshore zone, model predictions display no change or a slight displacement of birds from the LUD footprint (Figure 5.34).

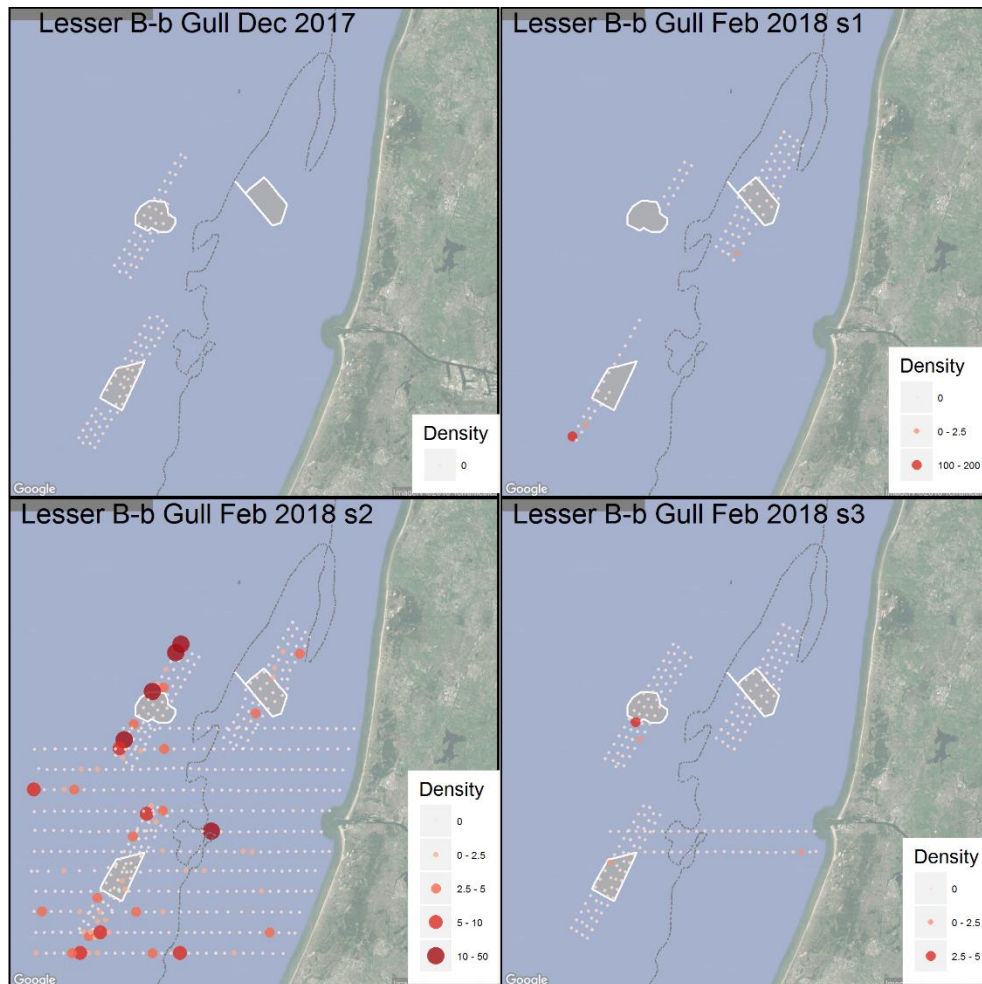


Figure 5.31. Observed density (birds/km²) of Lesser Black-backed Gull during LUD-T3 surveys 2017-2018. Densities have been corrected for distance bias.

Lesser Black-backed Gull, 2002-2018

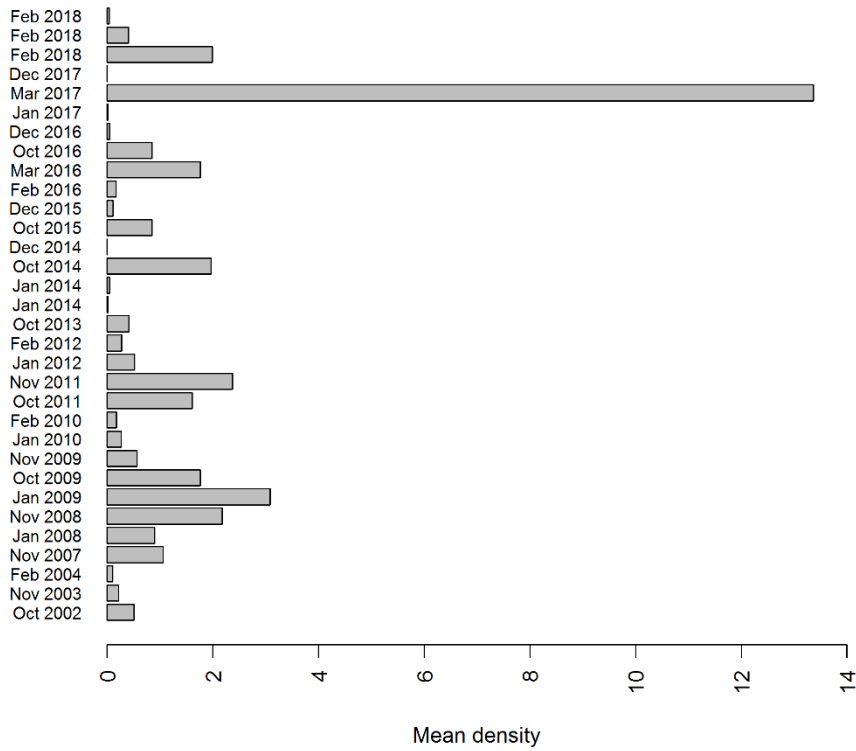


Figure 5.32. Mean observed density (birds/km²) of Lesser Black-backed Gull in the entire surveyed area during OWEZ, PAWP and LUD pre- and post-construction surveys. Densities have been corrected for distance bias.

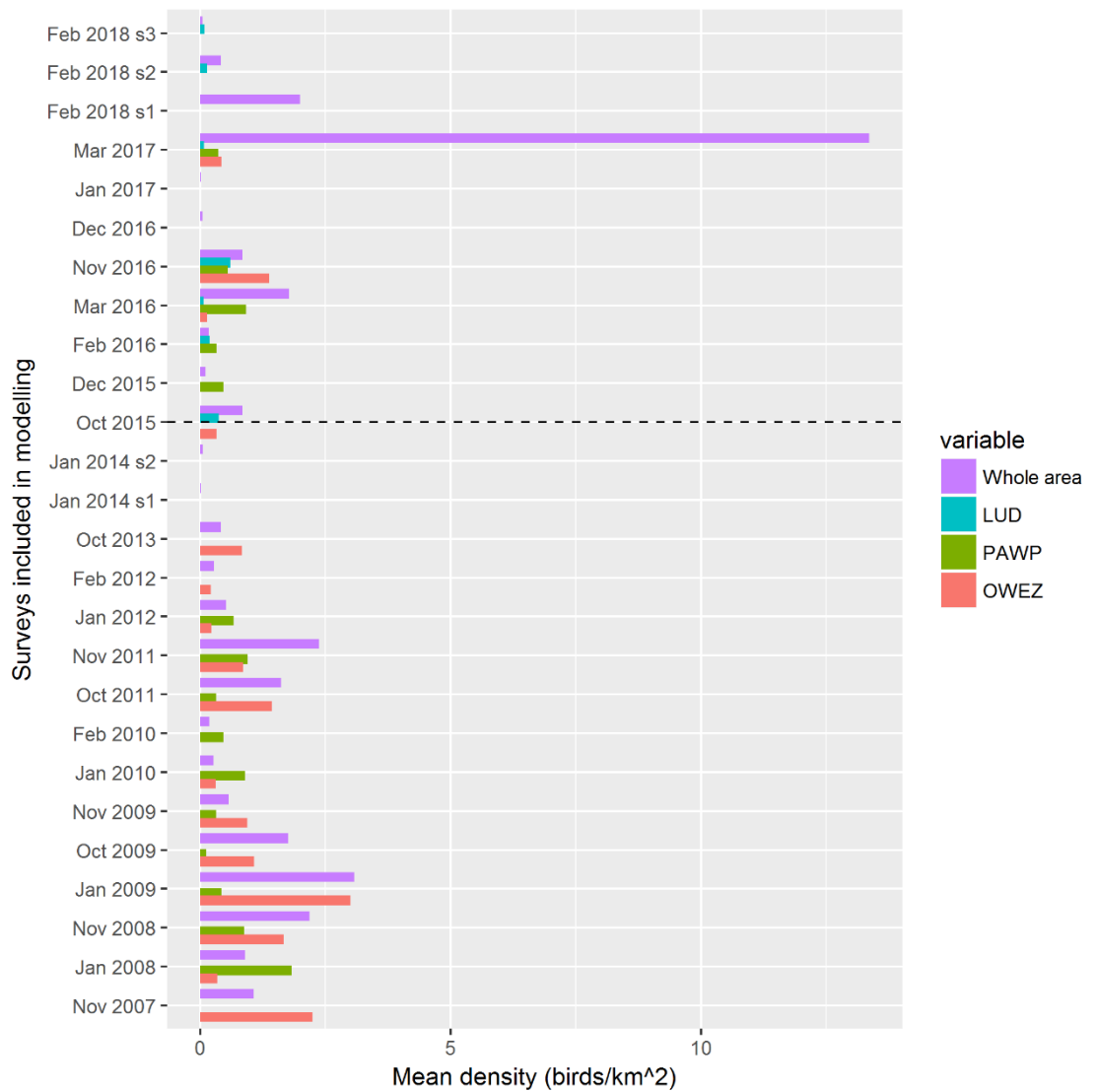


Figure 5.33. Mean density of Lesser Black-backed Gull during surveys included in the modelling. The mean density within each of the three wind farm footprints (OWEZ, PAWP and LUD) is shown as well as the mean in the whole surveyed area (including wind farms). Surveys above the dashed line are LUD post-construction surveys.

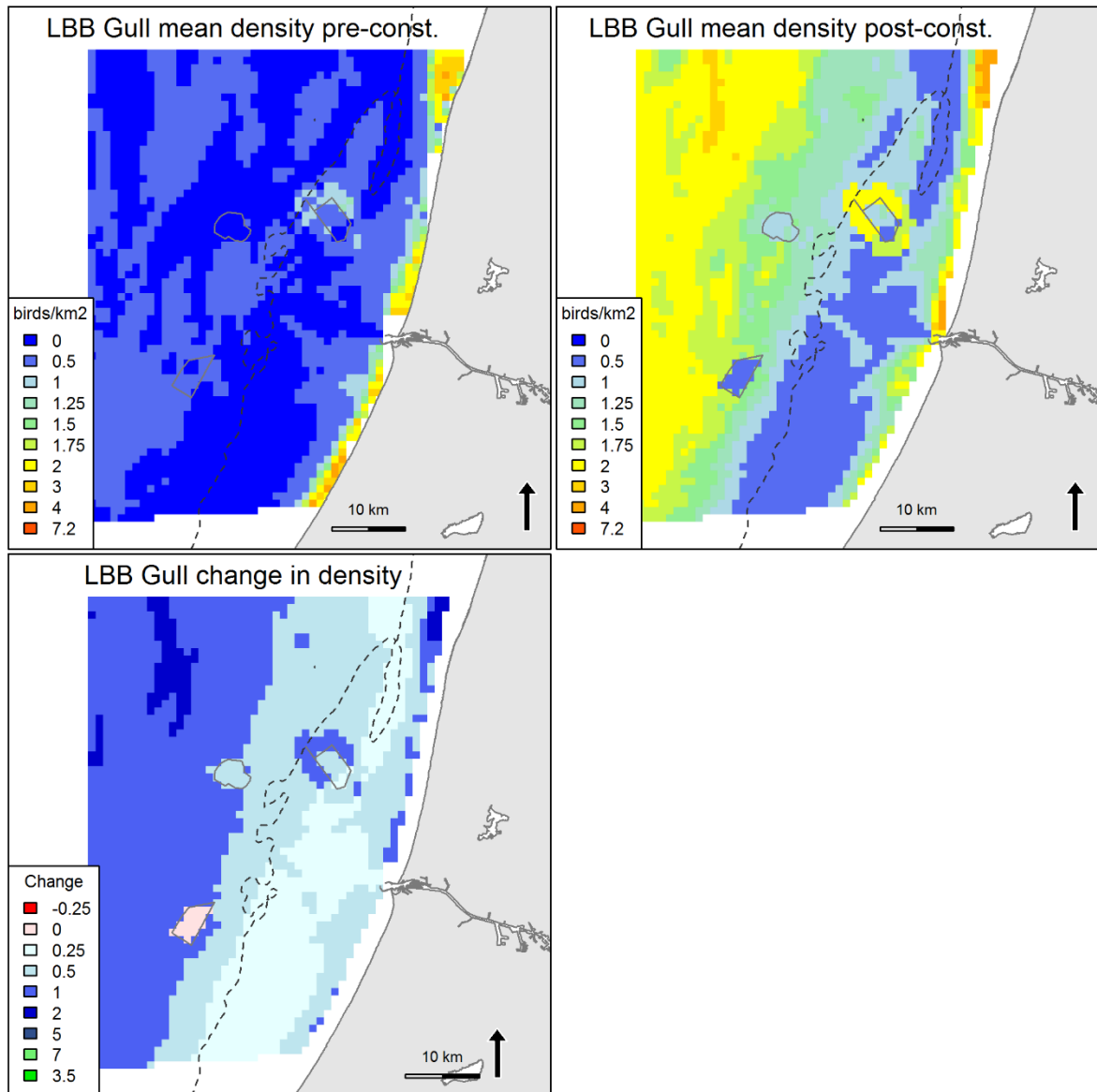


Figure 5.34. Predicted mean density (birds/km²) and distribution of wintering Lesser Black-backed Gull during eight LUD pre- and 12 LUD post-construction surveys, and the relative change in predicted density between the two periods. Note that all included surveys are OWEZ and PAWP post-construction surveys.

5.3.9 Herring Gull *Larus argentatus*

During the LUD-T3 surveys low-medium densities of Herring Gulls were observed without a clear spatial pattern (Figure 5.35). Highest mean density was observed during the LUD-T3-02 survey in February 2018 (Figure 5.36). Herring Gulls were observed in all three wind farms (Figure 5.38). No apparent general trends were present in the observed numbers of Herring Gulls between LUD pre- and post-construction periods (Figure 5.36, Figure 5.37).

Model results

According to the model the probability of presence was significantly higher in the LUD and PAWP footprints indicating an attraction to both wind farms. The probability of presence also significantly increased with decreasing current speed and increasing current speed (Appendix A). If present, an increase in density was explained by increasing frontal activity (current gradient, Appendix A) and salinity. Overall,

the model was poor with low explanation degree and predictive power (Appendix A). The mapped predictions indicate that the coastal waters are preferred by the Herring Gull (Figure 5.38), however as already indicated the model is poor and the birds were observed scattered around the whole study area (Figure 5.35). Further, the model predictions indicate a general increase in parts of the coastal zone during the LUD post-construction zone which may be linked to changes in oceanographic conditions between pre- and post-construction periods (Figure 5.38). The predicted localised increases in densities inside the three wind farms may be interpreted as an effect of attraction.

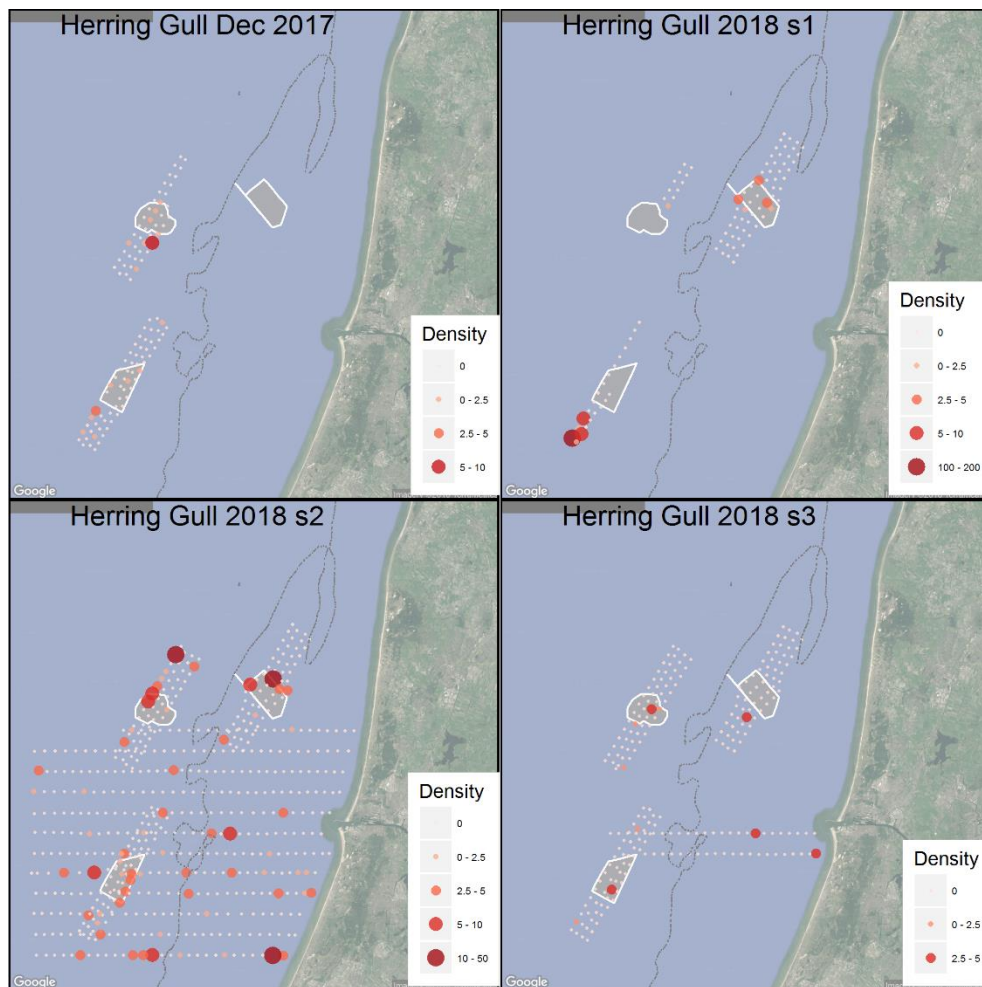


Figure 5.35. Observed density (birds/km²) of Herring Gull during LUD-T3 surveys 2017-2018. Densities have been corrected for distance bias.

Herring Gull, 2002-2018

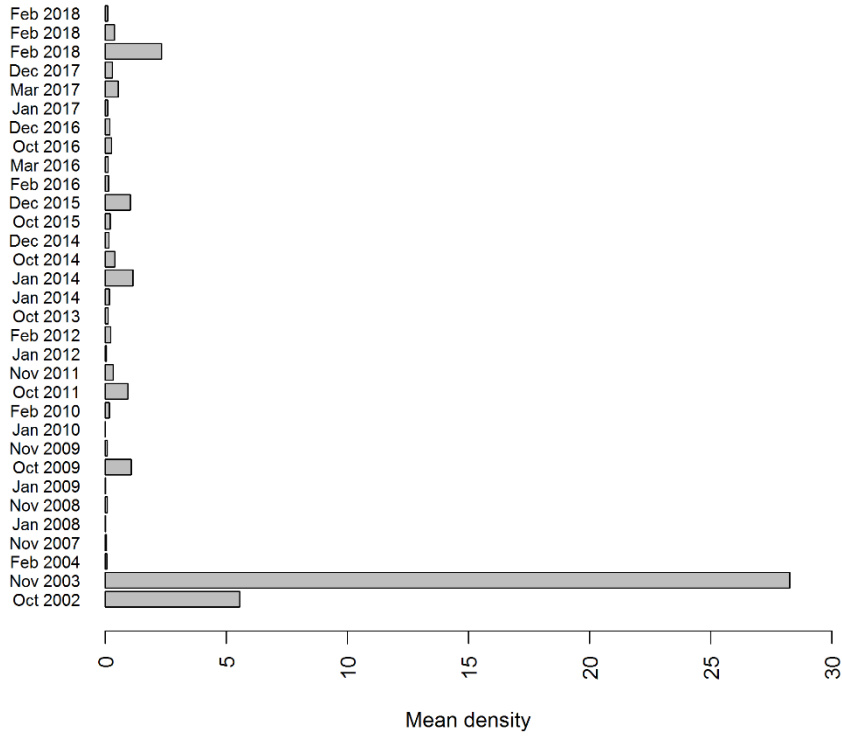


Figure 5.36. Mean observed density (birds/km²) of Herring Gull in the entire surveyed area during OWEZ, PAWP and LUD pre- and post-construction surveys. Densities have been corrected for distance bias.

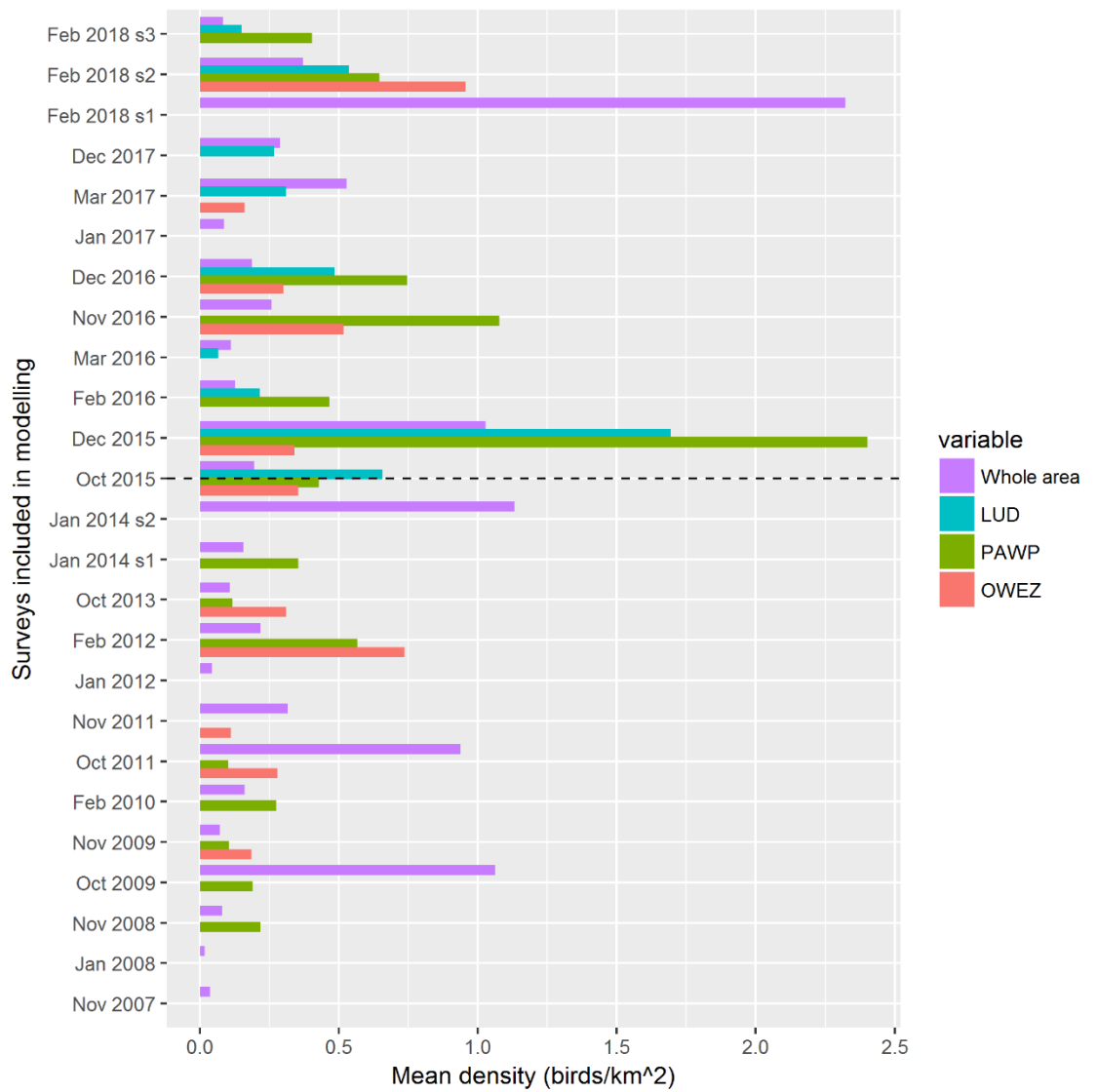


Figure 5.37. Mean density of Herring Gull during surveys included in the modelling. The mean density within each of the three wind farm footprints (OWEZ, PAWP and LUD) is shown as well as the mean in the whole surveyed area (including wind farms). Surveys above the dashed line are LUD post-construction surveys.

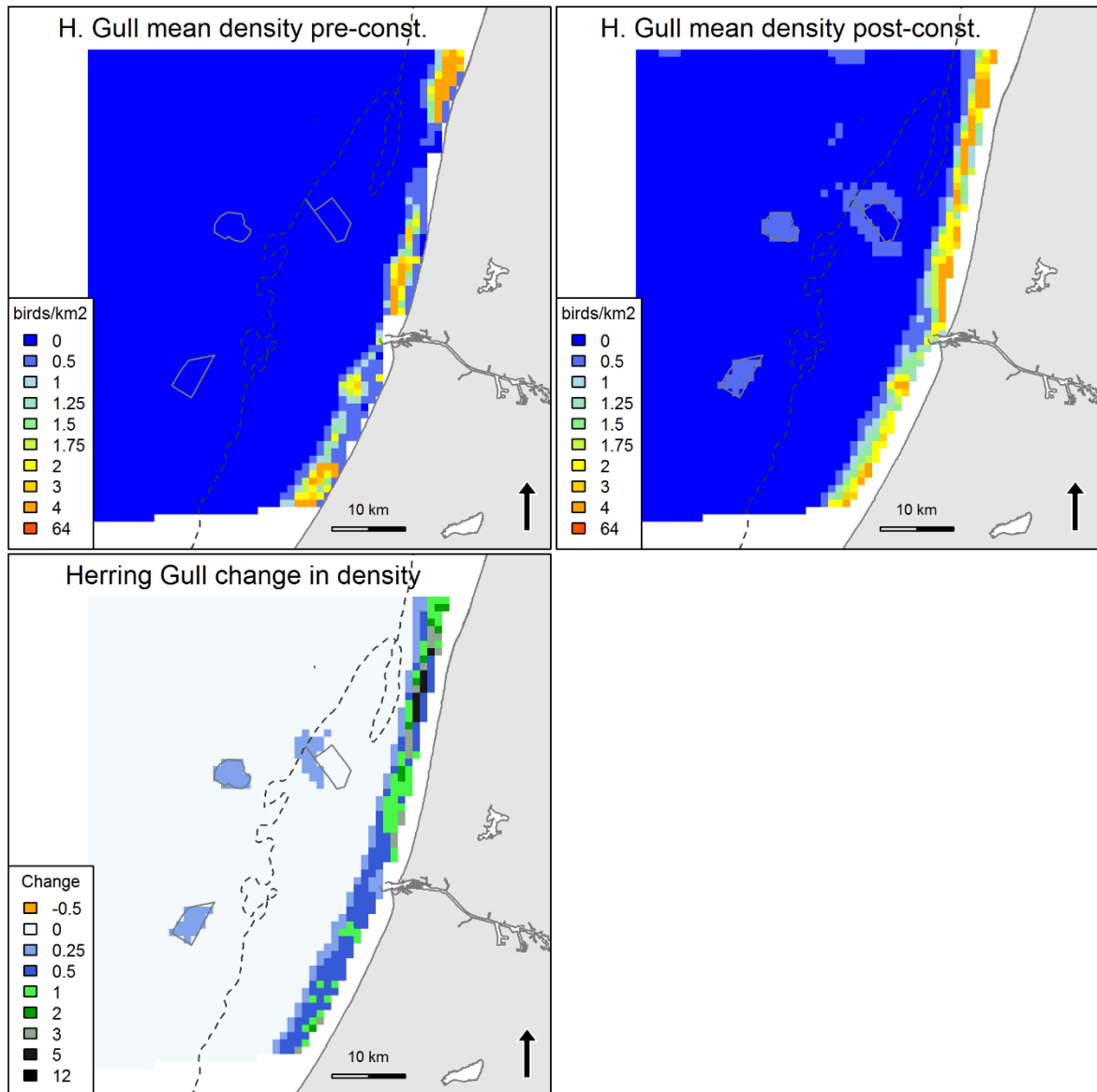


Figure 5.38. Predicted mean density (birds/km²) and distribution of wintering Herring Gull during eight LUD pre- and 12 LUD post-construction surveys, and the relative change in predicted density between the two periods. Note that all included surveys are OWEZ and PAWP post-construction surveys.

5.3.10 Great Black-backed Gull *Larus marinus*

Low to medium densities of Great Black-backed Gulls were observed during the LUD-T3 surveys (Figure 5.39). It is difficult to identify any clear distribution patterns but many observations were made in the vicinity of LUD and PAWP during LUD-T3-02. There is a weak declining trend in the observed numbers of Great Black-backed Gulls in the whole area between LUD pre- and post-construction periods (Figure 5.40, Figure 5.41). The changes in the three wind farms are less obvious, but seemingly more birds were observed in LUD and PWP during the post-construction period.

Model results

In accordance with the observations the model indicated an attraction to LUD and PAWP with a significantly higher probability within the LUD and PAWP footprint and the PAWP 2 km buffer ($p < 0.05$). Of the continuous variables only increasing frontal activity (current gradient) was included in both model parts. The predictions indicate a small increase in densities inside LUD and PAWP during the post-

construction period, in spite of general decline predicted in most of the other parts of the area (Figure 5.42). The predicted localised increases in densities inside the two wind farms may be interpreted as an effect of attraction. Highest densities were predicted close to the coast (Figure 5.42).

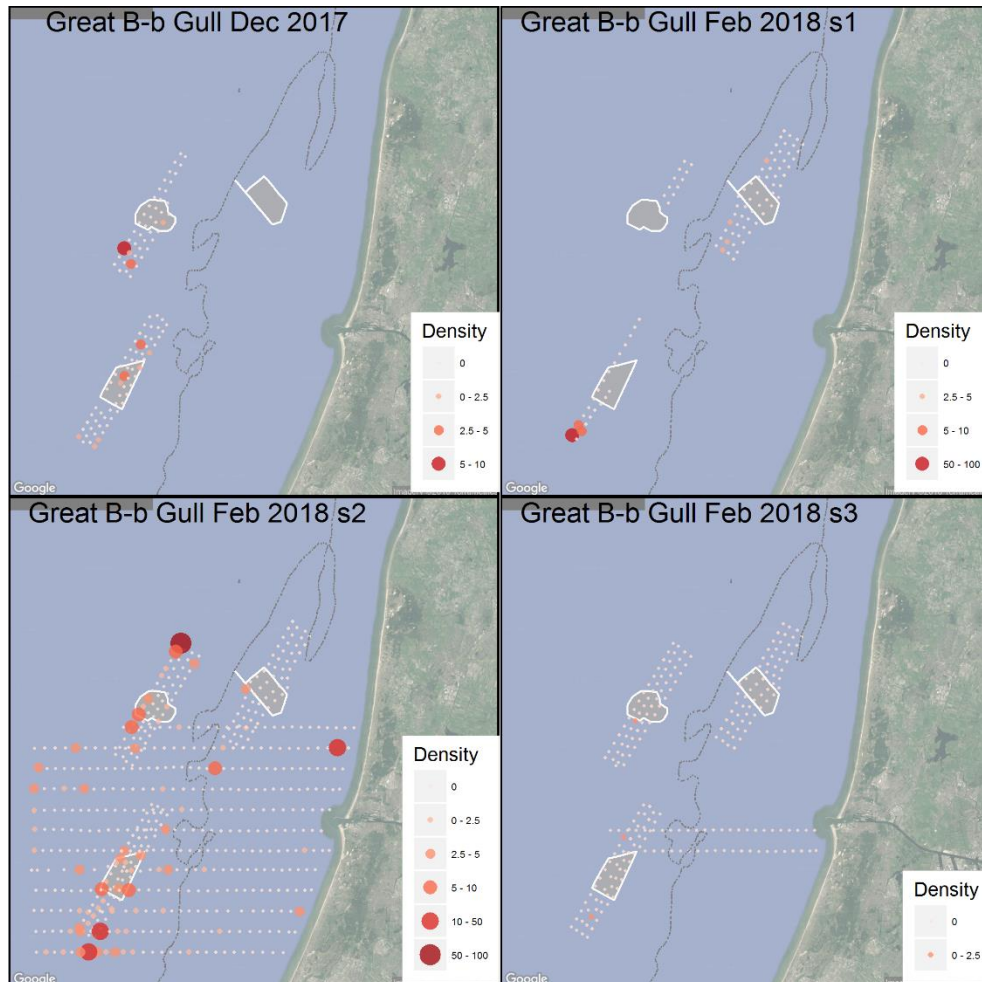


Figure 5.39. Observed density (birds/km²) of Great Black-backed Gull during LUD-T3 surveys 2017-2018. Densities have been corrected for distance bias.

Great Black-backed Gull, 2002-2018

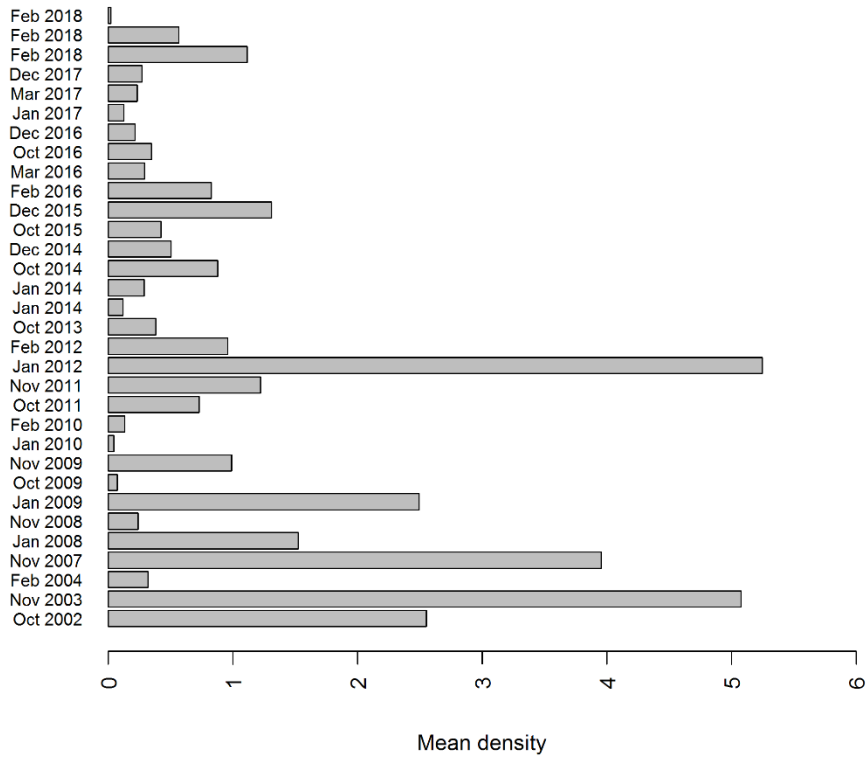


Figure 5.40. Mean observed density (birds/km²) of Great Black-backed Gull in the entire surveyed area during OWEZ, PAWP and LUD pre- and post-construction surveys. Densities have been corrected for distance bias.

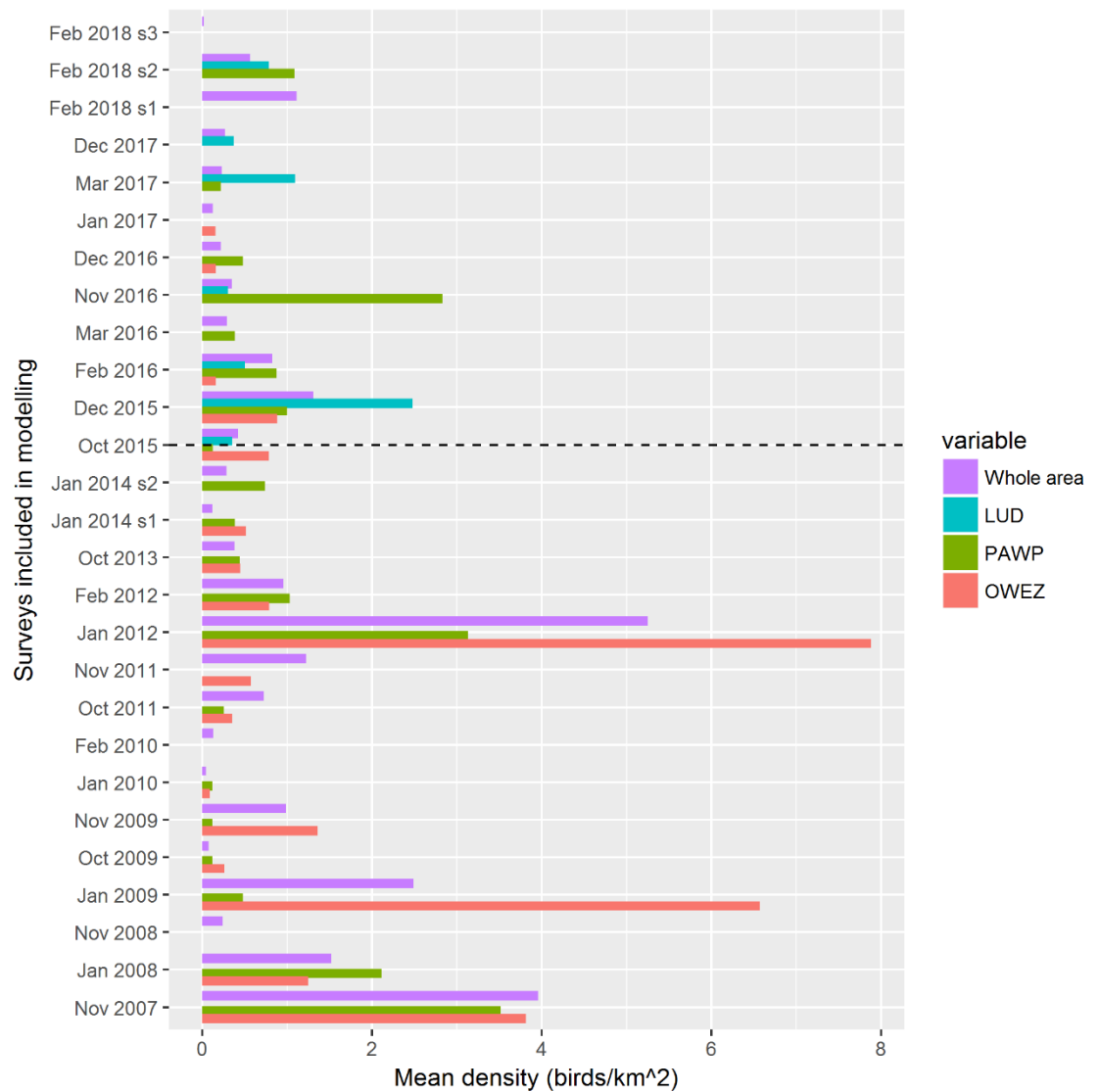


Figure 5.41. Mean density of Great Black-backed Gull during surveys included in the modelling. The mean density within each of the three wind farm footprints (OWEZ, PAWP and LUD) is shown as well as the mean in the whole surveyed area (including wind farms). Surveys above the dashed line are LUD post-construction surveys.

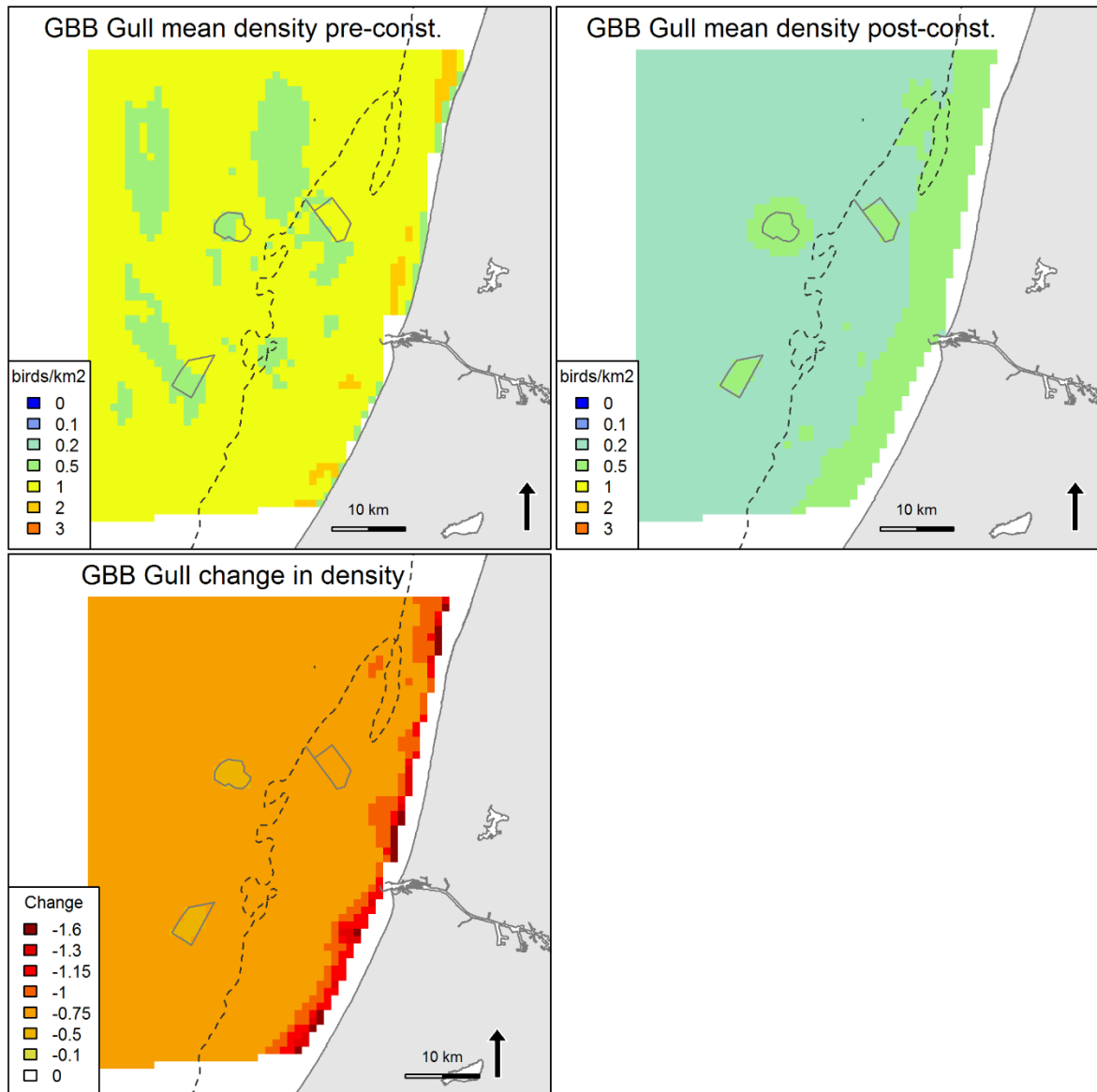


Figure 5.42. Predicted mean density (birds/km²) and distribution of wintering Great Black-backed Gull during eight LUD pre- and 12 LUD post-construction surveys, and the relative change in predicted density between the two periods. Note that all included surveys are OWEZ and PAWP post-construction

5.3.11 Black-legged Kittiwake *Rissa tridactyla*

High densities of Black-legged Kittiwakes were recorded during the LUD-T3-01 and LUD-T3-02 surveys, and medium densities during the LUD-T3-03 survey (Figure 5.43). During the December survey rather high densities were recorded inside LUD and PAWP. Lower densities were observed close to the coast. After the construction of LUD, a marked increase in the abundance of Black-legged Kittiwakes has been recorded over the whole area, including inside the LUD and PAWP footprints (Figure 5.44, Figure 5.45).

Model results

According to the model higher probability of presence was related to increasing water depth and salinity, - characteristics typical for the North Sea waters of the study area (Appendix A). The PAWP wind farm had a slight negative effect on the presence of kittiwakes. In the positive model, higher salinities and lower current speeds were influential factors, while the PAWP wind farm had a positive effect on densities of Kittiwakes (Appendix A). The explanatory degree of the distribution model for the Black-legged Kittiwake

was fair for the presence-absence part, but low for the positive part of the model (Appendix A). It can be concluded that based on the model results the distribution of Black-legged Kittiwake is strongly governed by the occurrence of North Sea water masses, and no clear displacement or attraction effect of the three wind farms can be detected. However, the predictions indicate a slightly stronger increase in densities inside PAWP during the post-construction period than in most other parts of the area, hence a small effect of attraction can be assumed (Figure 5.46).

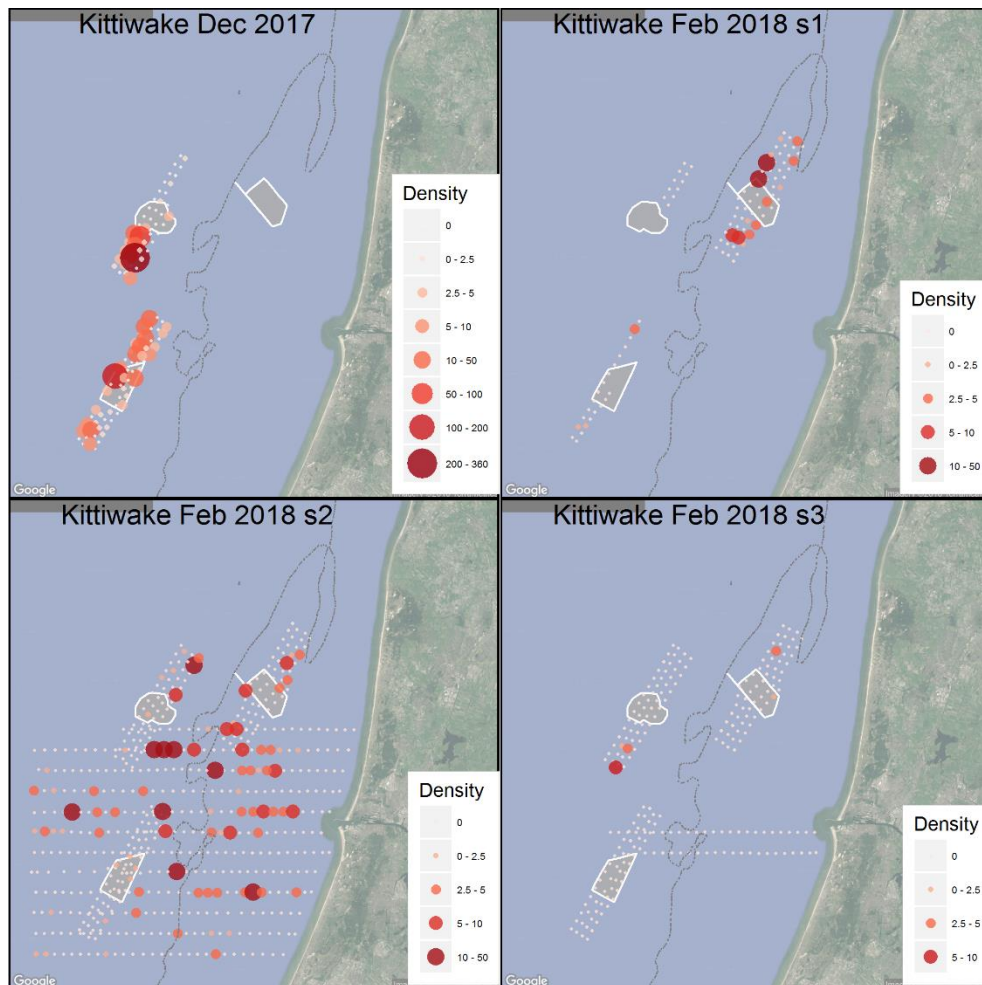


Figure 5.43. Observed density (birds/km²) of Black-legged Kittiwake during LUD-T3 surveys 2017-2018. Densities have been corrected for distance bias.

Kittiwake, 2002-2018

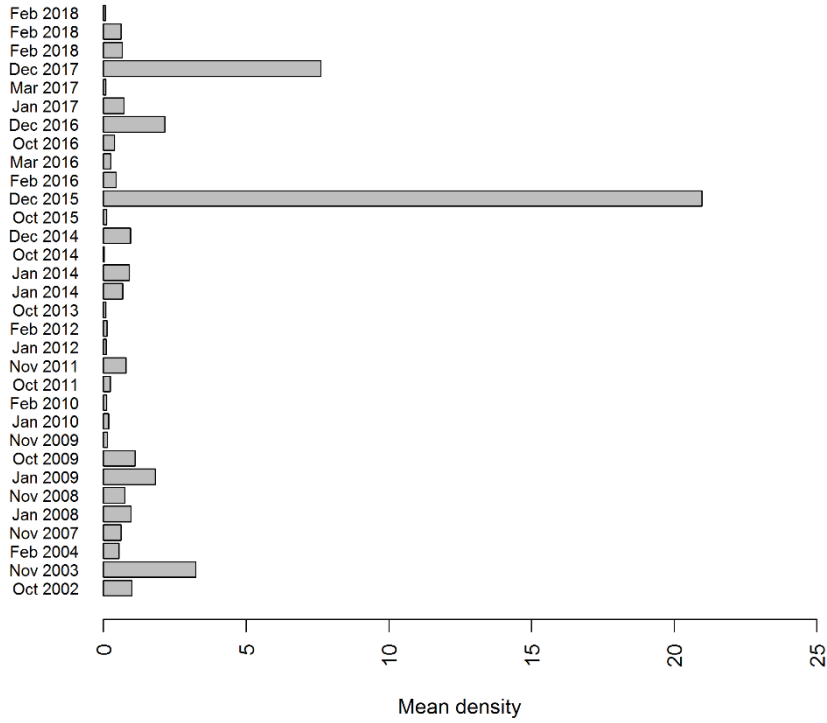


Figure 5.44. Mean observed density (birds/km²) of Black-legged Kittiwake in the entire surveyed area during OWEZ, PAWP and LUD pre- and post-construction surveys. Densities have been corrected for distance bias.

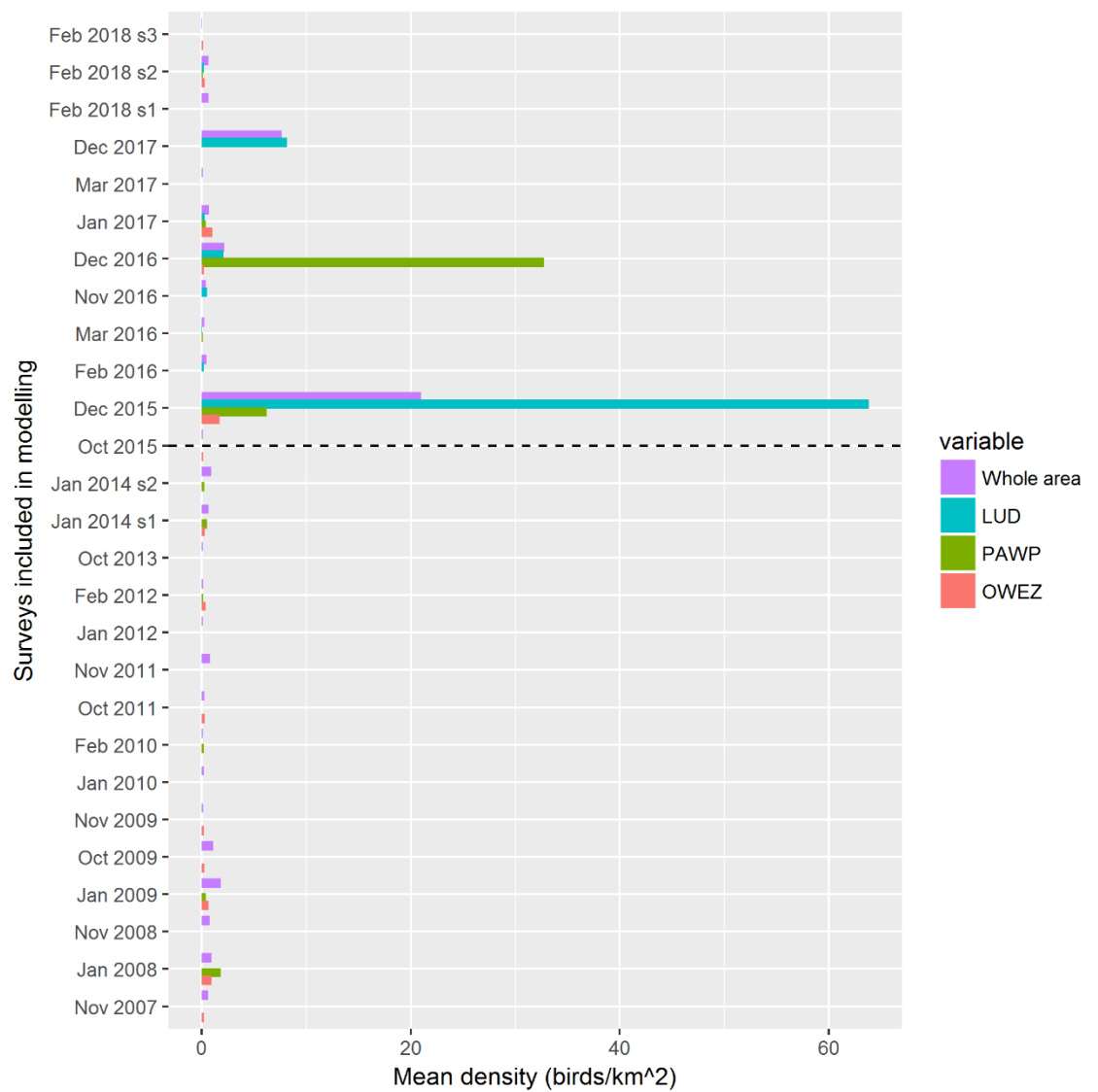


Figure 5.45. Mean density of Black-legged Kittiwake during surveys included in the modelling. The mean density within each of the three wind farm footprints (OWEZ, PAWP and LUD) is shown as well as the mean in the whole surveyed area (including wind farms). Surveys above the dashed line are LUD post-construction surveys.

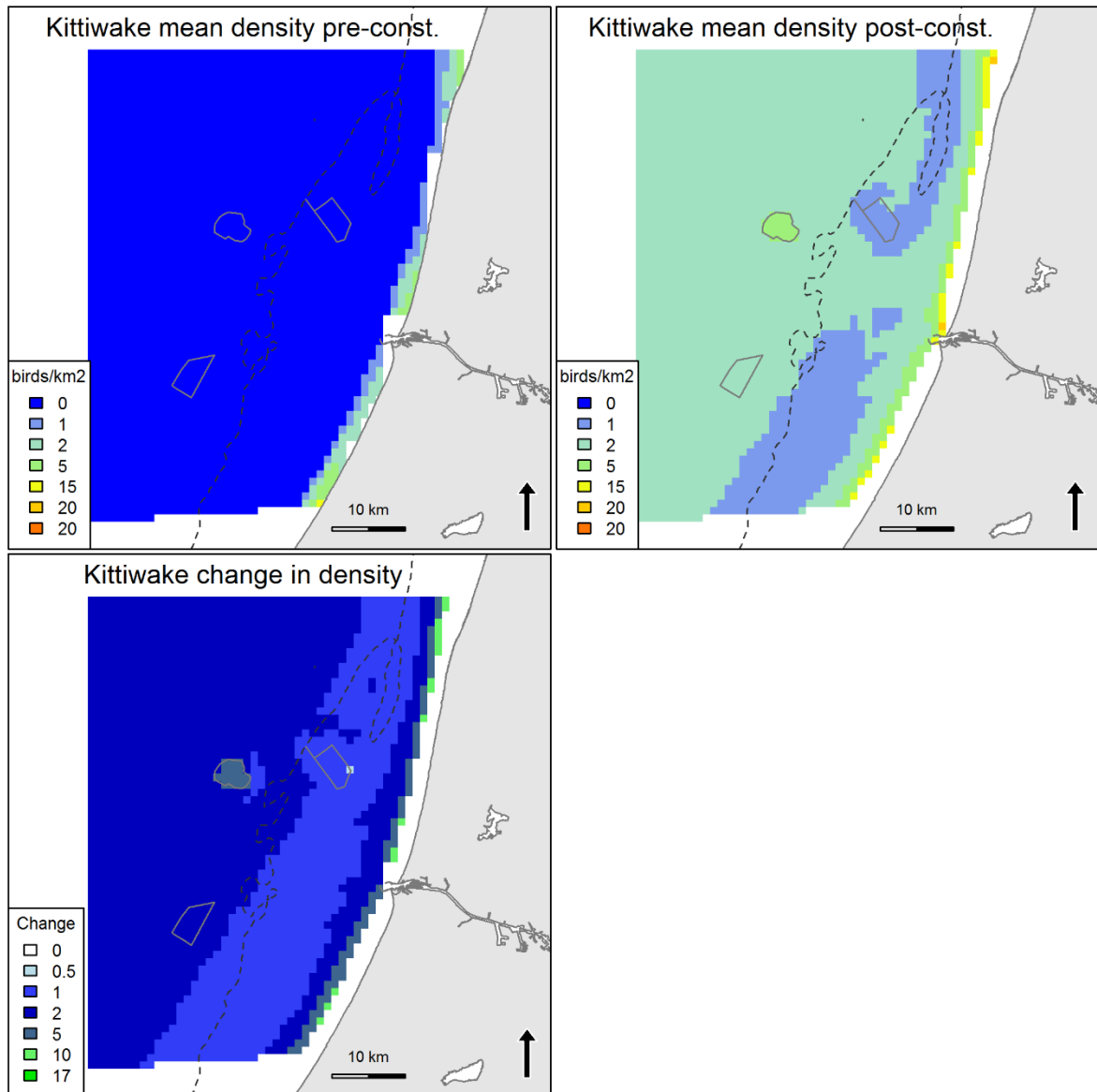


Figure 5.46. Predicted mean density (birds/km²) and distribution of wintering Black-legged Kittiwake during eight LUD pre- and 12 LUD post-construction surveys, and the relative change in predicted density between the two periods. Note that all included surveys are OWEZ and PAWP post-construction surveys.

5.3.12 Common Guillemot *Uria aalge*

During the LUD-T3 surveys high densities of Common Guillemot were recorded during all three surveys (Figure 5.47), and birds were seen in all three wind farms but in lower numbers than outside. The overall distribution reflected higher mean densities in the offshore parts of the study area, but with some high densities also close to the coast and lowest densities in between (Figure 5.47). A marked variation is apparent in the recorded densities of Common Guillemots between the 32 surveys of which 27 were included in the distribution analyses (Figure 5.48 Figure 5.49). After the construction of LUD, a marked increase in the abundance of Common Guillemot has been recorded over the whole area, including inside the OWEZ and PAWP footprints (Figure 5.48, Figure 5.49).

Model results

According to the model the probability of presence increased with increasing salinity and current speeds within areas with water depths between 15 and 25 m (Appendix A). Probability of presence was significantly ($p < 0.01$) lower in all wind farm footprints and within the 2km buffer around PAWP ($p < 0.01$) and OWEZ ($p < 0.05$). Higher density was further explained by increasing frontal activity (current gradient), both low and high current speeds and higher salinities. Significantly lower densities (when present) were predicted inside the footprints of PAWP ($p < 0.01$) and LUD ($p < 0.05$), but not inside the 2 km buffer zones (Appendix A). Hence, the model indicated a significant short-scale avoidance from all three wind farms (< 1 km), and strongest from PAWP (Figure 5.50). The explanatory degree of the distribution model for the Common Guillemot was fair for both the presence-absence (26 %) and the positive part (15 %) of the model and the predictive accuracy in terms of AUC and Spearman's correlation was high (Appendix A).

When evaluating predictions, by predicting on model input data with and without the response of the wind farm the results indicate that there is on average a 37% decrease in probability of detecting a Common Guillemot inside the LUD wind farm, in comparison to a case without a wind farm (Figure 5.51). When both model parts are combined there is on average a 52% decrease in density within the wind farm when comparing model predictions including the wind farm response (factor variable) with model predictions excluding the wind farm response (Figure 5.51). This can be regarded as an indication of level of displacement, however it is important to consider the model errors as well as potential unknown uncertainties around the estimates (Figure 5.51). For comparison, the levels of displacement for PAWP and OWEZ were 47%/70% for the predicted probabilities and 30%/28% for the predicted densities.

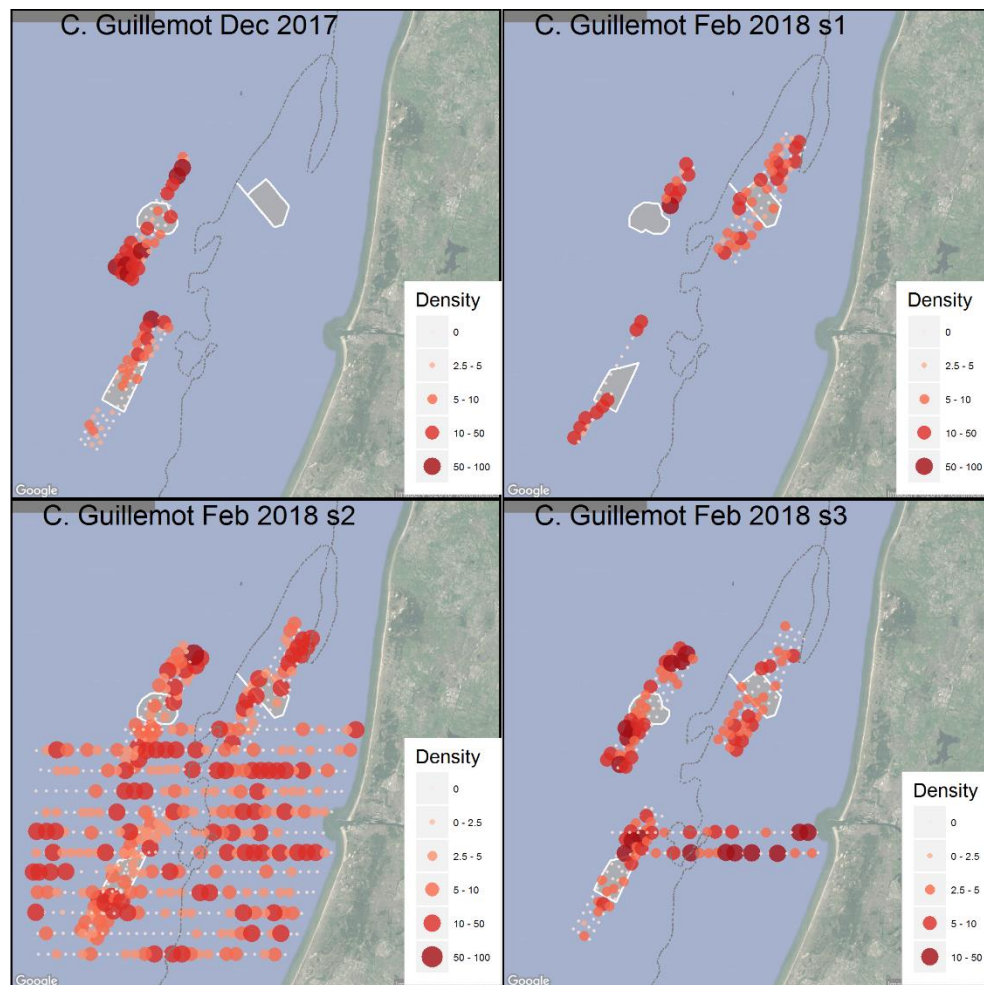


Figure 5.47. Observed density (birds/km²) of Common Guillemot during LUD-T3 surveys 2017-2018. Densities have been corrected for distance bias.

Common Guillemot, 2002-2018

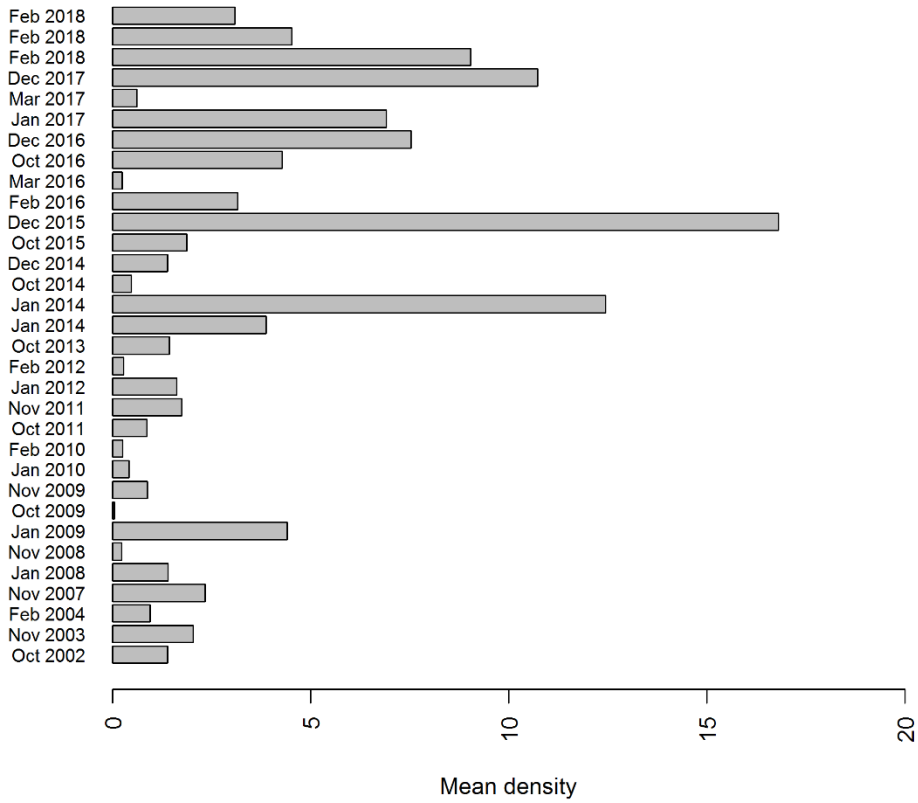


Figure 5.48. Mean observed density (birds/km²) of Common Guillemot in the entire surveyed area during OWEZ, PAWP and LUD pre-construction surveys (indicated by a blue rectangle) and post-construction surveys (green rectangle). Densities have been corrected for distance bias.

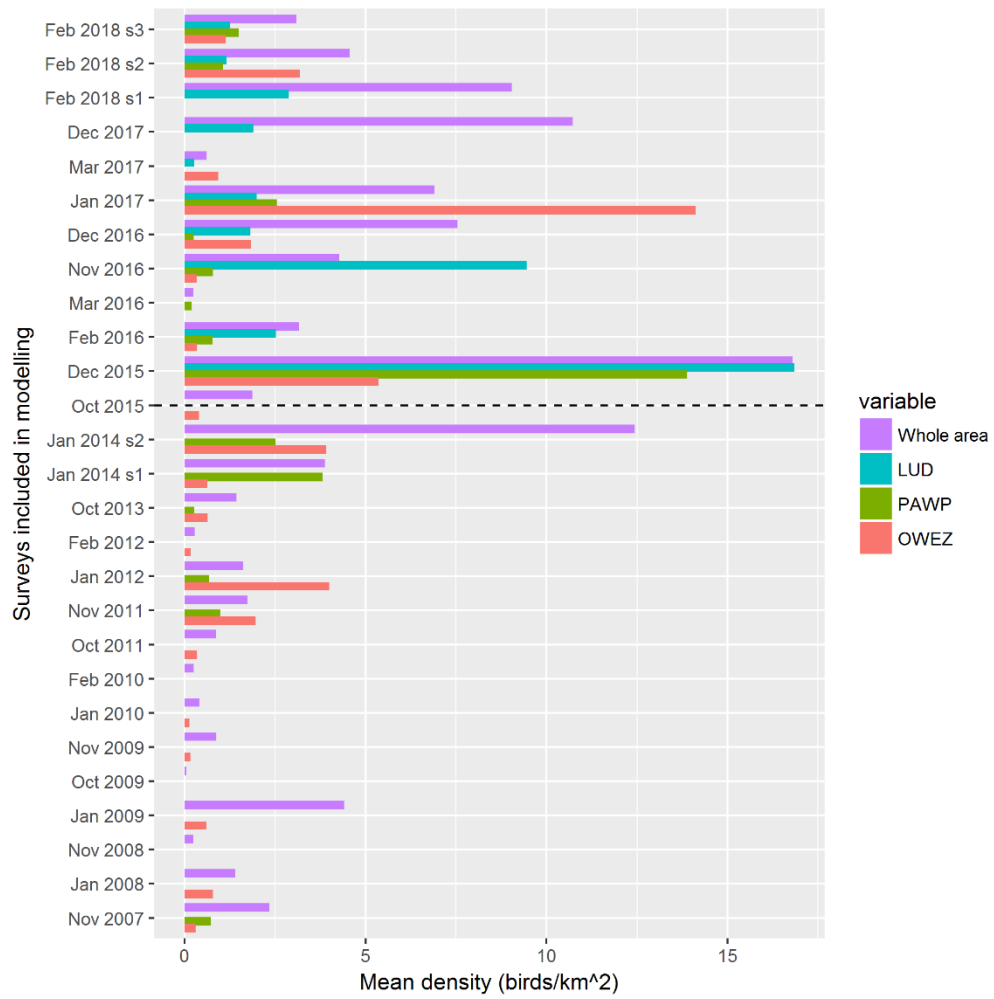


Figure 5.49. Mean density of Common Guillemot during surveys included in the modelling. The mean density within the three wind farm footprints (OWEZ, PAWP and LUD) are shown as well as the mean in the whole surveyed area. Surveys above the dashed line are LUD post-construction surveys.

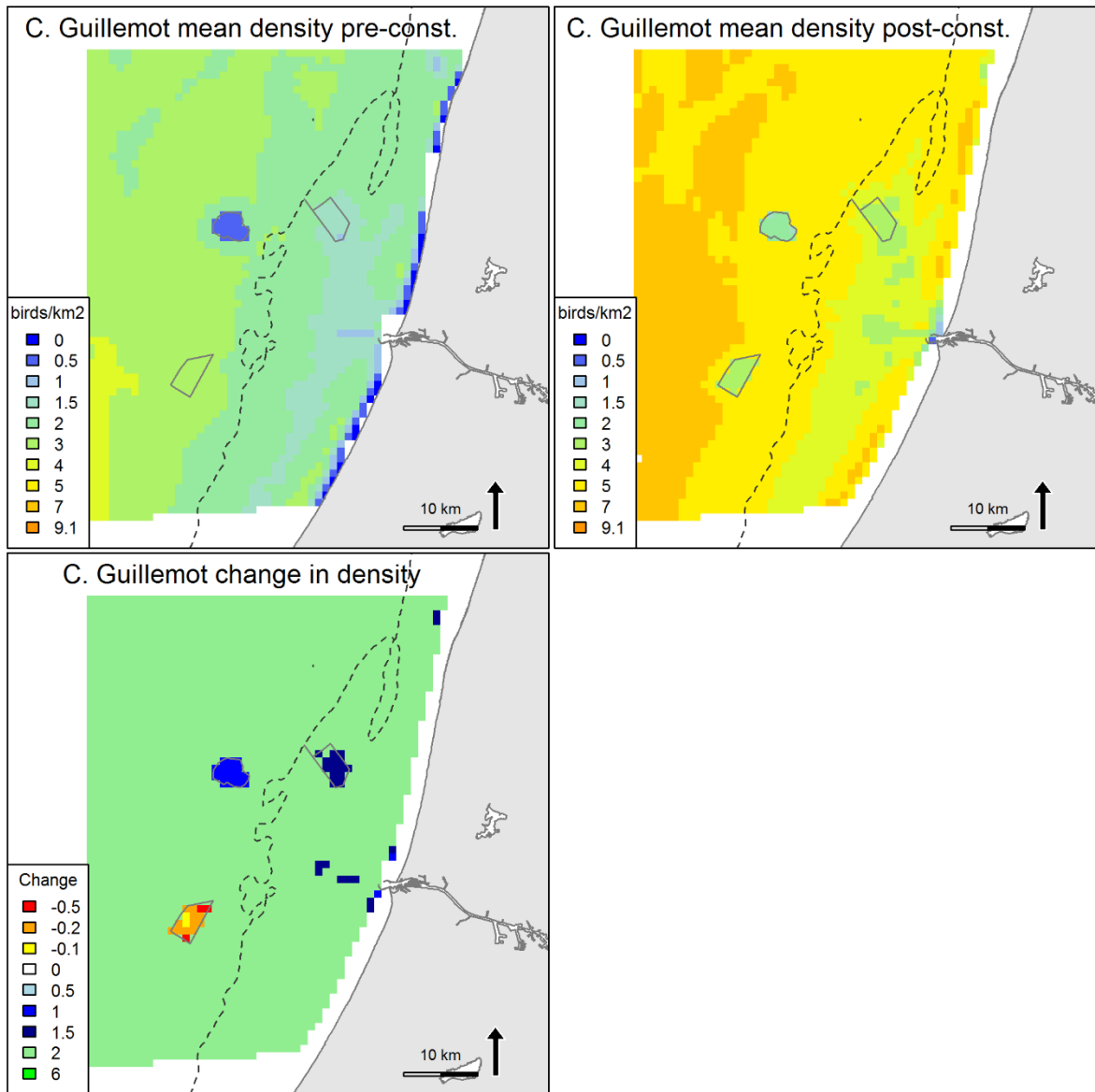


Figure 5.50. Predicted mean density (birds/km²) and distribution of wintering Common Guillemot during eight LUD pre- and 12 LUD post-construction surveys, and the relative change in predicted density between the two periods. Note that all included surveys are OWEZ and PAWP post-construction surveys.

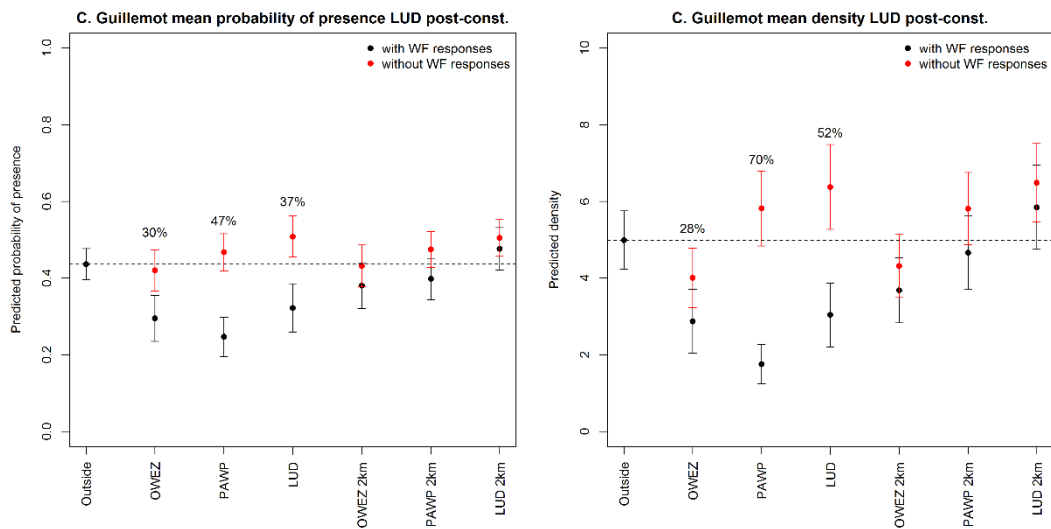


Figure 5.51. Model predictions (on model data) for Common Guillemot during the eight LUD post-construction surveys, with (fitted values) and without the response of the wind farm, when taking into account the dynamic environmental conditions. The difference indicate a mean displacement with model errors, i.e. what is the difference in probability of presence (to the left) or the density (to the right) if the wind farm(s) would not be present compared to a WF present. The mean displacement in % is indicated above the estimates for the footprints (GAMM model errors, SE, are indicated as error bars).

5.3.13 Razorbill *Alca torda*

During the LUD-T3 surveys Razorbills were frequently observed in offshore waters, including in all three wind farms, and more birds were recorded during the two first surveys (Figure 5.52). The overall distribution and trends during the monitoring projects resembles that of the Common Guillemot. After the construction of LUD, a marked increase in the abundance of Razorbill has been recorded over the whole area, including inside the LUD and PAWP footprints (Figure 5.53, Figure 5.54).

Model results

Highest probability of presence was associated with areas with lower water depth and high current speeds found in the interface between coastal waters and the North Sea. The negative effect of the footprints of LUD and PAWP on the presence of Razorbills was significant, while no significant effect was noted for OWEZ, and unlike the Common Guillemot no significant effect of the wind farm footprints on densities of Razorbills was detected (Appendix A). Yet, the response levels (Appendix A) indicate a lower probability of presence within all three wind farms, including LUD and therefore a reduction in the predicted density in LUD between pre- and post-construction can be seen (Figure 5.55). When evaluating predictions, by predicting on model input data with and without the response of the wind farm the results indicate that there is in average a 37% decrease in probability of detecting a Razorbill inside the LUD wind farm, in comparison to a case without a wind farm. However in both cases the probability is low, around 0.06 and 0.11 respectively. When both model parts are combined there is a 52% decrease in density within the wind farm when comparing model predictions including the wind farm response (factor variable) to model predictions excluding the wind farm response (Figure 5.56). This can be regarded as an indication of level of displacement, however it is important to consider the model errors as well as potential unknown uncertainties around the estimates (Figure 5.56). For comparison, the levels of displacement for PAWP and OWEZ were 53%/72% for the predicted probabilities and 36%/52% for the predicted densities.

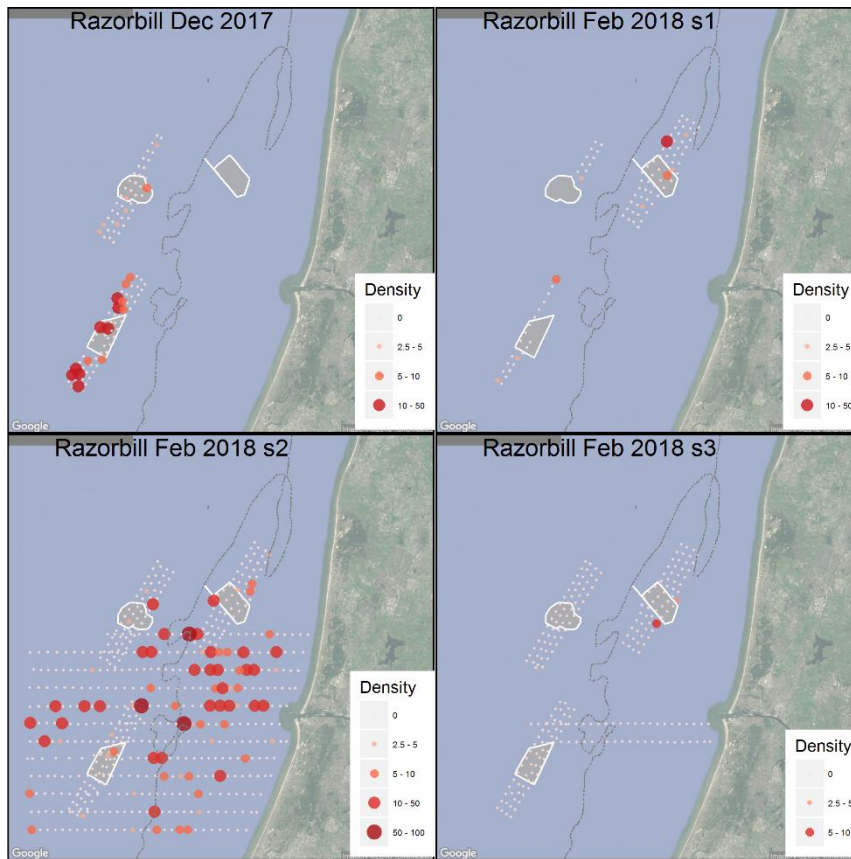


Figure 5.52. Observed density (birds/km²) of Razorbill during LUD-T3 surveys 2017-2018. Densities have been corrected for distance bias.

Razorbill, 2002-2018

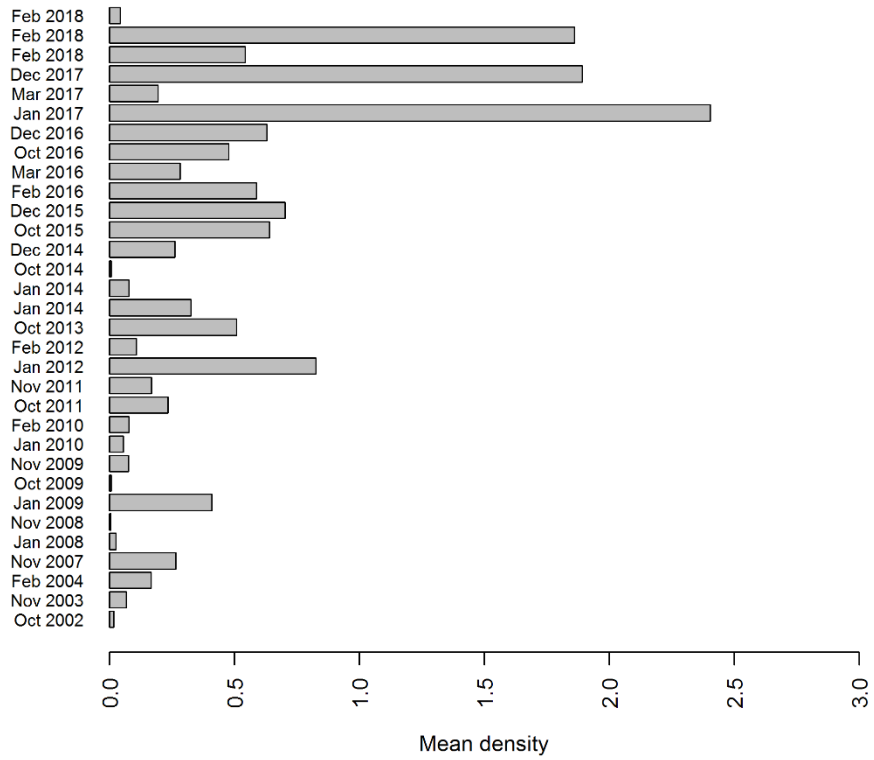


Figure 5.53. Mean observed density (birds/km²) of Razorbill in the entire surveyed area during OWEZ, PAWP and LUD pre- and post-construction surveys. Densities have been corrected for distance bias.

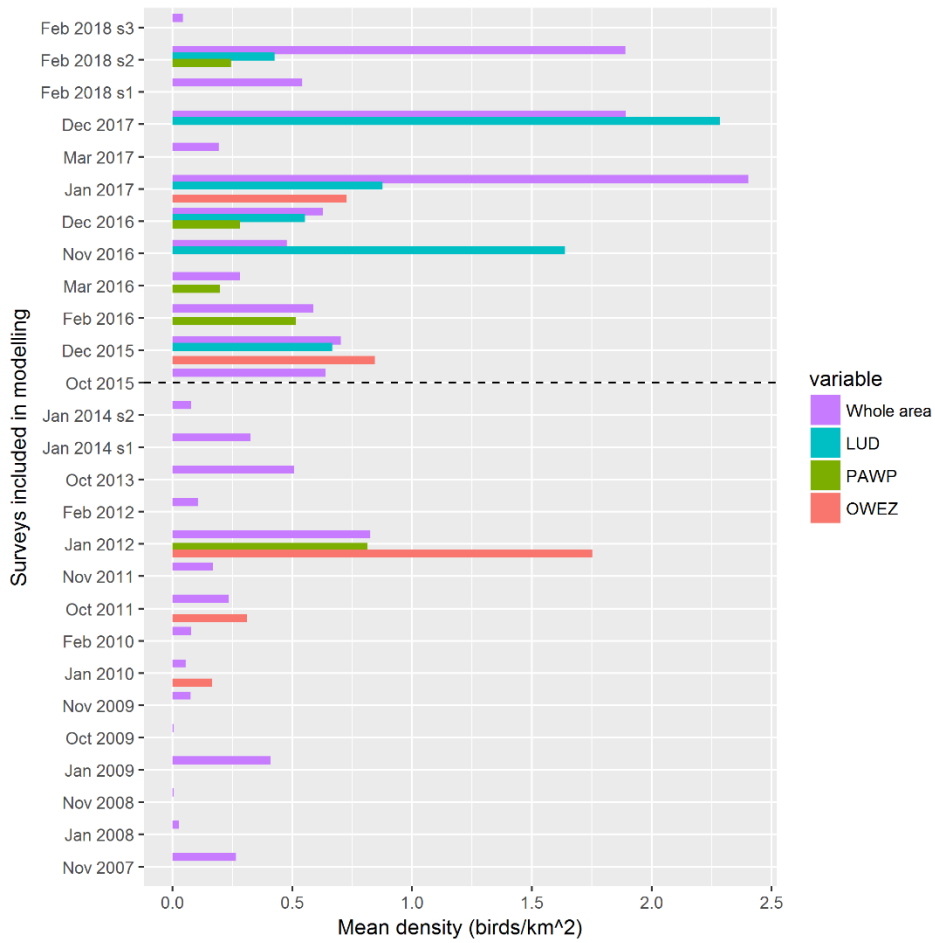


Figure 5.54. Mean density of Razorbill during surveys included in the modelling. The mean density within the three wind farm footprints (OWEZ, PAWP and LUD) are shown as well as the mean in the whole surveyed area. Surveys above the dashed line are LUD post-construction surveys.

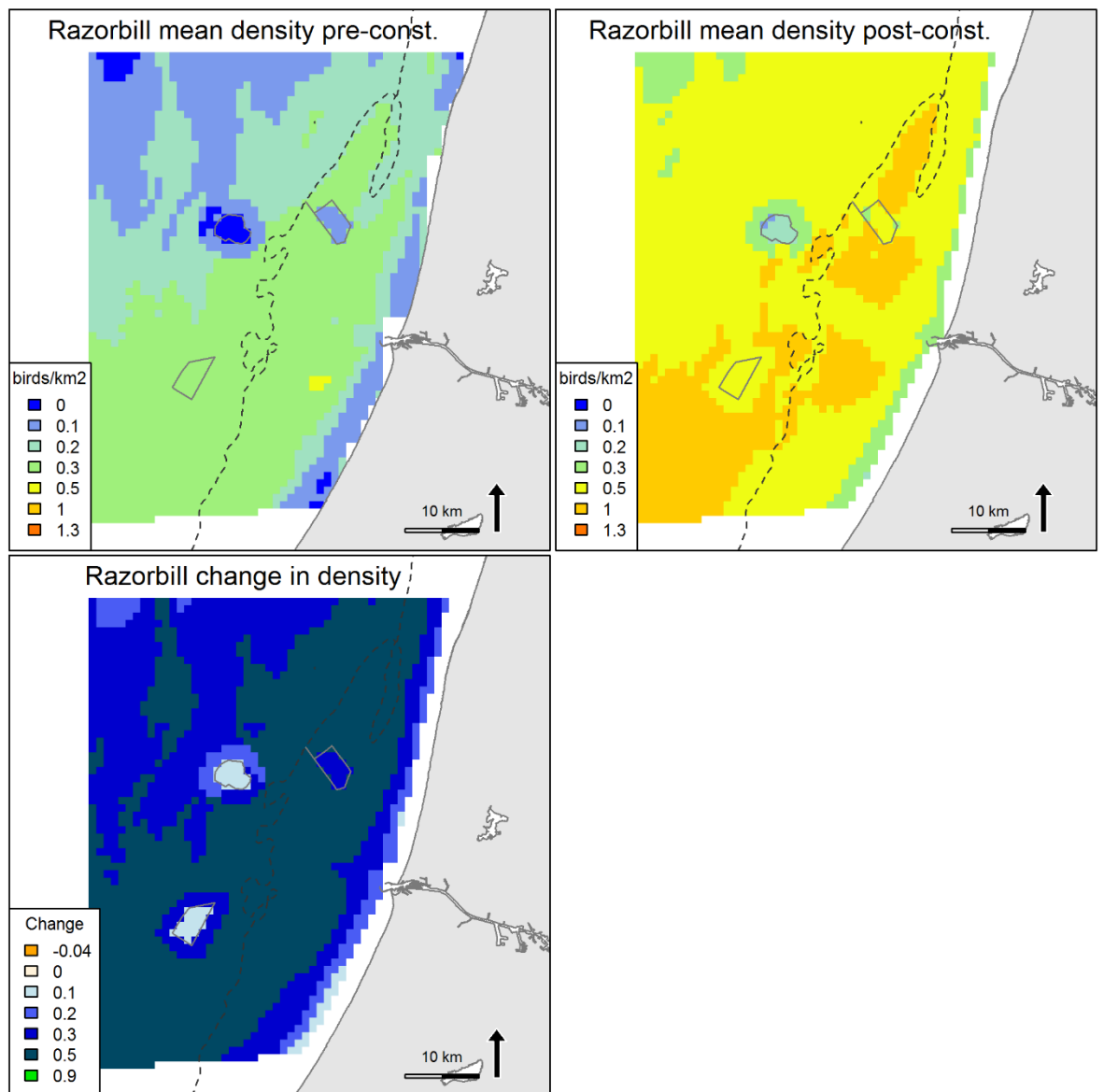


Figure 5.55. Predicted mean density (birds/km²) and distribution of wintering Razorbill during eight LUD pre- and 12 LUD post-construction surveys, and the relative change in predicted density between the two periods. Note that all included surveys are OWEZ and PAWP post-construction surveys.

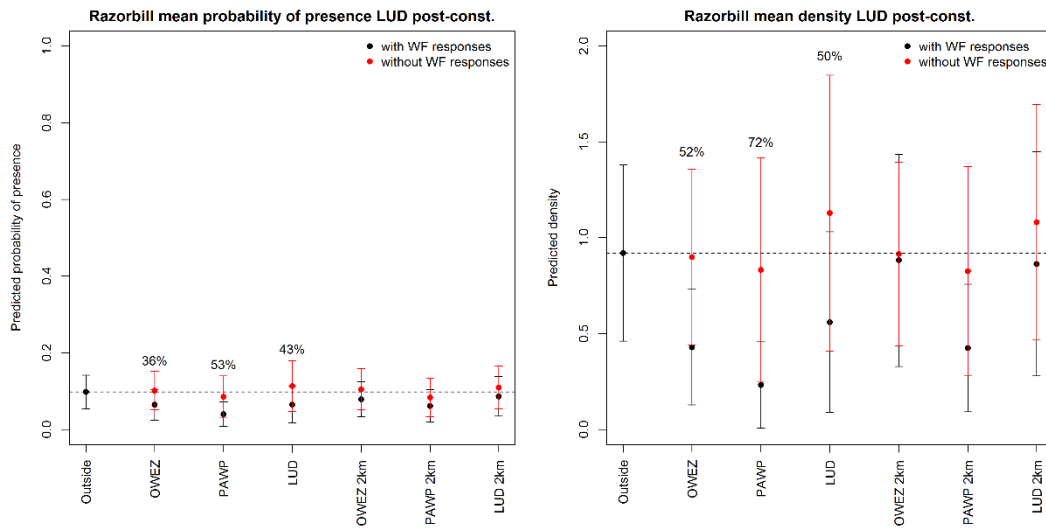


Figure 5.56. Model predictions (on model data) for Razorbill during the eight LUD post-construction surveys, with (fitted values) and without the response of the wind farm, when taking into account the dynamic environmental conditions. The difference indicate a mean displacement with model errors, i.e. what is the difference in probability of presence (to the left) or the density (to the right) if the wind farm(s) would not be present compared to a WF present. The mean displacement in % is indicated above the estimates for the footprints (GAMM model errors, SE, are indicated as error bars).

5.3.14 Marine mammal observations

A total of 116 sightings of marine mammals were made during the T-3 surveys, of which the majority (91) were harbour porpoise *Phocoena phocoena*, which were recorded in the whole area, including inside PAWP and LUD (Figure 5.57). With these observations the total number of marine mammal observations during the LUD Seabird monitoring program summed up to 480, of which 360 were harbour porpoises (Table 8). Although these data have not been analysed they form a rich source of information about the changes in distribution of marine mammals during the post-construction phases of the three wind farms.

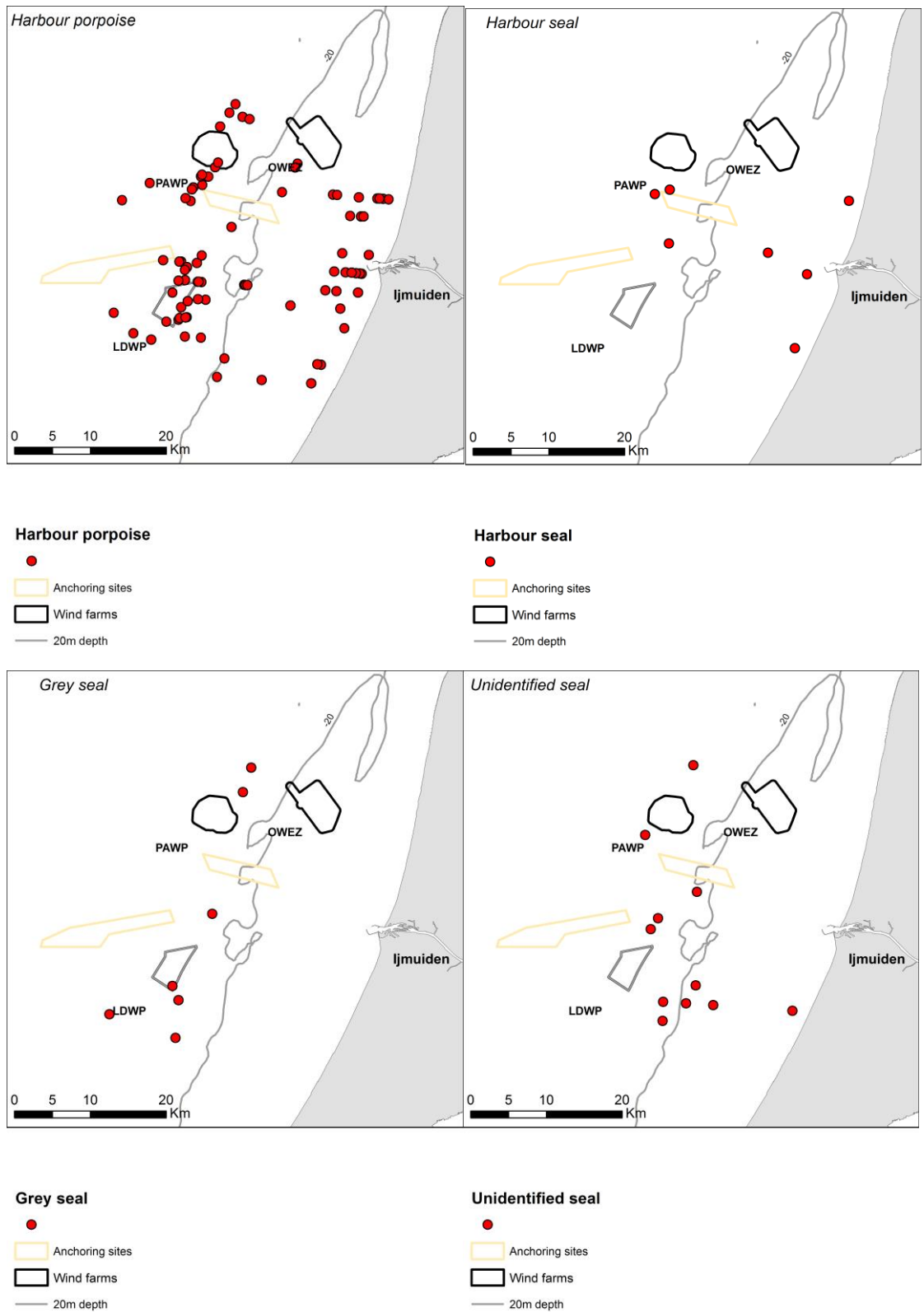


Figure 5.57. Observations of marine mammals during the LUD-T3 surveys 2017-2018. No corrections for possible double registrations have been made.

Table 8. Overview of observations of marine mammals during the LUD Seabird monitoring program 2014-2018

	Harbour porpoise	Harbour seal	Grey seal	Indet. seal sp.	Indet. dolphin sp	Total
T-0	108	4	0	2	1	115
T-con	20	3	1	0	0	24
T-1	51	15	8	3	0	77
T-2	90	38	12	8	0	148
T-3	91	7	7	11	0	116
Total	360	67	28	24	1	480

6 Discussion and conclusion

6.1 Characterisation of LUD site

The abundance and distribution of the different species of seabirds recorded during the Offshore Wind Farm Eneco Luchterduinen (LUD) T3 surveys largely follow the patterns from the LUD baseline, T-Constr, T1 and T2 periods with the overall impression that the waters around LUD are mainly characterised by high densities of Common Guillemot and low to moderate densities of other species of seabirds. However, during the LUD T3-02 survey, high abundance of Northern Gannet and Razorbill was also recorded.

A common feature of the surveys undertaken during the LUD Seabird Monitoring Program is the significant variation in the abundance of several species of seabirds from survey to survey in the whole region off the Dutch mainland coast, including inside the three wind farms. The high level of variability is in line with the experience from the monitoring undertaken in relation to PAWP and OWEZ (Leopold et al. 2013), although the LUD surveys covered the area south of PAWP and OWEZ in more detail. Superimposed on the short-imposed variability a general increase in the density of Northern Gannet, Razorbill and Common Guillemot has been recorded in the Dutch coastal waters since the onset of seabird monitoring related to OWEZ and PAWP in 2002.

The variability of seabird abundance at LUD is clearly related to the location of the wind farm at 18-22 m water depth in an area characterised by being at the interface between coastal and offshore water masses as reflected by the gradients in salinity, current speed and direction (Figure 6.1). Concentrations of several species of seabirds are located in the coastal water mass, whereas higher densities of pelagic species are found in the North Sea water mass in the deeper parts of the North Sea west of LUD. As a result of the dynamics of coastal and North Sea masses driven by tidal and estuarine circulations the distribution of all seabirds at the LUD is very dynamic and dominated by species which occur widely across the North Sea during winter. At the same time it should be noted that the interface between coastal and North Sea water masses marks a zone of hydrographic frontal activity off the Dutch coast which has a concentrating effect on the distribution of species like Lesser Black-backed Gull, Herring Gull, Great Black-backed Gull and Common Guillemot. As a consequence, the variation in the abundance of seabirds may be amplified as the front sweeps back and forth, with high abundance being recorded when the LUD site coincides with the location of the front.

Several species are strongly associated with the estuarine coastal water mass with a salinity below 32 psu, and few of these birds use the LUD site. Slight increases in the abundance of these species at the LUD have been observed during periods with an extensive coastal current. The species are Divers, Great Crested Grebe, Black-headed Gull and Common Gull.

The density of Northern Gannets in the region around LUD shows a general increasing density gradient from the coastal water mass to the North Sea water mass with the LUD located on the lower end of this gradient. As the Gannets are associated with the North Sea water mass densities at LUD tend to increase during periods characterised by a narrow width of the coastal current.

The highest densities of Great Cormorants are found in the shallowest areas, as well as in LUD, PAWP and OWEZ. No concentrations of feeding Common Scoter have been recorded during the LUD monitoring program, and the species is mainly recorded flying along the coast (Leopold et al. 2013). Even if food resources (*Spisula subtruncata*) may return to former levels along the Dutch coast, the LUD is not likely to host larger numbers of Common Scoters.

The monitored region is also characterised by shipping lanes with intense ship traffic. However, when evaluated against the oceanographic variability ship traffic only turned out to affect the distribution of Red-throated Diver, Great Crested Grebe and Little Gull negatively.

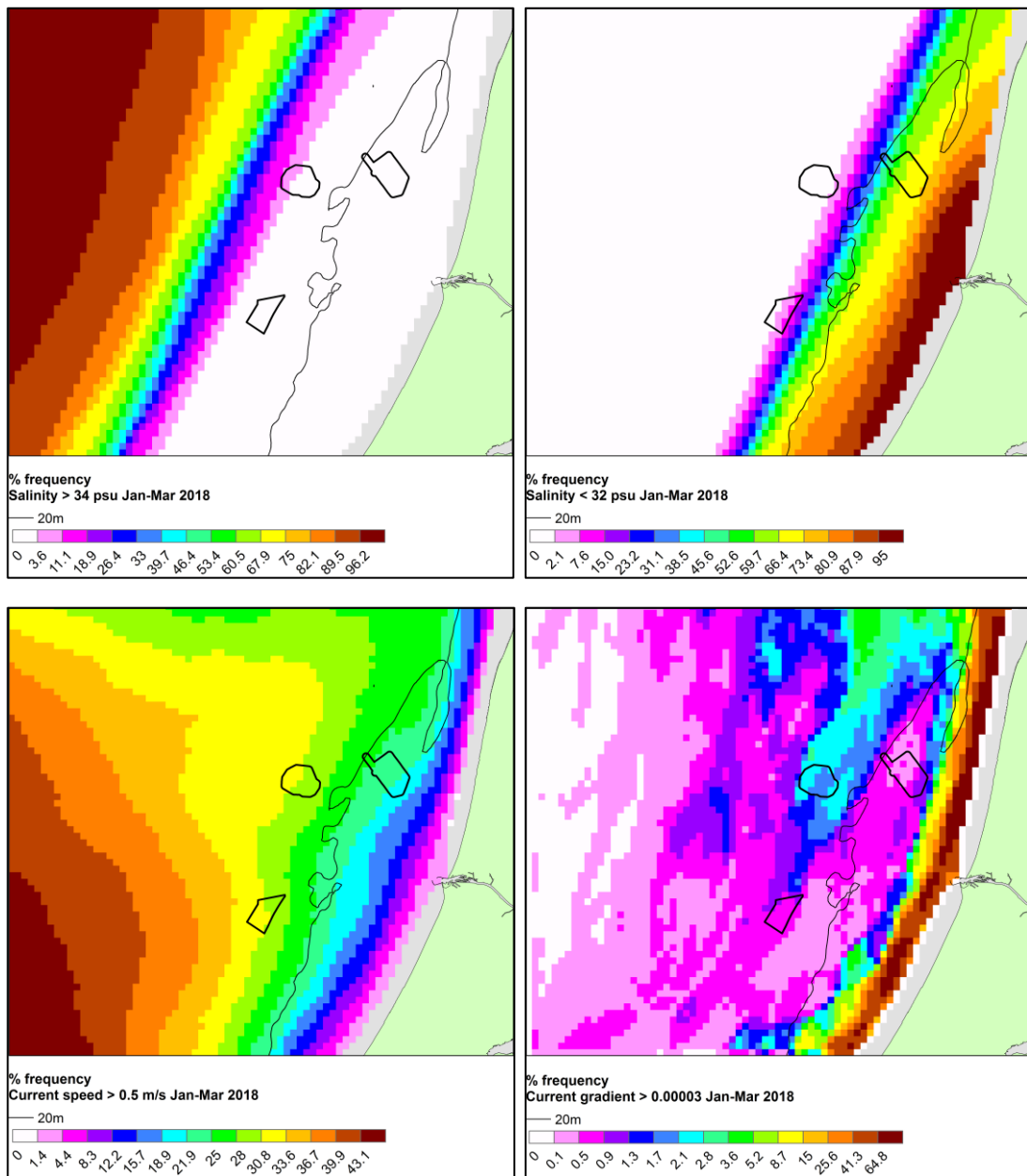


Figure 6.1. The distribution of the coastal and North Sea water masses and currents in relation to the location of the LUD site as reflected by the frequency (%) of modelled salinity (above 34 psu or below 32 psu), current speed (above 0.5 m/s) and current gradient (above 0.00003) at 10 m depth. The hydrodynamic model data from the period January-March 2018 have been processed. Areas close to the coast which are shallower than 10 m are shown with grey colour indicating no data values.

6.2 Monitoring design

The seabird winter density data which constitute the LUD baseline and post-construction periods have been collected over a 13-year long period of time. As the observed densities evidently display a high degree of short-term variability in response to the dynamics of the oceanography off the Dutch mainland coast the description of the distribution of seabirds at LUD and determination of the responses to this wind farm as well as to OWEZ and PAWP had to be based on an approach which solved the statistical challenge of

detecting a potentially small displacement effect in the presence of seabird movements and prominent dynamics of their marine habitats.

Given the attenuation of the displacement effect with distance from the wind farm, before-after and BACI designs (standard, repeated, asymmetrical) are all known to have less power than regression-based gradient designs (Ellis & Schneider 1997). However, in complex and dynamic habitats like the one found in the development area off the Dutch coast, a spatially explicit model design is preferred which includes all the factors causing the large variability and account for any unexplained spatial autocorrelation (Perez-Lapena et al. 2010). Yet, even with power considerations based on long-term monitoring data and with a considerable spatial coverage the challenge in the LUD Seabird Monitoring Program has been to disentangle the displacement effect from natural variability in the abundance of seabirds at the site of the wind farm as the effect of changing habitat might exceed the displacement effect.

Although model-based power and impact assessments are increasingly used for designing monitoring programs at offshore wind farms (e.g. MRSea Package in R <https://github.com/lindesaysh/MRSea/releases/tag/v1.0-beta>), confounding effects of wind farm and dynamic oceanographic habitat features on local seabird abundance are usually not accounted for, causing a risk for ambiguous monitoring results prone to type I errors (a result erroneously pointing at no impact) or to type II errors (a result erroneously pointing at an impact). In shelf environments local animal abundance typically changes over the scale of less than one day (Markones et al. 2008, Skov & Thomsen 2008), hence taking account of such short-term changes in local oceanography and its effect on animal distribution is a general constraint for detecting actual displacement of animals from offshore wind farms. The model-based solution developed for the LUD Seabird Monitoring Program made it possible to determine displacement effects by accounting for the short-term changes in the specific oceanographic habitats by integrated use of hind-casted data from a dedicated high-resolution hydrodynamic model. By describing the general habitat relationships during the surveys the changes in the recorded number of the different species of seabirds caused by changes in habitat features unrelated to the wind farms could be determined. In the same way, the changes in the distribution of seabirds which was caused by the wind farms could be determined.

6.3 Modelling approach and performance

The modelling approach has been designed to take account of environmental variability and describe the probability of presence and density in the wind farm footprints and adjacent areas in comparison to elsewhere in the study area. To avoid fitting specific spatial patterns related to the survey instance (snapshots) we decided not to include geographic predictors in the models. Relying on environmental space (environmental predictors) enables extrapolations in space and time and a description of habitat preferences. Models for species with clear habitat preferences therefore also results in models with a higher predictive accuracy and explanation degree. For example, divers and grebes are strongly related to the coastal water mass while Common Guillemot is strongly related to the more saline North Sea water mass and therefore also the explanation degree and predictive accuracy of these models is higher than for species with a more random distribution (e.g. gull species, see Appendix A). Absence of clear and strong environmental preferences (based on the predictors included in the analyses) are also important results and the factor variable including wind farms and buffers still indicates for all species whether there is a significant displacement or attraction effect.

It is nevertheless important to note that there is uncertainty related to all modelling exercises. This study is no exception and there is uncertainty related to each step of the modelling process as well as to the input data. Because it is not possible to assess all uncertainty components of the modelling exercise and data it is also not possible to estimate the overall uncertainty of the results. For example, the standard errors indicated in the estimated level of displacement are only describing the error related to the statistical models. The effort and spatial extent of the surveys are not the same which might cause a bias and this is also important to keep in mind when comparing mean densities between surveys. The OWEZ and PAWP surveys have a more northerly distribution than the LUD pre- and post-construction surveys. The effect of this potential spatial bias is however assumed to be small. The long-term temporal trend is accounted for in the models

on the survey level, but it could have been possible to also assess the trend by including a factor describing the year as well.

The results, in terms of displacement, of this study are, however, highly similar to other studies using other approaches which is an indication of reliability (see e.g. Welcker and Nehls 2016). In the present study the displacement effect is studied, however, what this means in terms of population impacts is unknown. An approach as used in this study capable of describing suitable habitats (not constrained by coordinates) will be highly useful in coming studies with the aim of defining a potential population impact.

6.4 Displacement and attraction effects

The LUD-T1 and LUD-T2 reports indicated that high power would be achievable after LUD-T3 for Common Guillemot (detection of a displacement of 50%), and possibly for Northern Gannet depending on the number of birds recorded. Displacement effects were detected for both Northern Gannet and Common Guillemot, and additionally also for Razorbill, Lesser Black-backed Gull (LUD only) and Black-legged Kittiwake (PAWP only). Although reductions in the number of several species were recorded and modelled during the LUD post-construction period, these changes were not related to the three wind farms. Red-throated/Black-throated Diver, Great Crested Grebe and Little Gull all declined in the coastal zone, and there was a general decline in the occurrence of Black-headed Gull. The reduction in the presence of Red-throated/Black-throated Diver in OWEZ and in the buffer zones of all three wind farms, of Little Gull in OWEZ and of Black-headed Gull in LUD (footprint and buffer) may therefore be unrelated to displacement, and rather reflects large-scale changes in environmental conditions beyond what was accounted for by the models.

When incorporating all data collected in relation to the monitoring programs of the three offshore wind farms the displacement impact on Northern Gannet from the three footprints was 74% for LUD, 89% for PAWP and 90% for OWEZ. The impact was manifested as a decline in the presence of the birds in spite of an increase in the occurrence of gannets in the offshore zone during the LUD post-construction period. No significant displacement impact on gannets could be detected beyond the footprints. Displacement impact on the presence of Lesser Black-backed Gull was detected in the LUD footprint and of Black-legged Kittiwake in PAWP in spite of a general increase of both species in the offshore zone during LUD post-construction.

The displacement impact on Common Guillemot was manifested as a decline in presence in all three offshore wind farm footprints and also in the PAWP buffer, as well as a decline in the density when present in the footprints of LUD and PAWP. The level of the displacement of guillemots was 52% in LUD, 70% in PAWP and 28% in OWEZ. The displacement impact on Razorbill presence was apparent in the footprints of all three wind farms, but only significant for LUD and PAWP. The level of displacement was 52% in LUD, 72% in PAWP and 52% in OWEZ. The displacements of Common Guillemot and Razorbill were detected in spite of the general recent increase in the occurrence of both species on the Dutch shelf. Overall the displacement of both species was highest in PAWP, followed by LUD and lowest in OWEZ, thus reflecting both the variation in the density of turbines between the three wind farms and the difference in terms of location relative to areas of highest densities of auks. It is difficult to disentangle the effects of turbine density and environmental differences.

Great Cormorants were clearly attracted to the footprints and buffers of all three wind farms. Although higher numbers of Common Gull, Herring Gull and Great Black-backed Gull were also recorded in LUD and PAWP during post-construction, only the Great Black-backed Gull may reflect attraction as this species was recorded in slightly lower numbers everywhere else during this period. Common Gull and Herring Gull displayed a general increase in occurrence off the Dutch coast during this period.

The results of the monitoring program are generally in line with other studies like Krijgsveld (2014) and Welcker & Nehls (2016). The updated results now indicate that displacement of Northern Gannet, Common Guillemot and Razorbill mainly takes place from the footprint and only the Guillemots seem to be displaced from the 2 km buffer around PAWP. The general distribution of diver species in the study area is largely out of range of the windfarms, however the model indicate that divers are also displaced from wind farms

and the buffers when present in accordance with studies (e.g. Welcker & Nehls 2016). Based on these results and the higher level of displacement seen in Guillemots and Razorbills in PAWP as compared to LUD and OWEZ it seems plausible that the distance between turbines plays an important role in determining the strength of displacement of seabirds. Even with a significant length of the post-construction period at OWEZ and PAWP no obvious signs of habituation of these target species to the wind farms have been observed over the period.

7 References

- Buckland, S.T., Anderson, D.R., Burnham, K.P., Laake, J.L., Borchers, D.L., and Thomas, L. 2001. Introduction to distance sampling - Estimating abundance of biological populations. Oxford University Press, Oxford. Burnham, K.P., and Anderson, D.R. 2002. Model Selection and Multimodel Inference: A Practical Information-Theoretic Approach, 2nd ed. Springer-Verlag. ISBN 0-387-95364-7. Camphuysen, C.J. & Garthe, S. 2004. Recording foraging seabirds at sea: standardised recording and coding of foraging behaviour and multi-species foraging associations. *Atlantic Seabirds* 5: 1-23.
- Burnham, K. P. & Anderson, D. R. 2002. Model selection and multimodel inference: a practical information-theoretic approach Springer.
- Camphuysen CJ, Fox TJ, Leopold MF & Petersen IK, 2004. Towards standardised seabirds at sea census techniques in connection with environmental impact assessments for offshore windfarms in the U.K. - A comparison of ship and aerial sampling methods for marine birds, and their applicability to offshore windfarm assessments. NIOZ Report to Cowrie / The Crown Estate.
- Ellis, J.I. & Schneider, D.C. 1997. Evaluation of a gradient sampling design for Environmental impact assessment. *Environmental Monitoring and Assessment* 48: 157–172.
- Hastie, T. & Tibshirani, R. 1990. Generalized Additive Models. Chapman & Hall, London. Leopold M.F., Camphuysen C.J., ter Braak C.J.F., Dijkman E.M., Kersting K. & van Lieshout S.M.J. 2004. Baseline studies North Sea windfarms: Lot 5 marine birds in and around the future sites Nearshore Windfarm (NSW) and Q7. Alterra-rapport 1048.
- Krijgsveld, K.L. 2014. Avoidance behaviour of birds around offshore windfarms. Overview of knowledge including effects of configuration. Bureau Waardenburg. Rijkswaterstaat Report no. 13-268.
- Leopold, M.F., van Bemmelen, R.S.A. & Zuur, A.F. 2013. Responses of Local Birds to the Offshore Windfarms PAWP and OWEZ off the Dutch mainland coast. Report number C151/12. Imares Report.
- Markones, N., Garthe, S., Dierschke, V., Adler, S. 2008. Small scale temporal variability of seabird distribution patterns in the south-eastern North Sea. In: Wollny-Goerke K, Eskildsen K (eds): Marine mammals and seabirds in front of offshore wind energy. MINOS – Marine warm-blooded animals in North and Baltic Seas. Teubner, Wiesbaden. pp. 115-140.
- Perez-Lapena, B., Wijnberg, K. M., Hulscher, S. J. M. H., & Stein, A. 2010. Environmental impact assessment of offshore wind farms: a simulation-based approach. *Journal of applied ecology*, 47(5), 1110-1118. DOI: 10.1111/j.1365-2664.2010.01850.x
- Petersen I.K., Christensen T.K., Kahlert J., Desholm M. & Fox A.D. 2006. Final results of bird studies at the offshore windfarms at Nysted and Horns Rev, Denmark. NERI Report, commissioned by DONG energy and Vattenfall A/S.
- R Development Core Team 2004. A language and environment for statistical computing. R Foundation for Statistical Computing, Vienna, Austria. <http://www.R-project.org>.
- Skov, H. & Thomsen, F. 2008. Resolving fine-scale spatio-temporal dynamics in the harbour porpoise *Phocoena phocoena*. *Mar Ecol Prog Ser* 373:173–186.
- Skov, H., Leonhard, S.B., Heinänen, S., Zydalis, R., Jensen, N.E., Durinck, J., Johansen, T.W., Jensen, B.P., Hansen, B.L., Piper, W., Grøn, P.N. 2012. Horns Rev 2 Monitoring 2010-2012. Migrating Birds. Orbicon, DHI, Marine Observers and Biola. Report commissioned by DONG Energy.
- Skov, H., Heinänen, S., Nyborg, L. & Lazcny, M. 2015. Offshore Windfarm Eneco Luchterduinen Ecological monitoring of seabirds. T0 report. Commissioned by Eneco. DHI.

Skov, H., Heinänen, S., Lazcny, M & Chudzinska, M. 2016. Offshore Windfarm Eneco Luchterduinen Ecological monitoring of seabirds. T0 report. Commissioned by Eneco. DHI.

Tasker M.L., Jones P.H., Dixon T.J. & Blake B.F. 1984. Counting seabirds at sea from ships: a review of methods employed and a suggestion for a standardized approach. *Auk* 101: 567-577.

Welcker, J. & Nehls, G. 2016. Displacement of seabirds by an offshore windfarm in the North Sea. *Mar Ecol Prog Ser*, 554: 173-182.

Wood, S.N. 2006. *Generalized Additive Models: An introduction* with R. Chapman and Hall, London, UK.

APPENDICES

APPENDIX A – Detailed results of species distribution models for the T-2 surveys

Red-throated and Black-throated Divers

Table A.1. Smooth terms, adjusted R-squared and evaluation statistics for the Red-throated and Black-throated Diver distribution models. F statistics and the approximate significance for the smooth terms and t-statistic, estimate and the significance for the parametric terms are shown. Variables not included in either the presence/absence or positive model part are indicated with a dash. The results of the evaluation test show AUC for presence/absence and the Spearman's correlation for the density predictions. 'n.s.' indicates terms with p-values > 0.05. The significant effect of the windfarms are marked in bold.

Smooth terms	Presence/absence			Positive density		
		F	p	F	p	
Depth		12.32	0.002	-	-	
Salinity		21.037	0	-	-	
Current speed		15.947	0	38.441	0	
Parametric terms	Estimate	t	p	Estimate	t	P
AIS	-0.017	-5.513	0	-0.007	-1.433	0.153
LUD WF not included	-	-	-	-	-	-
PAWP WF not included	-	-	-	-	-	-
OWEZ WF parametric	-1.849	-4.205	0	-	-	-
LUD (2 km buffer) parametric	-0.611	-2.299	0.022	-	-	-
PAWP (2 km buffer) parametric	-1.968	-8.302	0	-	-	-
OWEZ (2 km buffer) parametric	-0.799	-2.535	0.011	-	-	-
Survey 5	1.649	3.807	0	0.03	0.131	0.896
Survey 6	-0.793	-1.465	0.143	-1.214	-3.917	0
Survey 7	-0.423	-0.598	0.55	0.058	0.189	0.85
Survey 8	1.975	4.21	0	0.162	0.453	0.651
Survey 9	1.986	4.282	0	0.116	0.379	0.705
Survey 10	2.509	4.528	0	0.466	1.854	0.065
Survey 11	0.199	0.286	0.775	-0.886	-2.732	0.007
Survey 12	-0.172	-0.231	0.817	-0.818	-2.101	0.036
Survey 13	1.341	2.062	0.039	-0.591	-1.688	0.092
Survey 14	2.032	4.322	0	-0.258	-0.947	0.344
Survey 15	2.756	4.738	0	0.026	0.092	0.927
Survey 16	1.298	1.961	0.05	0.503	1.051	0.294
Survey 17	-0.509	-0.775	0.439	0.171	0.345	0.731
Survey 22	0.155	0.339	0.735	0.009	0.019	0.985
Survey 24	-0.896	-2.422	0.015	-0.014	-0.029	0.977
Survey 26	1.512	3.581	0	0.421	1.314	0.19
Survey 27	-0.422	-1.175	0.24	0.662	1.776	0.077
Survey 31	-1.533	-4.169	0	0.31	0.675	0.5
Sample size (n)		8,161			364	
AUC					0.87	
Adjusted R ²		19.30%			13.10%	
Spearman's corr.				0.41		

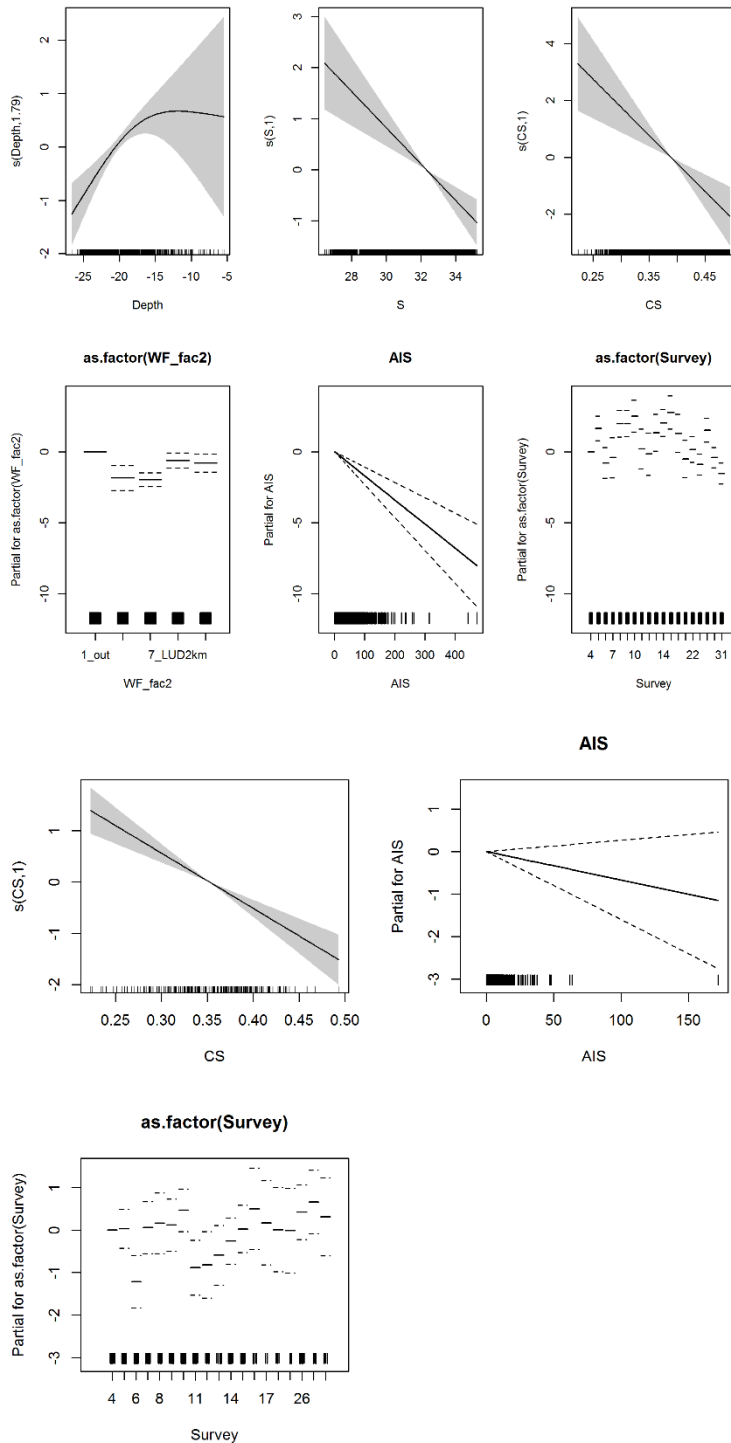


Figure A.1. Partial GAM plots for the Red-throated and Black-throated Diver distribution model – presence-absence (upper panel) and positive density (lower panel) parts. The values of the environmental variables are shown on the X-axis and the probability on the Y-axis in the scale of the linear predictor. The grey shaded areas and the dotted lines (for factors) show the 95% Bayesian confidence intervals. The degree of smoothing is indicated in the legend of the Y-axis.

Great Crested Grebe

Table A.2. Smooth terms, adjusted R-squared and evaluation statistics for the Great Crested Grebe distribution models. F statistics and the approximate significance for the smooth terms and t-statistic and the significance for the parametric terms are shown. Variables not included in either the presence/absence or positive model part are indicated with a dash. The results of the evaluation test show AUC for presence/absence and the Spearman's correlation for the density predictions. 'n.s.' indicates terms with p-values > 0.05. The significant effect of the windfarms are marked in bold.

Smooth terms	Presence/absence			Positive density		
	F	p		F	p	
Depth	13.155	0		5.726	0.005	
Salinity	56.593	0		7.124	0.008	
Current speed	9.977	0				
Parametric terms	Estimate	t	p	Estimate	t	p
AIS	-0.009	-3.458	0.001	-	-	-
LUD WF not included	-	-	-	-	-	-
PAWP WF not included	-	-	-	-	-	-
OWEZ WF parametric	-0.835	-2.216	0.027	0.112	0.077	0.938
LUD (2 km buffer) not included	-	-	-	-	-	-
PAWP (2 km buffer) not included	-	-	-	-	-	-
OWEZ (2 km buffer) not included	-	-	-	-	-	-
Survey 7	-2.606	-3.537	0	0.073	0.163	0.87
Survey 9	1.435	3.004	0.003	-0.871	-0.793	0.429
Survey 10	3.948	8.9	0	2.757	2.278	0.024
Survey 11	1.344	2.304	0.021	3.3	2.63	0.009
Survey 13	1.03	2.655	0.008	0.033	0.024	0.981
Survey 14	0.348	0.856	0.392	-1.413	-2.128	0.035
Survey 15	1.486	3.35	0.001	2.209	1.511	0.132
Survey 17	0.811	1.588	0.112	0.965	1.244	0.215
Survey 18	2.964	7.073	0	-0.482	-0.731	0.465
Survey 22	1.138	2.53	0.011	-1.209	-1.849	0.066
Survey 26	1.611	3.473	0.001	0.908	0.823	0.411
Survey 27	0.326	0.652	0.514	-2.611	-3.148	0.002
Survey 31	-1.953	-5.74	0	-2.593	-4.142	0
Survey 32	-0.585	-0.553	0.581	0.147	0.179	0.858
Sample size (n)	6,043			202		
Adjusted R ²	29.6%			4.0%		
AUC				0.93		
Spearman's corr.				0.34		

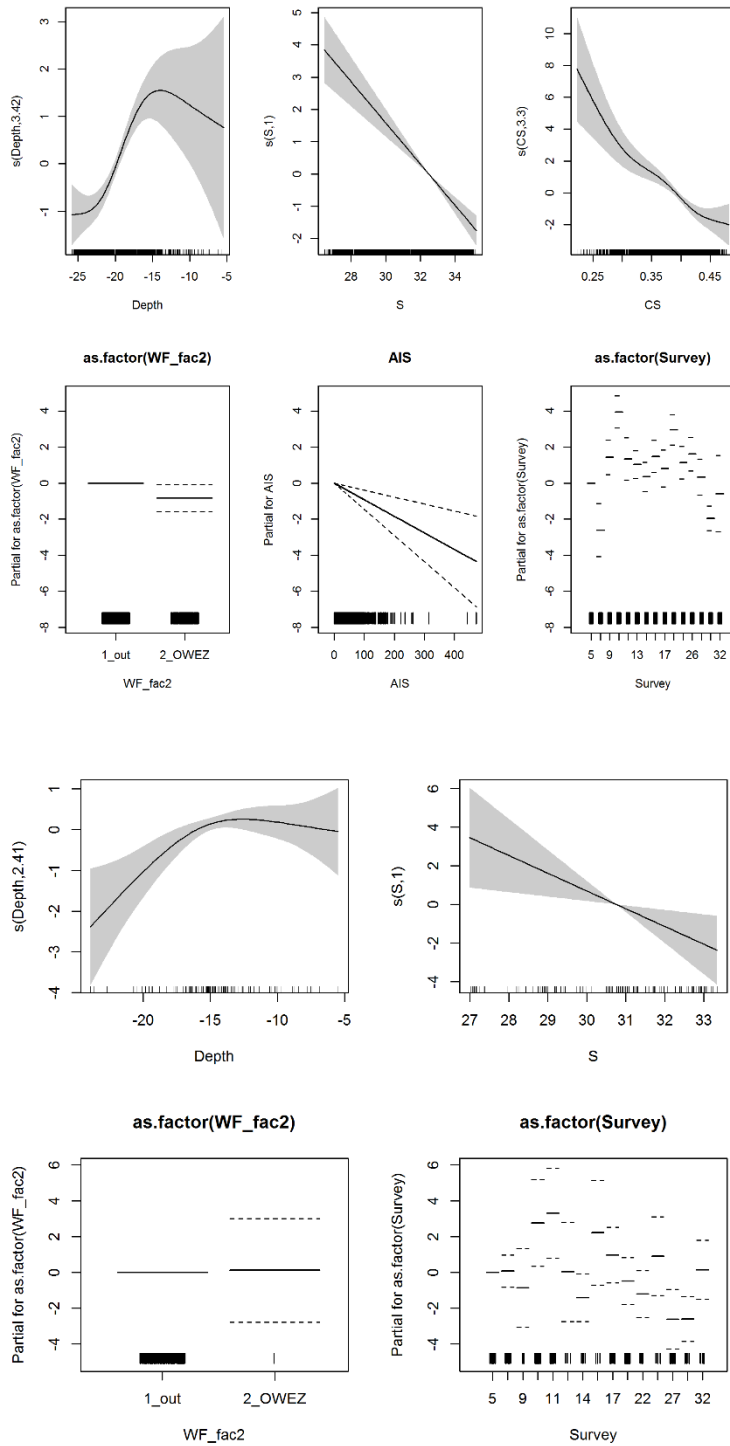


Figure A.2. Partial GAM plots for the Great Crested Grebe distribution model – presence-absence (upper panel) and positive density (lower panel) parts. The values of the environmental variables are shown on the X-axis and the probability on the Y-axis in the scale of the linear predictor. The grey shaded areas and the dotted lines (for factors) show the 95% Bayesian confidence intervals. The degree of smoothing is indicated in the legend of the Y-axis.

Northern Gannet

Table A.3. Smooth terms, adjusted R-squared and evaluation statistics for the Northern Gannet distribution models. F statistics and the approximate significance for the smooth terms and t-statistic and the significance for the parametric terms are shown. Variables not included in either the presence/absence or positive model part are indicated with a dash. The results of the evaluation test show AUC for presence/absence and the Spearman's correlation for the density predictions. 'n.s.' indicates terms with p-values > 0.05. The significant effect of the windfarms are marked in bold.

Smooth terms	Presence/absence			Positive density		
	F	p		F	p	
Depth	13.795	0		6.432	0.011	
Salinity	21.066	0		26.752	0	
Current speed	5.978	0.002		-	-	
Parametric terms	Estimate	t	p	Estimate	t	p
AIS	-0.003	-2.099	0.036	-	-	-
LUD WF parametric	-0.865	-3.861	0	-0.597	-1.387	0.166
PAWP WF parametric	-2.201	-10.357	0	-0.282	-0.478	0.632
OWEZ WF parametric	-2.054	-9.407	0	-0.207	-0.295	0.768
LUD (2 km buffer) parametric	-0.112	-0.637	0.524	-0.009	-0.038	0.97
PAWP (2 km buffer) parametric	-0.261	-1.611	0.107	0.028	0.15	0.881
OWEZ (2 km buffer) parametric	-0.457	-2.897	0.004	0.018	0.075	0.94
Survey 5	-2.618	-8.873	0	-1.412	-3.024	0.003
Survey 6	-0.41	-1.39	0.164	-0.406	-2.004	0.045
Survey 7	-1.101	-2.639	0.008	0.486	2.033	0.042
Survey 8	-1.718	-4.433	0	-1.547	-4.573	0
Survey 9	-0.68	-2.034	0.042	-0.458	-1.785	0.075
Survey 10	-2.212	-4.964	0	-1.349	-3.568	0
Survey 11	-1.477	-2.417	0.016	-0.848	-3.264	0.001
Survey 12	-0.718	-1.961	0.05	-0.772	-2.86	0.004
Survey 13	-1.178	-3.378	0.001	-1.49	-4.717	0
Survey 14	-1.982	-6.196	0	-1.113	-2.741	0.006
Survey 15	-2.47	-6.763	0	-1.268	-2.976	0.003
Survey 16	-1.393	-2.64	0.008	-1.478	-4.633	0
Survey 17	-5.113	-11.988	0	-1.759	-1.57	0.117
Survey 18	-3.696	-11.851	0	-1.363	-2.444	0.015
Survey 21	-2.038	-5.242	0	-1.52	-4.617	0
Survey 22	-0.808	-2.306	0.021	-0.325	-1.154	0.249
Survey 23	-1.559	-4.113	0	-1.104	-3.306	0.001
Survey 24	-3.246	-11.397	0	-1.588	-3.451	0.001
Survey 25	-1.285	-3.934	0	-1.121	-3.745	0
Survey 26	-1.866	-6.15	0	-1.089	-3.247	0.001
Survey 27	-1.119	-3.997	0	0	0.001	0.999
Survey 28	-1.25	-4.97	0	0.456	1.645	0.1
Survey 29	-1.088	-2.268	0.023	-0.503	-1.198	0.231
Survey 30	-2.775	-5.534	0	-0.378	-0.342	0.732
Survey 31	-0.644	-2.33	0.02	-0.198	-0.861	0.39
Survey 32	-2.198	-6.127	0	-1.196	-2.868	0.004
Sample size (n)	11,008			1,491		
Adjusted R ²	10.0%			2.5%		
AUC				0.76		
Spearman's corr.				0.16		

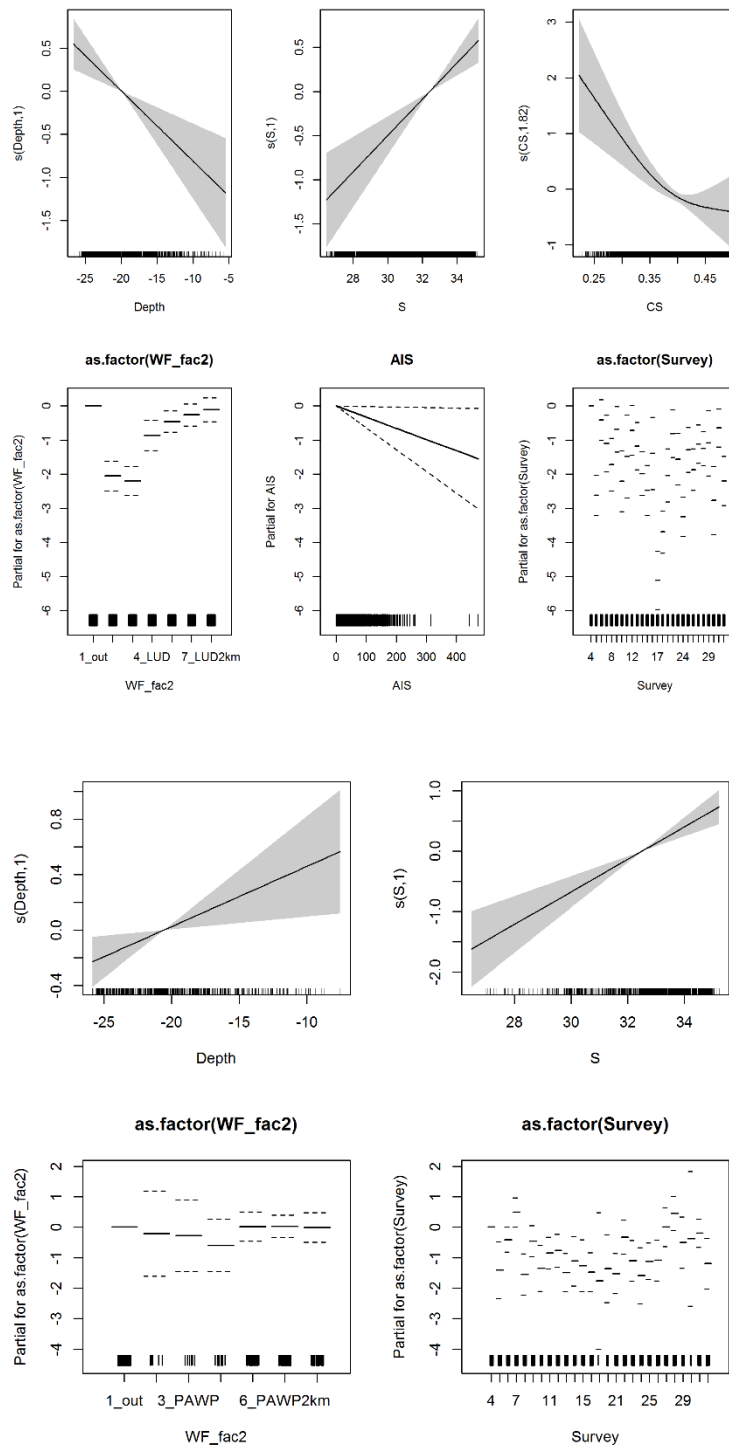


Figure A.3. Partial GAM plots for the Northern Gannet distribution model – presence-absence (upper panel) and positive density (lower panel) parts. The values of the environmental variables are shown on the X-axis and the probability on the Y-axis in the scale of the linear predictor. The grey shaded areas and the dotted lines (for factors) show the 95% Bayesian confidence intervals. The degree of smoothing is indicated in the legend of the Y-axis. .

Great Cormorant

Table A.4. Smooth terms, adjusted R-squared and evaluation statistics for the Great Cormorant distribution models. F statistics and the approximate significance for the smooth terms and t-statistic and the significance for the parametric terms are shown. Variables not included in either the presence/absence or positive model part are indicated with a dash. The results of the evaluation test show AUC for presence/absence and the Spearman's correlation for the density predictions. 'n.s.' indicates terms with p-values > 0.05. The significant effect of the windfarms are marked in bold.

Smooth terms	Presence/absence			Positive density		
		F	p		F	p
Depth		21.167	0		4.132	0.043
Salinity		6.481	0.011		2.836	0.093
Current speed		12.37	0		5.482	0.02
Parametric terms	Estimate	t	p	Estimate	t	p
AIS	-0.005	-2.132	0.033	-	-	-
LUD WF parametric	2.608	8.343	0	-0.067	-0.173	0.863
PAWP WF parametric	4.007	14.125	0	0.295	1.115	0.265
OWEZ WF parametric	1.647	5.325	0	1.329	4.784	0
LUD (2 km buffer) parametric	1.338	5.396	0	-0.112	-0.206	0.837
PAWP (2 km buffer) parametric	2.262	10.602	0	0.303	0.972	0.331
OWEZ (2 km buffer) parametric	1.359	6.326	0	1.045	4.587	0
Survey 5	0.205	0.558	0.577	-1.035	-1.734	0.083
Survey 6	-0.892	-2.381	0.017	1.541	2.763	0.006
Survey 7	-1.314	-2.358	0.018	0.672	1.171	0.242
Survey 8	2.21	5.285	0	-0.193	-0.304	0.761
Survey 9	1.475	3.226	0.001	-0.498	-0.879	0.38
Survey 10	0.721	1.286	0.198	-0.675	-1.092	0.275
Survey 11	-0.649	-0.889	0.374	-0.146	-0.243	0.808
Survey 12	-0.337	-0.705	0.481	-0.333	-0.544	0.587
Survey 13	0.777	1.631	0.103	-0.378	-0.591	0.555
Survey 14	0.698	1.364	0.173	-0.679	-0.974	0.33
Survey 15	0.126	0.262	0.793	0.017	0.024	0.981
Survey 16	-0.275	-0.501	0.616	-1.801	-2.263	0.024
Survey 17	-2.212	-3.855	0	-0.69	-0.678	0.498
Survey 18	-1.472	-4.188	0	-0.889	-0.901	0.368
Survey 21	-1.051	-2.267	0.023	-0.387	-0.557	0.578
Survey 22	-0.13	-0.233	0.816	-0.433	-0.606	0.545
Survey 23	0.342	0.696	0.486	-1.047	-1.504	0.133
Survey 24	-0.655	-1.862	0.063	0.094	0.142	0.888
Survey 25	0.291	0.685	0.493	-0.715	-1.077	0.282
Survey 26	0.989	2.282	0.023	-0.788	-1.304	0.193
Survey 27	0.225	0.715	0.474	0.232	0.351	0.725
Survey 28	0.243	0.788	0.431	-0.92	-1.533	0.126
Survey 29	0.042	0.101	0.919	0.427	0.597	0.551
Survey 30	1.032	2.55	0.011	0.229	0.345	0.73
Survey 31	0.076	0.271	0.786	0.567	1.029	0.304
Survey 32	-1.45	-2.987	0.003	-0.083	-0.112	0.911
Sample size (n)		11,008			575	
Adjusted R ²		13.4%			-3.6%	
AUC					0.81	
Spearman's corr.					0.11	

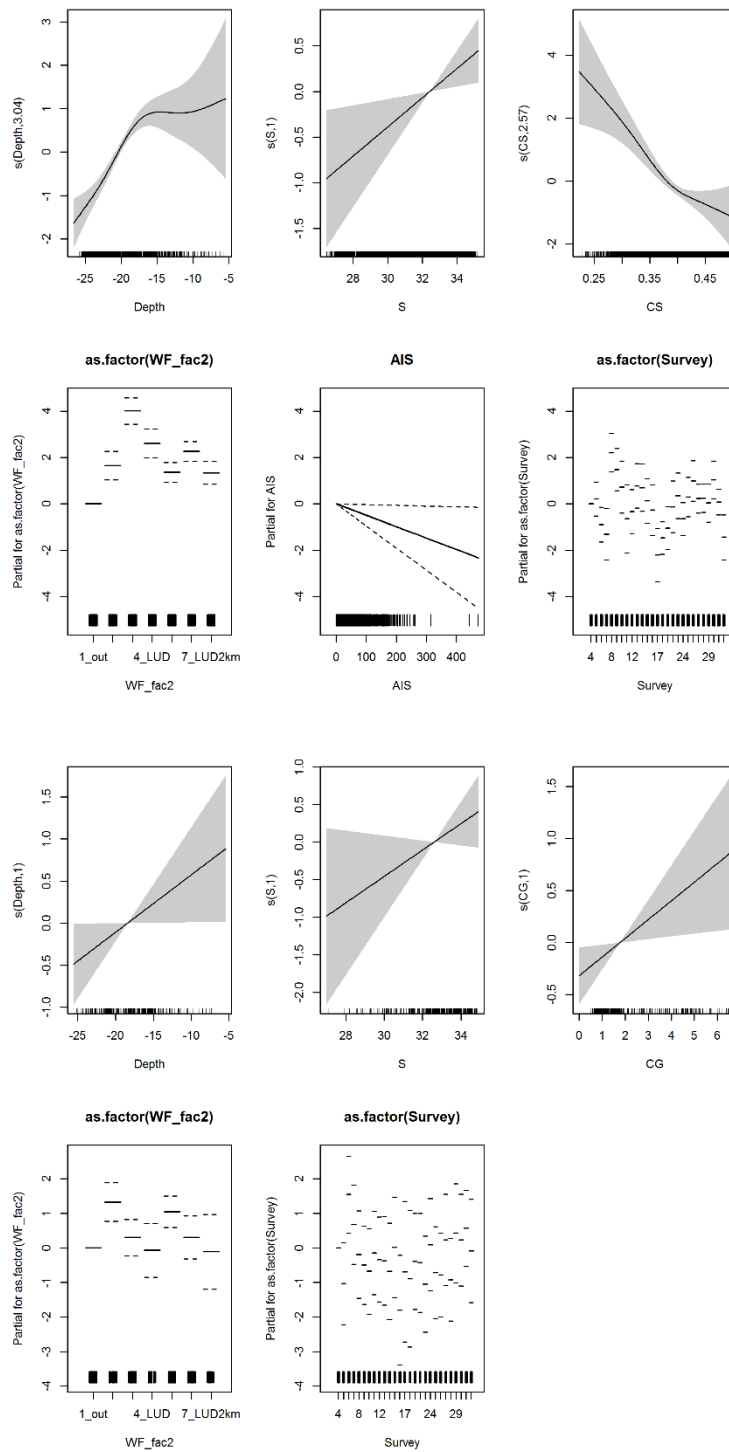


Figure A.4. Partial GAM plots for the Great Cormorant distribution model – presence-absence (upper panel) and positive density (lower panel) parts. The values of the environmental variables are shown on the X-axis and the probability on the Y-axis in the scale of the linear predictor. The grey shaded areas and the dotted lines (for factors) show the 95% Bayesian confidence intervals. The degree of smoothing is indicated in the legend of the Y-axis.

Little Gull

Table A.5. Smooth terms, adjusted R-squared and evaluation statistics for the Little Gull distribution models. F statistics and the approximate significance for the smooth terms and t-statistic and the significance for the parametric terms are shown. Variables not included in either the presence/absence or positive model part are indicated with a dash. The evaluation test did not converge due to too low sample size. 'n.s.' indicates terms with p-values > 0.05. The significant effect of the windfarms are marked in bold.

Smooth terms	Presence/absence			Positive density		
	F	p		F	p	
Depth	22.709	0		-	-	
Salinity	6.775	0.009		-	-	
Current speed	-	-		2.885	0.05	
Current gradient	2.746	0.097		-	-	
Parametric terms	Estimate	t	p	Estimate	t	p
AIS	-0.007	-2.646	0.008	-	-	-
LUD WF not included	-	-	-	-	-	-
PAWP WF not included	-	-	-	-	-	-
OWEZ WF parametric	-1.075	-2.778	0.005	-0.636	-0.785	0.433
LUD (2 km buffer) parametric	-0.057	-0.174	0.862	0.615	1.115	0.266
PAWP (2 km buffer) parametric	-0.015	-0.055	0.956	-0.696	-1.389	0.166
OWEZ (2 km buffer) parametric	-0.444	-1.53	0.126	-0.483	-1.094	0.275
Survey 5	-0.711	-1.152	0.249	0.053	0.092	0.927
Survey 6	-0.248	-0.464	0.643	-1.022	-1.953	0.052
Survey 7	-0.961	-2.129	0.033	-0.687	-0.875	0.382
Survey 8	-0.283	-0.576	0.565	0.437	1.022	0.308
Survey 9	-1.749	-4.448	0	0.047	0.063	0.95
Survey 10	0.014	0.032	0.974	1.101	2.558	0.011
Survey 11	-1.497	-3.127	0.002	-0.248	-0.344	0.731
Survey 12	-1.502	-2.535	0.011	-0.247	-0.351	0.726
Survey 13	-0.302	-0.448	0.654	-0.105	-0.211	0.833
Survey 14	-1.182	-1.686	0.092	-0.577	-0.767	0.443
Survey 16	0.6	1.229	0.219	0.461	0.828	0.409
Survey 17	-0.43	-0.76	0.447	-0.462	-0.891	0.374
Survey 18	-0.104	-0.183	0.855	0.139	0.305	0.76
Survey 21	-1.6	-3.327	0.001	0.31	0.452	0.651
Survey 22	-1.273	-3.138	0.002	0.012	0.017	0.986
Survey 23	-1.637	-3.486	0	0.736	0.906	0.366
Survey 24	-0.225	-0.547	0.584	0.976	2.211	0.028
Survey 25	-1.786	-3.867	0	-0.604	-0.767	0.444
Survey 27	-0.358	-0.894	0.371	0.235	0.381	0.704
Survey 28	1.141	3.181	0.001	1.086	2.686	0.008
Survey 31	-0.196	-0.378	0.706	0.531	1.137	0.256
Sample size (n)	9,751			313		
Adjusted R ²	2.9%			2.9%		
AUC						
Spearman's corr.						

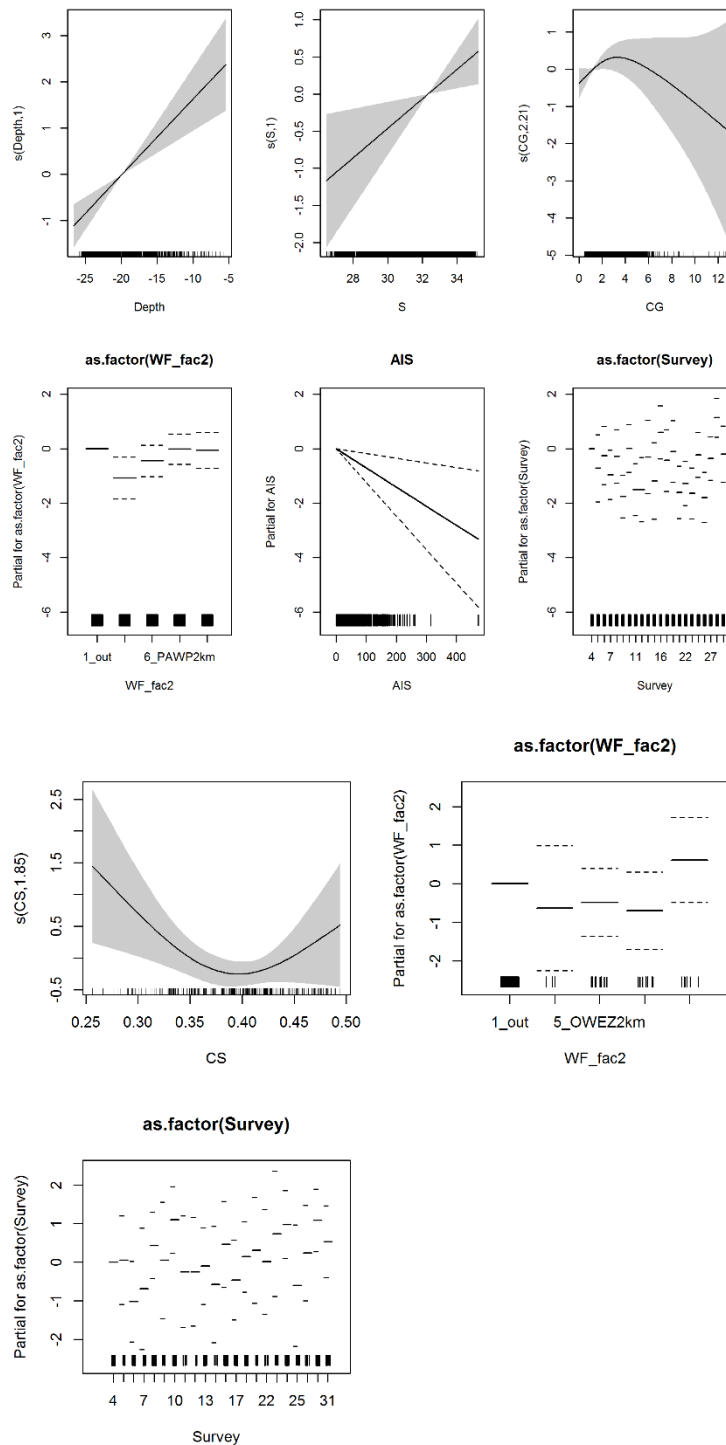


Figure A.5. Partial GAM plots for the Little Gull distribution model – presence-absence (upper panel) and positive density (lower panel) parts. The values of the environmental variables are shown on the X-axis and the probability on the Y-axis in the scale of the linear predictor. The grey shaded areas and the dotted lines (for factors) show the 95% Bayesian confidence intervals. The degree of smoothing is indicated in the legend of the Y-axis.

Black-headed Gull

Table A.6. Smooth terms, adjusted R-squared and evaluation statistics for the Black-headed Gull distribution models. F statistics and the approximate significance for the smooth terms and t-statistic and the significance for the parametric terms are shown. Variables not included in either the presence/absence or positive model part are indicated with a dash. The evaluation test did not converge due to too low sample size. 'n.s.' indicates terms with p-values > 0.05. The significant effect of the windfarms are marked in bold.

Smooth terms	Presence/absence			Positive density		
		F	p		F	p
Depth		10.642	0		2.712	0.05
Salinity		14.814	0		-	-
Current speed		3.747	0.053		7.435	0
Current gradient		7.251	0.007		-	-
Parametric terms	Estimate	t	p	Estimate	t	p
AIS	-	-	-	-	-	-
LUD WF parametric	-0.497	-2.143	0.032	-1.404	-0.92	0.358
PAWP WF parametric	0.001	0.003	0.997	-0.067	-0.202	0.84
OWEZ WF parametric	-0.15	-0.634	0.526	-0.219	-0.879	0.379
LUD (2 km buffer) parametric	-0.746	-3.969	0	-0.624	-0.577	0.564
PAWP (2 km buffer) parametric	0.038	0.228	0.82	0.09	0.396	0.692
OWEZ (2 km buffer) parametric	-0.164	-0.996	0.319	0.018	0.104	0.917
Survey 5	0.627	2.924	0.003	-0.32	-1.525	0.127
Survey 6	1.404	5.224	0	-0.859	-3.752	0
Survey 7	1.192	3.368	0.001	-0.001	-0.003	0.997
Survey 8	0.513	2.008	0.045	-0.137	-0.537	0.592
Survey 9	0.239	0.925	0.355	-0.1	-0.357	0.721
Survey 10	2.218	4.438	0	0.252	1.376	0.169
Survey 11	0.483	0.958	0.338	-1.168	-4.459	0
Survey 12	-0.331	-0.827	0.408	-0.937	-3.256	0.001
Survey 13	0.797	2.017	0.044	-0.079	-0.338	0.736
Survey 14	0.814	2.298	0.022	0.063	0.258	0.797
Survey 15	1.233	1.382	0.167	-0.18	-0.799	0.424
Survey 16	-0.765	-1.24	0.215	0.244	0.555	0.579
Survey 17	-3.671	-6.74	0	-0.905	-0.619	0.536
Survey 18	-2.089	-5.266	0	1.226	2.319	0.021
Survey 21	-1.269	-2.687	0.007	-0.677	-1.604	0.109
Survey 22	-0.867	-2.045	0.041	-0.137	-0.362	0.717
Survey 23	-2.958	-4.68	0	-1.026	-0.954	0.34
Survey 24	-2.621	-6.982	0	0.268	0.441	0.659
Survey 25	-1.365	-4.288	0	0.304	0.63	0.529
Survey 26	-1.935	-8.456	0	-0.007	-0.012	0.99
Survey 27	-2.209	-12.925	0	0.652	1.293	0.196
Survey 28	-2.801	-16.721	0	0.146	0.22	0.826
Survey 29	-2.319	-6.503	0	0.306	0.146	0.884
Survey 30	-1.052	-2.878	0.004	-0.555	-0.833	0.405
Survey 31	-2.467	-12.711	0	-0.282	-0.528	0.598
Survey 32	-3.412	-10.039	0	-1.583	-1.091	0.275
Sample size (n)		11,008			1,313	
Adjusted R ²		24.1%			6.2%	
AUC						
Spearman's corr.						

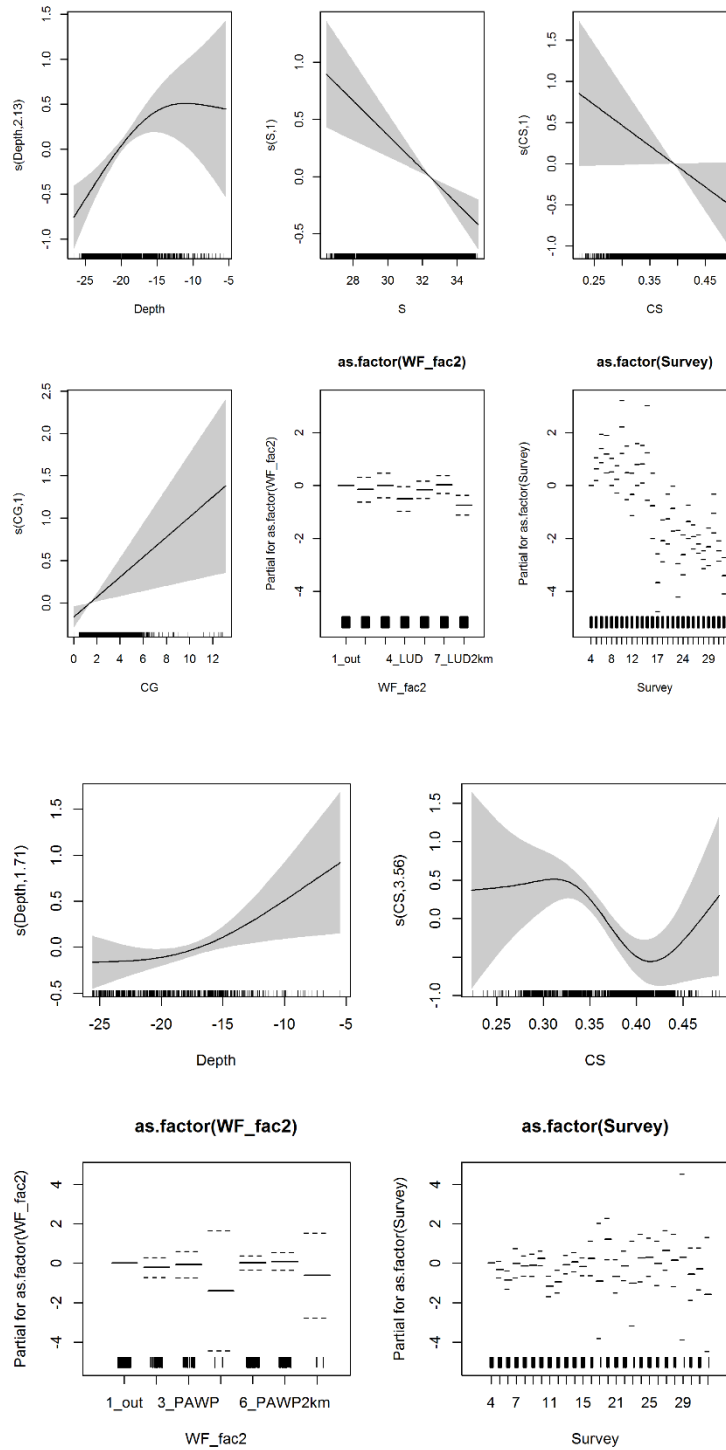


Figure A.6. Partial GAM plots for the Black-headed Gull distribution model – presence-absence (upper panel) and positive density (lower panel) parts. The values of the environmental variables are shown on the X-axis and the probability on the Y-axis in the scale of the linear predictor. The grey shaded areas and the dotted lines (for factors) show the 95% Bayesian confidence intervals. The degree of smoothing is indicated in the legend of the Y-axis.

Common Gull

Table A.7. Smooth terms, adjusted R-squared and evaluation statistics for the Common Gull distribution models. F statistics and the approximate significance for the smooth terms and t-statistic and the significance for the parametric terms are shown. Variables not included in either the presence/absence or positive model part are indicated with a dash. The evaluation test did not converge due to too low sample size. 'n.s.' indicates terms with p-values > 0.05.

Smooth terms	Presence/absence			Positive density		
	F	p		F	p	
Depth	5.731	0.001		-	-	
Salinity	-	-		2.51	0.113	
Current speed	7.618	0.006		-	-	
Current gradient	-	-		14.191	0	
Parametric terms	Estimate	t	p	Estimate	t	p
LUD WF	0.22	0.985	0.325	0.12	0.462	0.644
PAWP WF parametric	0.074	0.357	0.721	-0.079	-0.261	0.794
OWEZ WF parametric	-0.28	-1.238	0.216	0.133	0.433	0.665
LUD (2 km buffer) parametric	-0.027	-0.147	0.884	0.725	2.584	0.01
PAWP (2 km buffer) parametric	0.307	1.797	0.072	0.228	0.951	0.342
OWEZ (2 km buffer) parametric	-0.067	-0.391	0.696	0.071	0.337	0.737
Survey 5	0.731	1.281	0.2	-1.627	-2.631	0.009
Survey 6	-0.477	-0.629	0.529	-1.341	-1.988	0.047
Survey 9	2.187	4.105	0	-0.235	-0.44	0.66
Survey 10	-0.71	-1.272	0.203	-1.385	-1.571	0.117
Survey 11	0.176	0.336	0.737	-0.183	-0.294	0.769
Survey 12	-1.059	-2.047	0.041	-1.114	-1.221	0.222
Survey 13	-1.206	-2.459	0.014	-0.926	-0.799	0.425
Survey 14	1.701	3.56	0	-0.745	-1.32	0.187
Survey 15	0.04	0.087	0.931	-0.831	-1.051	0.294
Survey 16	2.009	4.023	0	-1.157	-2.023	0.043
Survey 17	0.602	1.233	0.218	-1.27	-2.003	0.045
Survey 18	1.867	4.023	0	-0.238	-0.445	0.656
Survey 21	2.21	4.519	0	-0.601	-1.118	0.264
Survey 22	2.364	5.086	0	-0.153	-0.285	0.776
Survey 23	2.895	5.887	0	-0.415	-0.782	0.435
Survey 24	1.813	3.916	0	-0.743	-1.428	0.153
Survey 25	2.416	5.049	0	-0.807	-1.515	0.13
Survey 26	3.022	6.591	0	-0.23	-0.441	0.659
Survey 27	2.82	5.833	0	0.278	0.579	0.563
Survey 28	1.239	2.393	0.017	0.186	0.343	0.732
Survey 29	2.093	2.401	0.016	0.247	0.391	0.696
Survey 30	2.767	2.923	0.003	-0.258	-0.443	0.658
Survey 31	2.359	4.91	0	-0.464	-0.937	0.349
Survey 32	2.099	3.927	0	-1.05	-1.866	0.062
Sample size (n)	10,242			1,021		
Adjusted R ²	6.7%			2.1%		
AUC						
Spearman's corr.						

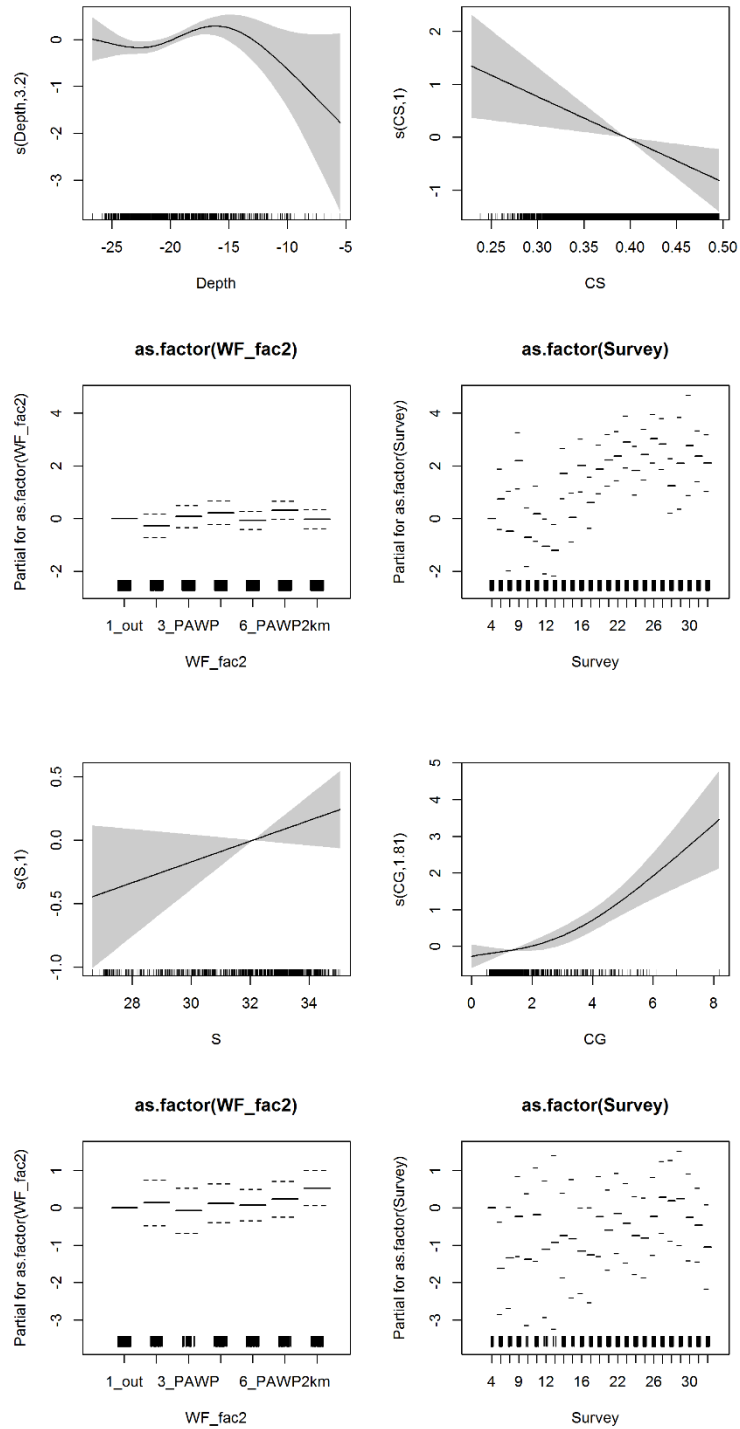


Figure A.7. Partial GAM plots for the Common Gull distribution model – presence-absence (upper panel) and positive density (lower panel) parts. The values of the environmental variables are shown on the X-axis and the probability on the Y-axis in the scale of the linear predictor. The grey shaded areas and the dotted lines (for factors) show the 95% Bayesian confidence intervals. The degree of smoothing is indicated in the legend of the Y-axis.

Lesser Black-backed Gull

Table A.8. Smooth terms, adjusted R-squared and evaluation statistics for the Lesser Black-backed Gull distribution models. F statistics and the approximate significance for the smooth terms and t-statistic and the significance for the parametric terms are shown. Variables not included in either the presence/absence or positive model part are indicated with a dash. The evaluation test did not converge due to too low sample size. 'n.s.' indicates terms with p-values > 0.05.

Smooth terms	Presence/absence			Positive density		
	F	p		F	p	
Depth	22.62	0		2.51	0.048	
Salinity	24.749	0		12.835	0	
Current speed				-	-	
Current gradient	4.33	0.037		5.475	0.019	
Parametric terms	Estimate	t	p	Estimate	t	p
AIS						
LUD WF parametric	-0.543	-2.755	0.006	-0.499	-0.749	0.454
PAWP WF parametric	0.25	1.331	0.183	-0.583	-1.488	0.137
OWEZ WF parametric	0.046	0.238	0.812	-0.033	-0.087	0.93
LUD (2 km buffer) parametric	-0.113	-0.72	0.472	0.185	0.405	0.686
PAWP (2 km buffer) parametric	-0.077	-0.54	0.589	0.023	0.071	0.944
OWEZ (2 km buffer) parametric	0.185	1.31	0.19	0.565	2.17	0.03
Survey 5	-0.189	-0.605	0.545	-1.03	-2.691	0.007
Survey 6	0.367	1.614	0.107	-0.145	-0.463	0.644
Survey 7	-0.485	-1.791	0.073	0.41	0.988	0.323
Survey 8	-0.807	-2.728	0.006	-1.247	-2.56	0.011
Survey 9	-1.283	-4.448	0	-0.868	-2.002	0.045
Survey 10	-1.846	-4.2	0	-1.129	-2.214	0.027
Survey 11	-1.994	-2.69	0.007	-1.463	-2.657	0.008
Survey 12	-0.609	-2.046	0.041	-0.647	-1.494	0.135
Survey 13	-0.944	-2.739	0.006	-0.588	-1.185	0.236
Survey 14	-0.901	-2.201	0.028	-1.063	-2.327	0.02
Survey 15	-2.145	-5.533	0	-1.335	-2.271	0.023
Survey 16	-1.882	-6.203	0	-0.922	-1.746	0.081
Survey 17	-5.628	-17.649	0	-0.888	-0.344	0.731
Survey 18	-4.621	-16.178	0	-0.44	-0.333	0.739
Survey 21	-1.233	-2.217	0.027	-0.982	-1.983	0.048
Survey 22	-2.847	-8.408	0	-1.134	-1.597	0.11
Survey 23	-2.636	-9.433	0	-0.84	-1.291	0.197
Survey 24	-1.449	-5.176	0	0.453	1.023	0.306
Survey 25	-1.097	-3.768	0	-0.661	-1.47	0.142
Survey 26	-3.697	-13.655	0	-1.495	-1.588	0.113
Survey 27	-3.655	-16.593	0	-0.645	-0.496	0.62
Survey 28	-0.738	-3.201	0.001	2.206	5.865	0
Survey 30	-2.825	-8.139	0	2.16	1.43	0.153
Survey 31	-1.538	-6.498	0	-0.412	-0.923	0.356
Survey 32	-3.999	-12.255	0	-1.221	-0.914	0.361
Sample size (n)	10,901			1,782		
Adjusted R ²	12.3%			0.8%		
AUC						
Spearman's corr.						

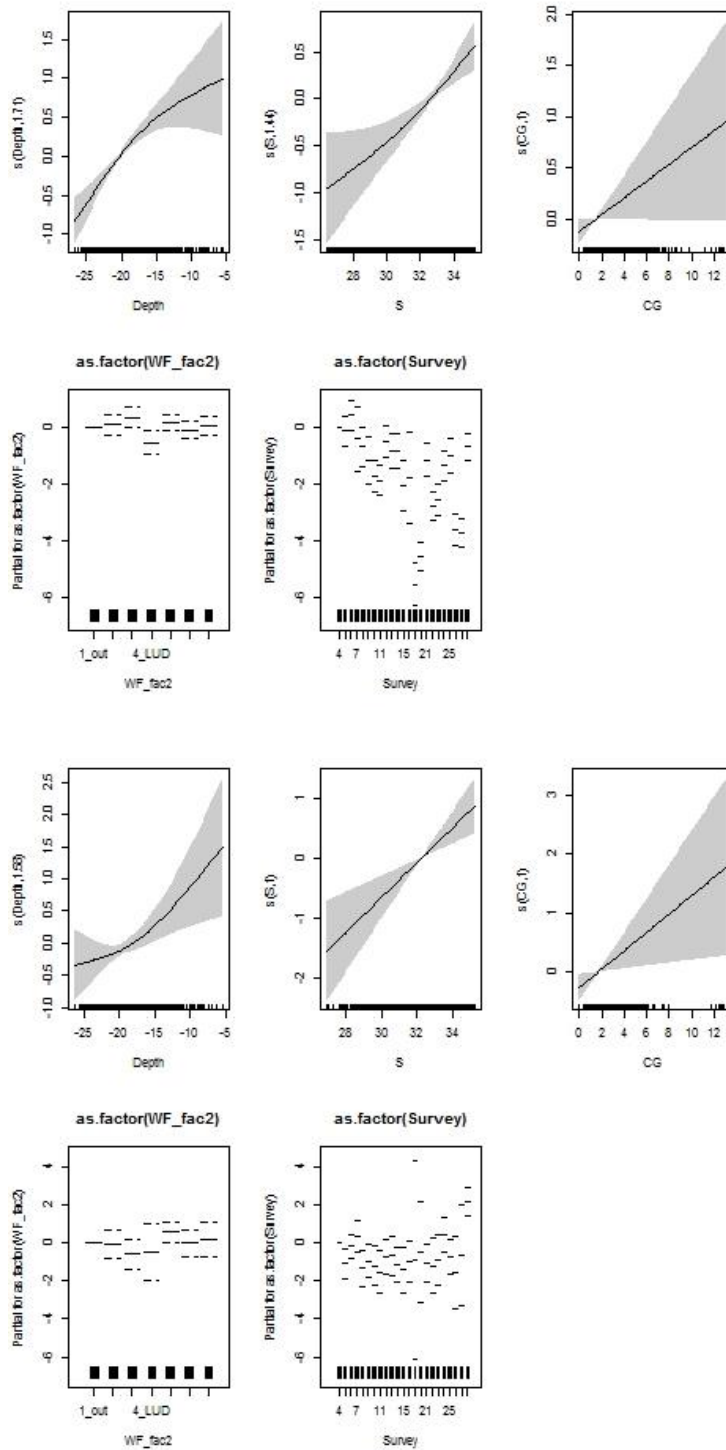


Figure A.8. Partial GAM plots for the Lesser Black-backed Gull distribution model – presence-absence (upper panel) and positive density (lower panel) parts. The values of the environmental variables are shown on the X-axis and the probability on the Y-axis in the scale of the linear predictor. The grey shaded areas and the dotted lines (for factors) show the 95% Bayesian confidence intervals. The degree of smoothing is indicated in the legend of the Y-axis.

Herring Gull

Table A.9. Smooth terms, adjusted R-squared and evaluation statistics for the Herring Gull distribution models. F statistics and the approximate significance for the smooth terms and t-statistic and the significance for the parametric terms are shown. Variables not included in either the presence/absence or positive model part are indicated with a dash. The results of the evaluation test show AUC for presence/absence and the Spearman's correlation for the density predictions. 'n.s.' indicates terms with p-values > 0.05.

Smooth terms	Presence/absence			Positive density		
		F	p		F	p
Depth		-	-		-	-
Salinity		3.212	0.028		2.828	0.093
Current speed		34.691	0		-	-
Current gradient		-	-		42.051	0
Parametric terms	Estimate	t	p	Estimate	t	p
AIS	-	-	-	-	-	-
LUD WF parametric	0.659	2.256	0.024			
PAWP WF parametric	0.729	3.001	0.003			
OWEZ WF parametric	-0.131	-0.515	0.606			
LUD (2 km buffer) parametric	0.177	0.72	0.472			
PAWP (2 km buffer) parametric	0.264	1.393	0.164			
OWEZ (2 km buffer) parametric	0.264	1.444	0.149			
Survey 5	-0.29	-1.121	0.262	-1.014	-1.217	0.224
Survey 6	0.438	1.218	0.223	-0.619	-1.075	0.283
Survey 8	2.963	9.022	0	-0.403	-0.702	0.483
Survey 9	1.677	4.517	0	-0.672	-1.125	0.261
Survey 11	1.092	2.742	0.006	-0.8	-1.437	0.151
Survey 12	2.767	7.703	0	-0.238	-0.441	0.659
Survey 13	1.487	4.225	0	-0.833	-1.37	0.171
Survey 14	0.789	2.789	0.005	-0.372	-0.496	0.62
Survey 15	2.342	7.502	0	-0.474	-0.803	0.422
Survey 16	1.417	3.598	0	0.395	0.566	0.571
Survey 17	0.871	1.754	0.079	-0.199	-0.32	0.749
Survey 18	2.215	7.312	0	-0.044	-0.08	0.936
Survey 21	1.446	3.711	0	-0.651	-1.136	0.256
Survey 22	3.165	8.161	0	0.544	1.003	0.316
Survey 23	1.898	5.174	0	-0.048	-0.078	0.938
Survey 24	0.834	2.965	0.003	-0.058	-0.098	0.922
Survey 25	2.458	8.409	0	-0.125	-0.221	0.825
Survey 26	1.739	3.817	0	-0.288	-0.492	0.623
Survey 27	1.422	2.745	0.006	0.066	0.104	0.917
Survey 28	1.701	5.411	0	1.024	1.83	0.068
Survey 29	2.034	4.943	0	-0.419	-0.688	0.492
Survey 30	2.21	5.221	0	1.788	2.744	0.006
Survey 31	2.191	7.988	0	0.086	0.162	0.872
Survey 32	0.293	0.561	0.575	-0.412	-0.593	0.553
Sample size (n)		10,298			759	
Adjusted R ²		5.9%			-3.7%	
AUC						
Spearman's corr.						

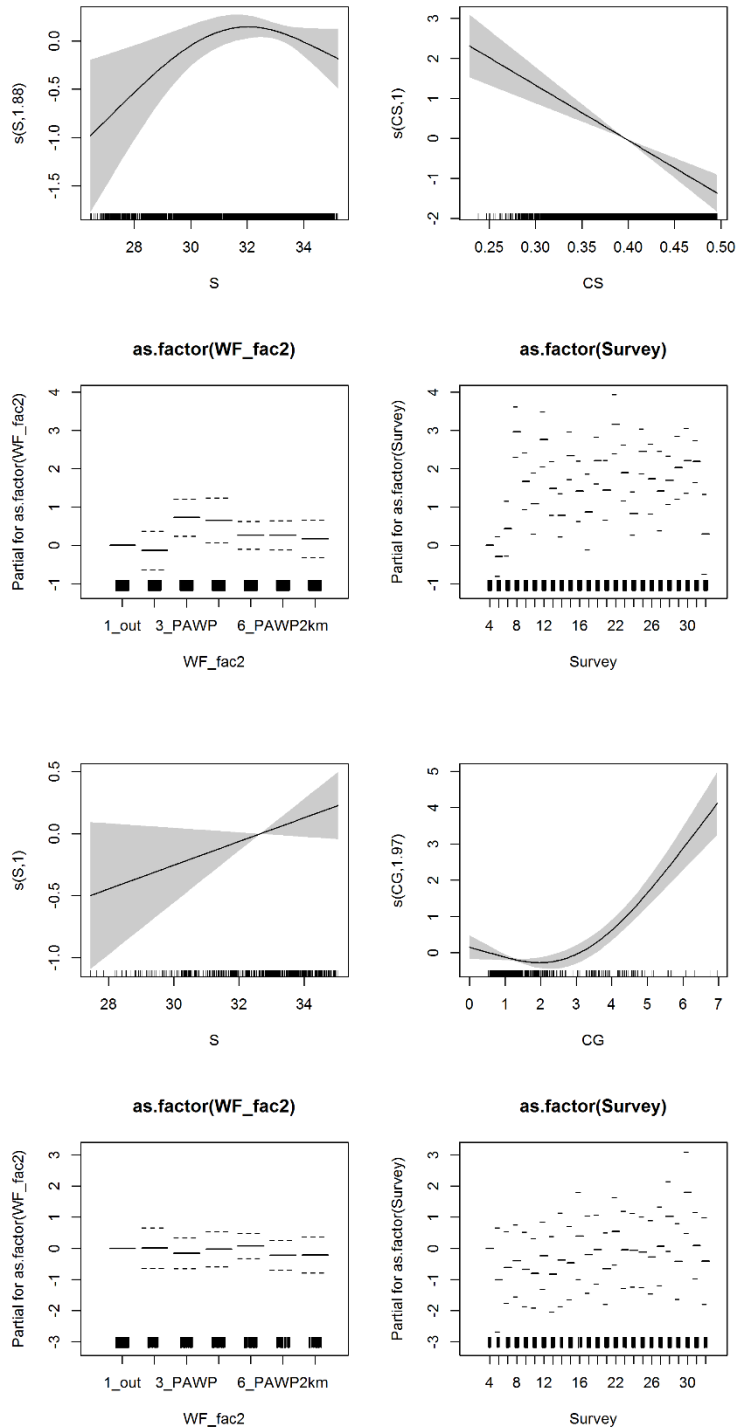


Figure A.9. Partial GAM plots for the Herring Gull distribution model – presence-absence (upper panel) and positive density (lower panel) parts. The values of the environmental variables are shown on the X-axis and the probability on the Y-axis in the scale of the linear predictor. The grey shaded areas and the dotted lines (for factors) show the 95% Bayesian confidence intervals. The degree of smoothing is indicated in the legend of the Y-axis.

Great Black-backed Gull

Table A.10. Smooth terms, adjusted R-squared and evaluation statistics for the Great Black-backed Gull distribution models. F statistics and the approximate significance for the smooth terms and t-statistic and the significance for the parametric terms are shown. Variables not included in either the presence/absence or positive model part are indicated with a dash. The results of the evaluation test show AUC for presence/absence and the Spearman's correlation for the density predictions. 'n.s.' indicates terms with p-values > 0.05. The significant effect of the windfarms are marked in bold.

Smooth terms	Presence/absence			Positive density		
		F	p		F	p
Depth		-	-		-	-
Salinity		-	-		-	-
Current speed		-	-		-	-
Current gradient		5.695	0.017		10.456	0.001
Parametric terms	Estimate	t	p	Estimate	t	p
AIS	-	-	-	-	-	-
LUD WF parametric	0.447	2.101	0.036	-0.154	-0.449	0.653
PAWP WF parametric	0.638	3.373	0.001	-0.364	-1.554	0.12
OWEZ WF parametric	0.288	1.441	0.149	-0.091	-0.367	0.714
LUD (2 km buffer) parametric	0.233	1.372	0.17	-0.227	-0.742	0.458
PAWP (2 km buffer) parametric	0.369	2.559	0.011	-0.112	-0.623	0.533
OWEZ (2 km buffer) parametric	0.135	0.951	0.342	-0.127	-0.693	0.488
Survey 5	-0.536	-1.055	0.291	-0.523	-2.73	0.006
Survey 6	-2.252	-5.893	0	-1.094	-3.961	0
Survey 7	-0.217	-0.56	0.575	-0.14	-0.727	0.467
Survey 8	-3.552	-9.599	0	-1.032	-2.297	0.022
Survey 9	-1.434	-3.782	0	-0.374	-1.852	0.064
Survey 10	-3.937	-9.128	0	-1.123	-1.944	0.052
Survey 11	-3.606	-7.558	0	-0.351	-0.706	0.48
Survey 12	-1.645	-4.09	0	-0.441	-1.913	0.056
Survey 13	-1.121	-2.794	0.005	-0.329	-1.47	0.142
Survey 14	0.127	0.314	0.754	0.346	1.936	0.053
Survey 15	-0.93	-2.293	0.022	-0.726	-3.576	0
Survey 16	-2.178	-5.273	0	-0.666	-2.388	0.017
Survey 17	-3.105	-7.161	0	-0.883	-1.894	0.058
Survey 18	-3.437	-8.597	0	0.037	0.089	0.929
Survey 21	-2.046	-4.647	0	-0.694	-2.636	0.008
Survey 22	-1.854	-4.152	0	0.288	1.184	0.237
Survey 23	-2.222	-5.286	0	0.133	0.475	0.635
Survey 24	-2.562	-6.647	0	-0.592	-2.157	0.031
Survey 25	-2.444	-6.122	0	-0.443	-1.487	0.137
Survey 26	-2.832	-7.642	0	-0.73	-2.16	0.031
Survey 27	-3.258	-8.668	0	-0.779	-1.988	0.047
Survey 28	-2.774	-7.408	0	-0.505	-1.537	0.124
Survey 29	-2.496	-3.316	0.001	-0.847	-1.553	0.121
Survey 30	-2.717	-3.418	0.001	0.86	1.25	0.212
Survey 31	-2.096	-5.416	0	-0.293	-1.186	0.236
Survey 32	-4.766	-11.789	0	-1.402	-1.364	0.173
Sample size (n)		11,008			1,817	
Adjusted R ²		17.9%			3.4%	
AUC						
Spearman's corr.						

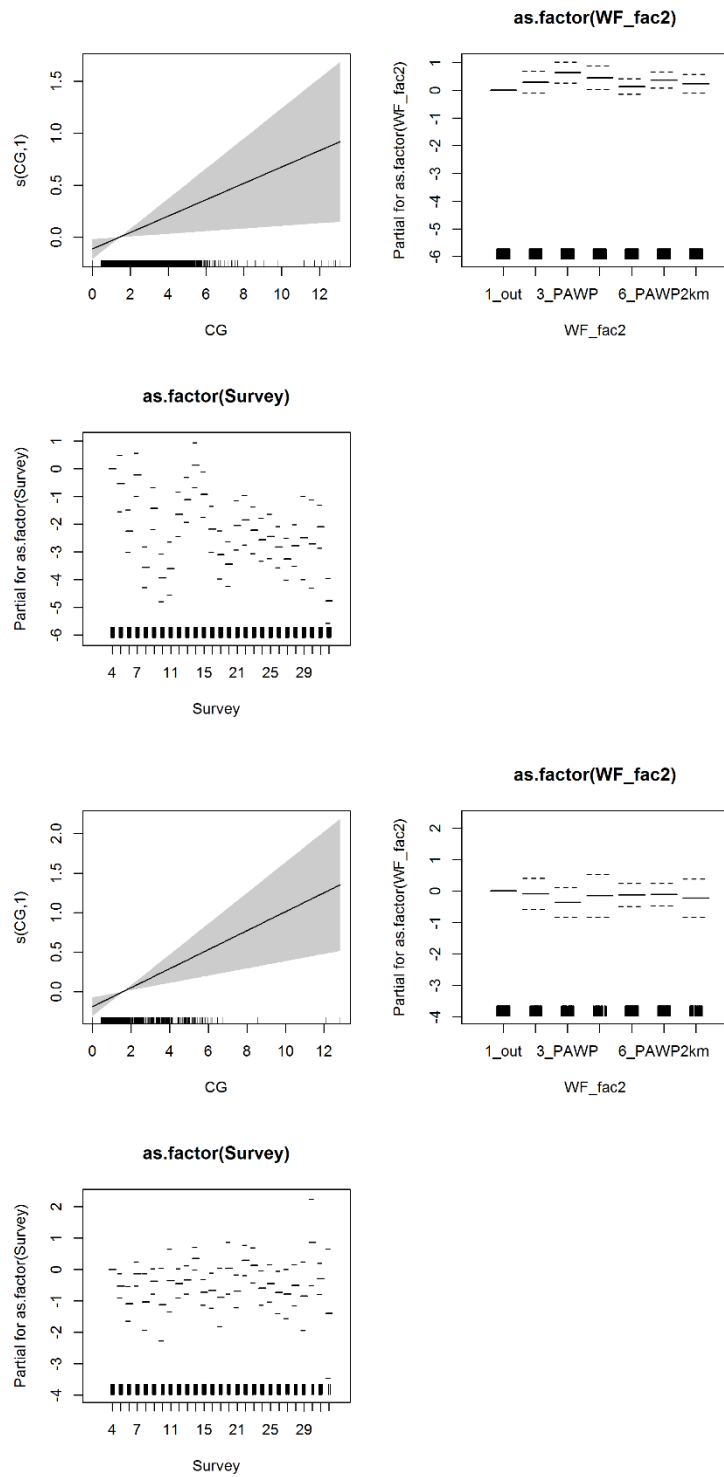


Figure A.10. Partial GAM plots for the Great Black-backed Gull distribution model – presence-absence (upper panel) and positive density (lower panel) parts. The values of the environmental variables are shown on the X-axis and the probability on the Y-axis in the scale of the linear predictor. The grey shaded areas and the dotted lines (for factors) show the 95% Bayesian confidence intervals. The degree of smoothing is indicated in the legend of the Y-axis.

Black-legged Kittiwake

Table A.11. Smooth terms, adjusted R-squared and evaluation statistics for the Black-legged distribution models. F statistics and the approximate significance for the smooth terms and t-statistic and the significance for the parametric terms are shown. Variables not included in either the presence/absence or positive model part are indicated with a dash. The evaluation test did not converge due to low sample size. 'n.s.' indicates terms with p-values > 0.05. The significant effect of the windfarms are marked in bold.

Smooth terms	Presence/absence			Positive density		
		F	p		F	p
Depth		21.333	0		-	-
Salinity		14.87	0		12.993	0
Current speed		2.911	0.054		8.958	0
Current gradient		-	-		-	-
Parametric terms	Estimate	t	p	Estimate	t	p
AIS	-	-	-	-	-	-
LUD WF parametric	0.114	0.537	0.591	0.275	0.692	0.489
PAWP WF parametric	-0.683	-3.506	0	1.067	2.067	0.039
OWEZ WF parametric	-0.351	-1.754	0.079	-0.34	-0.734	0.463
LUD (2 km buffer) parametric	0.075	0.426	0.67	0.149	0.438	0.661
PAWP (2 km buffer) parametric	-0.299	-2.015	0.044	-0.078	-0.203	0.839
OWEZ (2 km buffer) parametric	-0.256	-1.744	0.081	-0.029	-0.089	0.929
Survey 5	0.988	2.628	0.009	-1.063	-2.663	0.008
Survey 6	0.27	0.772	0.44	-1.609	-3.353	0.001
Survey 7	0.843	1.522	0.128	-2.041	-3.451	0.001
Survey 8	-1.233	-3.154	0.002	-0.277	-0.524	0.6
Survey 9	-1.64	-4.167	0	-0.686	-1.185	0.236
Survey 10	-1.134	-3.568	0	-1.25	-2.121	0.034
Survey 11	-1.205	-3.282	0.001	-2.92	-4.199	0
Survey 12	-0.635	-1.631	0.103	-1.98	-3.54	0
Survey 13	-1.816	-5.254	0	-0.07	-0.086	0.932
Survey 14	-1.402	-4.755	0	-0.955	-1.328	0.184
Survey 15	-1.385	-3.988	0	-1.284	-2.002	0.046
Survey 16	-2.684	-6.054	0	-0.602	-0.662	0.508
Survey 17	0.123	0.285	0.776	-1.65	-3.016	0.003
Survey 18	-0.211	-0.696	0.486	-0.271	-0.622	0.534
Survey 21	-1.581	-4.373	0	-1.914	-2.686	0.007
Survey 22	0.764	2.316	0.021	2.154	4.863	0
Survey 23	-0.926	-2.137	0.033	-0.258	-0.428	0.669
Survey 24	-1.526	-5.177	0	-0.317	-0.513	0.608
Survey 25	-0.99	-2.783	0.005	-0.282	-0.503	0.615
Survey 26	0.227	0.709	0.478	-0.087	-0.199	0.842
Survey 27	0.702	2.637	0.008	0.601	1.37	0.171
Survey 28	-1.943	-7.295	0	-0.723	-0.923	0.356
Survey 29	2.101	4.358	0	0.522	1.065	0.287
Survey 30	0.313	0.646	0.518	-0.21	-0.311	0.756
Survey 31	-0.008	-0.026	0.979	-0.257	-0.618	0.537
Survey 32	-2.17	-4.309	0	-1.498	-1.267	0.205
Sample size (n)		11,008			1,447	
Adjusted R ²		10.9%			0.5%	
AUC						
Spearman's corr.						

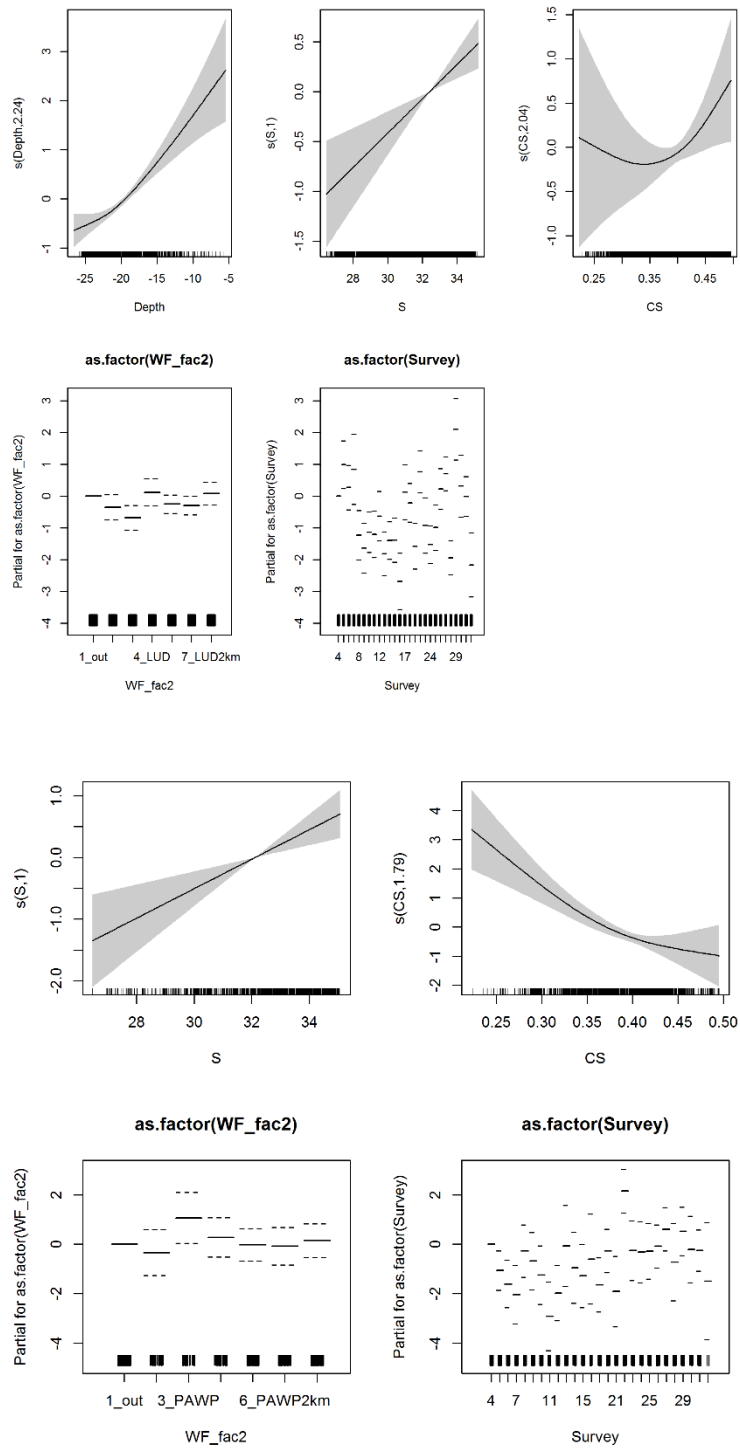


Figure A.11. Partial GAM plots for the Kittiwake distribution model – presence-absence (upper panel) and positive density (lower panel) parts. The values of the environmental variables are shown on the X-axis and the probability on the Y-axis in the scale of the linear predictor. The grey shaded areas and the dotted lines (for factors) show the 95% Bayesian confidence intervals. The degree of smoothing is indicated in the legend of the Y-axis.

Common Guillemot

Table A.12. Smooth terms, adjusted R-squared and evaluation statistics for the Common Guillemot distribution models. F statistics and the approximate significance for the smooth terms and t-statistic and the significance for the parametric terms are shown. Variables not included in either the presence/absence or positive model part are indicated with a dash. The results of the evaluation test show AUC for presence/absence and the Spearman's correlation for the density predictions. 'n.s.' indicates terms with p-values < 0.05. The significant effect of the windfarms are marked in bold.

Smooth terms	Presence/absence			Positive density		
	F	p		F	p	
Depth	5.07	0.004		1.225	0.177	
Salinity	15.694	0		6.193	0.013	
Current speed	7.145	0		6.551	0.002	
Current gradient				11.543	0.001	
Parametric terms	Estimate	t	p	Estimate	t	p
AIS	-0.002	-1.49	0.136	-0.001	-0.623	0.533
LUD WF parametric	-0.953	-5.16	0	-0.343	-2.593	0.01
PAWP WF parametric	-1.218	-7.774	0	-0.634	-4.589	0
OWEZ WF parametric	-0.661	-3.987	0	-0.003	-0.022	0.983
LUD (2 km buffer) parametric	-0.147	-0.998	0.318	-0.055	-0.626	0.531
PAWP (2 km buffer) parametric	-0.402	-3.313	0.001	-0.067	-0.76	0.447
OWEZ (2 km buffer) parametric	-0.265	-2.22	0.026	-0.044	-0.49	0.624
Survey 5	-0.358	-0.845	0.398	-0.652	-3.242	0.001
Survey 6	-1.988	-6.538	0	-1	-3.793	0
Survey 7	0.072	0.18	0.857	-0.326	-1.169	0.242
Survey 8	-3.931	-12.861	0	-1.473	-3.647	0
Survey 9	-1.052	-3.545	0	-0.962	-4.685	0
Survey 10	-1.408	-5.088	0	-1.059	-4.664	0
Survey 11	-2.9	-8.857	0	-0.525	-1.574	0.116
Survey 12	-1.364	-4.31	0	-0.746	-3.245	0.001
Survey 13	-0.081	-0.255	0.799	-0.79	-3.732	0
Survey 14	0.004	0.013	0.99	-0.737	-3.749	0
Survey 15	-1.818	-6.121	0	-1.472	-5.808	0
Survey 16	-1.591	-4.027	0	-0.92	-3.731	0
Survey 17	0.086	0.241	0.81	-0.245	-1.089	0.276
Survey 18	1.62	6.111	0	0.405	2.376	0.018
Survey 21	-0.704	-2.175	0.03	-0.519	-2.286	0.022
Survey 22	1.477	5.009	0	0.68	3.65	0
Survey 23	-0.606	-1.695	0.09	-0.675	-2.919	0.004
Survey 24	-2.116	-8.131	0	-0.945	-4.038	0
Survey 25	-0.293	-1.024	0.306	-0.054	-0.27	0.787
Survey 26	0.698	2.451	0.014	0.209	1.138	0.255
Survey 27	2.142	7.84	0	0.261	1.678	0.093
Survey 28	-1.284	-5.019	0	-0.542	-2.607	0.009
Survey 29	1.03	0.936	0.349	0.678	2.835	0.005
Survey 30	1.353	1.248	0.212	0.559	2.391	0.017
Survey 31	0.973	3.361	0.001	-0.1	-0.646	0.518
Survey 32	0.247	0.688	0.491	-0.563	-2.46	0.014
Sample size (n)	11,008			3,629		
Adjusted R ²	25.7%			14.8%		
AUC	0.80					
Spearman's corr.				0.43		

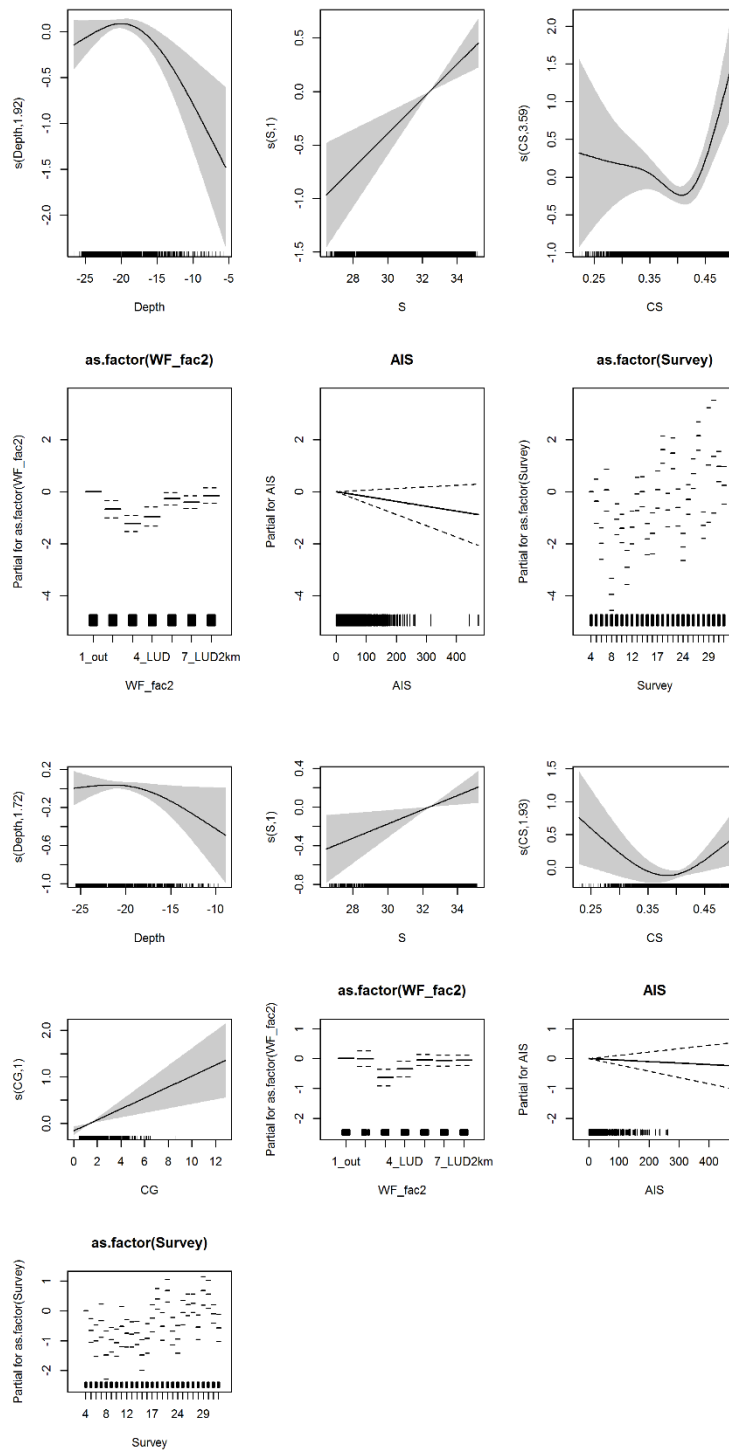


Figure A.12. Partial GAM plots for the Common Guillemot distribution model – presence-absence (upper panel) and positive (lower panel) parts. The values of the environmental variables are shown on the X-axis and the probability on the Y-axis in the scale of the linear predictor. The grey shaded areas and the dotted lines (for factors) show the 95% Bayesian confidence intervals. The degree of smoothing is indicated in the legend of the Y-axis.

Razorbill

Table A.13. Smooth terms, adjusted R-squared and evaluation statistics for the Razorbill distribution models. F statistics and the approximate significance for the smooth terms and t-statistic and the significance for the parametric terms are shown. Variables not included in either the presence/absence or positive model part are indicated with a dash. The evaluation test did not converge due to low sample size. 'n.s.' indicates terms with p-values < 0.05. The significant effect of the windfarms are marked in bold.

Smooth terms	Presence/absence			Positive density		
	F	p		F	p	
Depth	16.954	0.001		-	-	
Salinity	-	-		-	-	
Current speed	9.597	0.002		5.776	0.017	
Current gradient	-	-		-	-	
Parametric terms	Estimate	t	p	Estimate	t	p
AIS	-	-	-	-	-	-
LUD WF parametric	-0.656	-2.119	0.034	-0.138	-0.592	0.554
PAWP WF parametric	-0.842	-3.173	0.002	-0.525	-1.619	0.106
OWEZ WF parametric	-0.521	-1.709	0.087	-0.291	-1.081	0.28
LUD (2 km buffer) parametric	-0.284	-1.099	0.272	0.017	0.096	0.923
PAWP (2 km buffer) parametric	-0.349	-1.668	0.095	-0.359	-1.723	0.085
OWEZ (2 km buffer) parametric	-0.335	-1.567	0.117	0.249	1.301	0.194
Survey 5	-1.31	-1.851	0.064	-0.937	-1.39	0.165
Survey 6	-1.798	-3.495	0	-1.455	-1.577	0.115
Survey 7	1.969	3.241	0.001	-0.072	-0.207	0.836
Survey 8	-2.897	-6.759	0	-1.843	-1.972	0.049
Survey 9	-1.492	-3.194	0.001	-0.692	-1.419	0.156
Survey 10	-0.453	-0.973	0.33	-1.377	-3.26	0.001
Survey 11	-0.359	-0.598	0.55	-0.102	-0.2	0.842
Survey 12	0.794	1.704	0.088	-0.449	-1.343	0.18
Survey 13	0.685	1.587	0.113	-1.105	-3.156	0.002
Survey 14	1.977	4.552	0	-1.06	-3.696	0
Survey 15	0.152	0.343	0.731	-1.524	-4.168	0
Survey 16	-0.033	-0.064	0.949	-0.579	-1.576	0.116
Survey 17	0.726	1.445	0.148	-0.089	-0.246	0.805
Survey 18	-0.744	-1.752	0.08	-1.122	-2.79	0.005
Survey 21	1.661	3.835	0	-0.232	-0.815	0.415
Survey 22	1.103	2.617	0.009	-0.861	-2.787	0.005
Survey 23	0.343	0.642	0.521	-0.788	-2.221	0.027
Survey 24	0.391	0.982	0.326	-0.432	-1.368	0.172
Survey 25	0.208	0.43	0.667	-0.499	-1.471	0.142
Survey 26	1.17	2.322	0.02	-0.695	-2.38	0.018
Survey 27	2.288	2.779	0.005	-0.405	-1.453	0.147
Survey 28	-0.383	-0.829	0.407	-0.283	-0.743	0.458
Survey 29	2.818	1.202	0.23	-0.114	-0.366	0.715
Survey 30	1.427	0.619	0.536	-0.746	-1.916	0.056
Survey 31	1.846	2.692	0.007	0.114	0.431	0.667
Survey 32	-0.466	-0.534	0.593	-0.917	-1.31	0.191
Sample size (n)	11,008			627		
Adjusted R ²	7.3%			6.5%		
AUC						
Spearman's corr.						

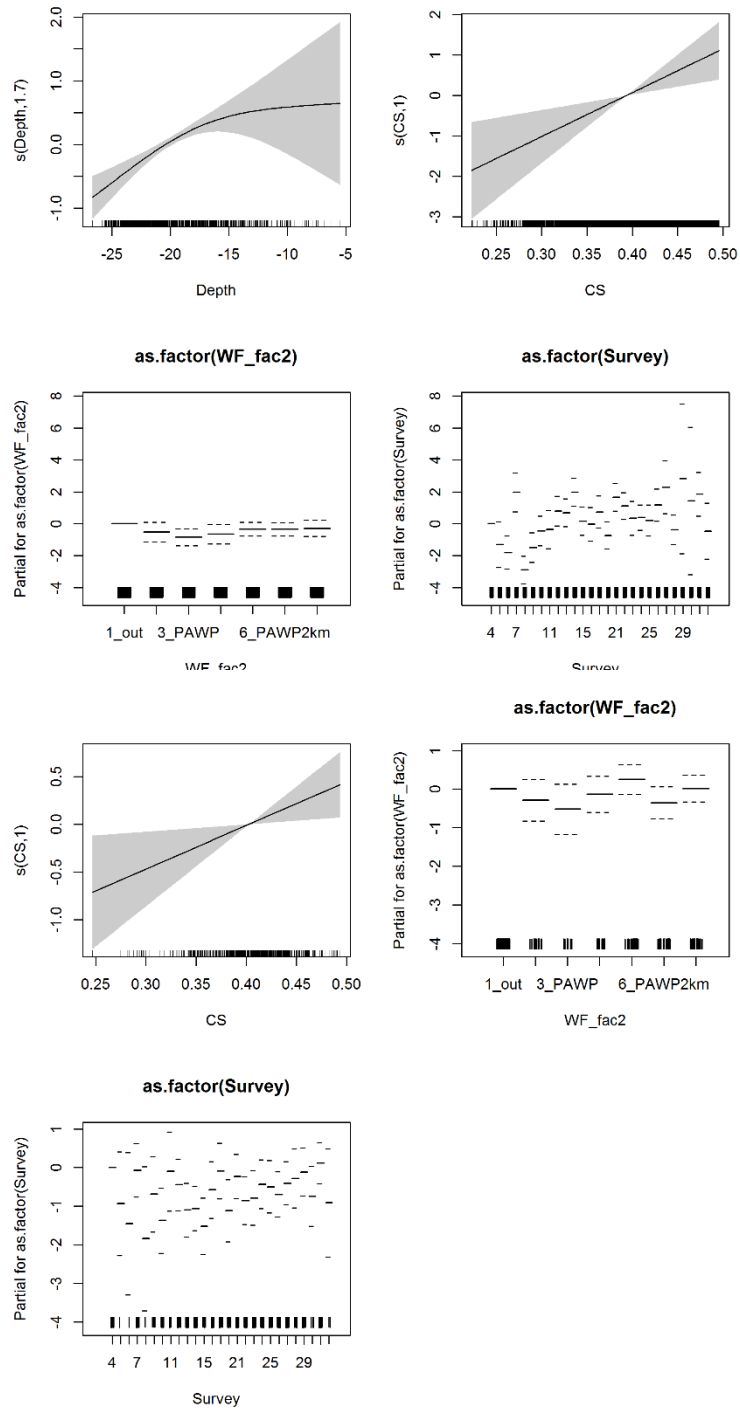


Figure A13. Partial GAM plots for the Razorbill distribution model – presence-absence (upper panel) and positive density (lower panel) parts. The values of the environmental variables are shown on the X-axis and the probability on the Y-axis in the scale of the linear predictor. The grey shaded areas and the dotted lines (for factors) show the 95% Bayesian confidence intervals. The degree of smoothing is indicated in the legend of the Y-axis.